



<https://theses.gla.ac.uk/>

Theses Digitisation:

<https://www.gla.ac.uk/myglasgow/research/enlighten/theses/digitisation/>

This is a digitised version of the original print thesis.

Copyright and moral rights for this work are retained by the author

A copy can be downloaded for personal non-commercial research or study, without prior permission or charge

This work cannot be reproduced or quoted extensively from without first obtaining permission in writing from the author

The content must not be changed in any way or sold commercially in any format or medium without the formal permission of the author

When referring to this work, full bibliographic details including the author, title, awarding institution and date of the thesis must be given

Enlighten: Theses

<https://theses.gla.ac.uk/>  
[research-enlighten@glasgow.ac.uk](mailto:research-enlighten@glasgow.ac.uk)

THESIS FOR THE DEGREE OF DOCTOR OF PHILOSOPHY.

A STUDY OF THE DEGRADATION OF  
POLYOXYMETHYLENE

By

Rodney S. Roche, B.Sc., A.R.I.C.

Department of Chemistry,  
University of Glasgow.

March 1965.

ProQuest Number: 10984195

All rights reserved

INFORMATION TO ALL USERS

The quality of this reproduction is dependent upon the quality of the copy submitted.

In the unlikely event that the author did not send a complete manuscript and there are missing pages, these will be noted. Also, if material had to be removed, a note will indicate the deletion.



ProQuest 10984195

Published by ProQuest LLC (2018). Copyright of the Dissertation is held by the Author.

All rights reserved.

This work is protected against unauthorized copying under Title 17, United States Code  
Microform Edition © ProQuest LLC.

ProQuest LLC.  
789 East Eisenhower Parkway  
P.O. Box 1346  
Ann Arbor, MI 48106 – 1346

## PREFACE.

The work described in this thesis was done during the period October 1961 to December 1964 in the Physical Chemistry Laboratories of the University of Glasgow under the general supervision of Professor J. Monteath Robertson, C.B.E., F.R.S. and Dr. Norman Grassie, Senior Lecturer in Macromolecular Chemistry.

My thanks are due to BX Plastics Limited for the award of a research scholarship for the academic year 1961/62 and to the University of Glasgow for my appointment to an Assistant Lectureship for the period 1962-1965 during the tenure of which this work was done.

Thanks are also due to Dr. E. Clayton for expert collaboration in the mass spectrometric product analyses and those members of the technical staff, particularly Mr. R. Smith, who provided technical assistance during the course of the work.

The supply of research samples by BX Plastics Limited and the Distillers' Company is gratefully acknowledged.

## SUMMARY

This thesis is primarily concerned with the kinetics and mechanism of the thermal degradation of linear high molecular weight polyoxymethylene with hydroxyl and acetate chain-ends.

An introduction to the thesis (Chapter 1) briefly reviews the various modes of polymerisation of formaldehyde to linear polyoxymethylene. Evidence for the structure of the polymer provided by modern physical methods (X-ray diffraction and I.R. spectroscopy), which substantiates the conclusions of Staudinger and others, is also reviewed. The thirty year hiatus between the classical work and modern work culminating in industrially useful thermoplastic materials is also discussed. A review of earlier work on the degradation of polyoxymethylene reveals the need for the more detailed study described in this thesis.

The apparatus and experimental techniques used in this study are described in chapter 2.

In order to isolate the thermal degradation from other degradation reactions, particularly oxidation, the reaction is studied in high vacuum.

The thermal stability of high polymers can be discussed from two standpoints - thermodynamic and kinetic. The thermodynamic aspects of the thermal stability of polyoxymethylene is the subject of Chapter 3. The relationship between the heat of polymerisation,

## II

$\Delta H_p$ , and the facility with which the reverse process, depolymerisation, occurs is discussed. This discussion leads to a consideration of the value of  $\Delta H_p$  for formaldehyde. Estimates of this quantity, based on (a) heats of solution of formaldehyde in polar solvents, (b) heats of combustion of polymer and monomer, and (c) a hypothetical polymerisation reaction path, suggest a value of  $\Delta H_p$  in the region of 15 k cal mole<sup>-1</sup>. The polyoxymethylenes with hydroxyl chain-ends,  $\text{HO}(\text{CH}_2\text{O})_n\text{H}$ , are "living" polymers in the sense that the chain-ends are stable "active centres" through which polymer-monomer equilibrium can be achieved. Dainton exploited this fact in his determination of  $\Delta H_p$  and  $\Delta S_p$  from equilibrium measurements. However, Dainton noted an unacceptable discrepancy of 11.2 entropy units between the "Second Law" entropy and the more reliable "Third Law" value based on heat capacity measurements in the temperature range 20-300°K. The values for the thermodynamic functions obtained in this study are in better agreement with the "Third Law" and theoretical values.

The thermodynamic ceiling temperature of polyoxymethylene has been calculated for five polymer samples and found to be near 120°C. This temperature represents the upper limit of thermodynamic stability of the polymer. Metastability of the polymer above the ceiling temperature due to kinetic factors can extend its useful temperature range up to 270°C in high vacuum and thus a study of the kinetics of degradation is of fundamental and practical interest.

The kinetics and mechanism of the degradation of several polyoxymethylenes with hydroxyl and acetate chain-ends are discussed in chapters 4 and 5. It is shown that the high molecular weight polymers with hydroxyl chain-ends are completely degradable at  $130^{\circ}\text{C}$ , detectable degradation occurring in high vacuum at temperatures in excess of  $100^{\circ}\text{C}$ , which is some  $80^{\circ}$  below the M.p.t ( $178-180^{\circ}\text{C}$ ) of the polymer. The thermal depolymerisation reaction is 1st order at all temperatures in excess of  $130^{\circ}\text{C}$ , showing a deviation from first order behaviour which occurs later in the reaction the higher the temperature. Possible explanations for this deviation are discussed. In contrast the acetates are much more stable than the parent glycols showing little degradation below  $165^{\circ}\text{C}$ . It is found that whereas the polymer with acetate chain-ends shows uniform 1st order behaviour with an activation energy of  $58 \text{ k cal. mole}^{-1}$  throughout the reaction the activation energy for volatilisation of monomer from the glycols shows complex behaviour increasing to a maximum of  $52 \text{ k. cal. mole}^{-1}$  as the reaction proceeds. Tentatively, this effect is explained in terms of the crystalline-amorphous transition becoming rate controlling as the more readily degradable amorphous phase is removed.

The molecular weight of the polymer was measured during the course of degradation and the results confirm that the thermal depolymerisation of polyoxymethylenes is chain-end initiated and that no random chain-scission or chain transfer reactions occur during the reaction.

Within the limits of sensitivity of the analytical techniques available evidence for products that could conceivably arise from a free - radical reaction, initiated at the polymer chain-end, is lacking and further the action of free-radical inhibitors gives scant support to a free-radical mechanism (Chapter 5)

It has been established (Chapter 5) that the degradation is susceptible to base-catalysis. It is concluded, however, that the most plausible mechanism for the thermal depolymerisation of both the polyoxymethylene glycols and acetates is a molecular mechanism involving 4 or 6 membered transition states.

The characterisation of the polymer in terms of dilute solution properties was hampered initially by the lack of a suitable room-temperature solvent. The fact that aqueous perfluoroacetone hydrate was found to dissolve the polymer at room-temperature provided a key to this problem. In Chapter 6 the solubility of the polymer and some of its solution properties are discussed. In Chapter 7 a brief survey of the photo- and photo-oxidative degradation of polyoxymethylene is presented.

An appendix contains information on the characterisation of perfluoroacetone hydrate.



## CONTENTS

<u>CHAPTER 1</u>	<u>Introduction</u>	<u>Page</u>
	Introduction	1
	Polymerisation of Formaldehyde	1
	A. Solution Polymerisation	2
	(1) Polymerisation in aqueous solutions	2
	(2) Polymerisation non-aqueous solvents	5
	Anionic Polymerisation	6
	Cationic Polymerisation	8
	B. Bulk Polymerisation of Formaldehyde	10
	C. Polymerisation of Gaseous Formaldehyde	10
	The Structure of the Polymer	12
	The Degradation of Polyoxymethylene	16
	Introduction	16
	(a) Thermal Degradation	19
	(b) Thermal Chain Scission	20
	(c) Thermal Oxidation	20
	(d) Hydrolytic degradation	21
	Aims of this work	22

## CONTENTS

	<u>Page</u>
<u>CHAPTER 2.</u>	<u>Experimental</u> 23
2.1.	Introduction 23
2.2.	Preparation of Polymers 23
2.3.	Characterisation of the Polymers 26
2.3.1.	Viscometry 26
2.3.2.	Infrared End group analysis 28
2.4.	<u>Degradation Apparatus and Techniques</u> 30
2.4.1.	Introduction 30
2.4.2. (a)	The Pirani gauge and the measurement of Rates of Volatilisation 31
2.4.2. (b)	Calibration of the Pirani gauge 34
2.4.2. (c)	The Kinetics of Thermal Degradation and the Evaluation of Activation Energies 36
2.4.2. (d)	Vacuum Manometric apparatus 40 Procedure for measuring Rates of Degradation 42 Catalysis and Inhibition Experiments 44
2.5.	Gas Analysis Apparatus 45 Calibration of the Apparatus 46

## CONTENTS

	<u>Page</u>
2.6.	Equilibration Apparatus 48
2.7.	Measurement of Polymer density 50
2.8.	Photochemical Techniques 51
2.9.	Preparation of Perfluoroacetone hydrate 52
2.10	Mass Spectrometric Product Analysis 53
 <u>CHAPTER 3</u>	
	<u>The Thermodynamic Properties of Polyoxymethylene</u> 55
3.1.	Introduction 55
3.2.	<u>The Heat of Polymerisation of gaseous</u>
	<u>Formaldehyde</u> 57
3.2.1.	Introduction 57
3.2.2.	Estimation of $\Delta H$ for polymerisation of formaldehyde 57
3.2.3.	Experimental Determination of $-\Delta H^{\circ}_{gc}$ 61
3.3.	<u>The Ceiling Temperature of Polyoxymethylene</u> 68
3.4.	<u>Discussion</u> 69
 <u>CHAPTER 4</u>	
	<u>The Thermal Depolymerisation of Polyoxymethylene</u>
4.1.	<u>General Introduction</u> 74
4.2.	Thermal Depolymerisation of Polyoxymethylene 80
	glycols and acetates Part 1 - Kinetics 80

## CONTENTS

	<u>Page</u>
4.2.1. <u>Introduction</u>	80
4.2.2. <u>The Degradation Variables</u>	80
4.2.2. (a)    Temperature and the Activation Energy of the reaction	80
4.2.2. (b)    Mode of Preparation and Molecular weight	88
4.2.2. (c)    Weight as a reaction variable	96
4.2.2. (d)    Time as a reaction variable	97
4.2.3        Polymer density as a function of percentage depolymerisation	102
4.2.4. $\bar{M}_n$ as a function of conversion to monomer	106

## CHAPTER 5

### The Thermal Depolymerisation of Polyoxymethylene

#### Part 2                    The Mechanism of the Reaction

5.1.1. <u>Introduction</u>	110
5.2.        Mechanistic Schemes - Theoretical	111
5.2.        The Molecular Mechanism	111
5.2.2.        The Free Radical Mechanism	113
5.2.3.        The Ionic Mechanism	120
5.3.        Product Analysis	122
5.3.1.        Non-condensables	122

## CONTENTS

	<u>Page</u>
5.3.2. Mass Spectrometric Analysis	126
5.4. Catalysis and Inhibition Experiments	128
 <u>CHAPTER 6</u>	
<u>The Solubility and Some solution properties</u>	
<u>of Polyoxymethylene</u>	
	133
6.1. <u>Introduction</u>	133
6.2. Perfluoroacetone hydrate as a solvent for polyoxymethylene	134
6.3. The Viscosity of P.O.M. in P.F.A.H./H <sub>2</sub> O mixtures	139
6.4. The Mark - Houwink exponent, $a$	143
 <u>CHAPTER 7</u>	
<u>The Photochemical and Photo-oxidative</u>	
<u>Degradation of Polyoxymethylene</u>	
	144
7.1. <u>Introduction</u>	144
7.2. Photochemical degradation in High Vacuum	144
7.3. The Photo-oxidation of Polyoxymethylene	146
7.3. (a) The hydroxyl band	147
7.3. (b) The carbonyl band	148
7.4. Discussion	150
APPENDIX I	152
REFERENCES	

## CHAPTER 1

### Introduction.

An increasingly important branch of polymer science and technology is associated with the heterochain macromolecules known as polyethers<sup>(1)</sup>. The carbon-oxygen polyethers, known also as polyalkylene oxides, are best known and it is with the linear polymer of formaldehyde, which is structurally the simplest of this class of materials, that this thesis is concerned. The I.U.P.A.C. nomenclature committee recommended the name poly(methylene oxide) for this polymer<sup>(2)</sup> but the classical nomenclature is retained here because it serves as a link with the earlier work of Staudinger and is in common use today.

Polymers of formaldehyde were first observed by Butlerov in 1859<sup>(3)</sup> and contributions were made by Auerbach and Barschall<sup>(4)</sup> to an understanding of the nature of the white polymeric powders but it was Staudinger who established that they had a polyoxymethylene chain structure.

#### Polymerisation of Formaldehyde

Formaldehyde (M.Pt.  $-118^{\circ}\text{C}$ ; B.Pt.  $-19^{\circ}\text{C}$ )<sup>(6)</sup>, may be polymerised directly from the gas phase, in bulk, or in solution in aqueous and non-aqueous solvents.

## A. Solution Polymerisation

### (1) Polymerisation in aqueous solution

At room temperature concentrated solutions of formaldehyde become cloudy and ultimately precipitate a white powder which Staudinger showed to be polyoxymethylene glycol,  $\text{HO}(\text{CH}_2\text{O})_n\text{H}$  ( $n = 6 - 100$ ). Considerable evidence has accumulated about the mechanism of the reaction (1)(5)(7) and there is now little doubt that it is ionic. Formaldehyde dissolves exothermically, ( $-\Delta H = 15 \text{ Kcals.mole}^{-1}$ )(7), in polar solvents, existing in water as the hydrate methylene glycol, which is in equilibrium with unhydrated formaldehyde,



$$K_1 = \frac{(\text{CH}_2\text{O}) \cdot (\text{H}_2\text{O})}{(\text{HOCH}_2\text{OH})} = 10^{-4}, \text{ at } 20^\circ\text{C} \text{ (8)}$$

The hydrate dissociates both as an acid and as a base,

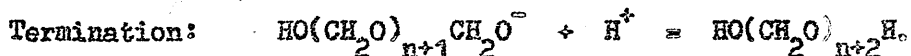
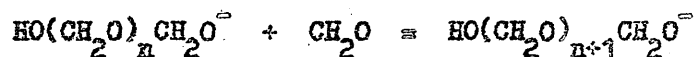
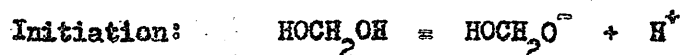
$$K_a = 0.4 \times 10^{-13}, \text{ at } 20^\circ\text{C} \text{ (9)}$$

$$K_b = 1.62 \times 10^{-20}, \text{ at } 20^\circ\text{C} \text{ (10)}$$

It may be calculated from these data that in a 1 M solution of formaldehyde,

$$(\text{HOCH}_2\text{O}^-) = 10^{-7}; (\text{HOCH}_2^+) = 10^{-13}; (\text{CH}_2\text{O}) = 10^{-4}.$$

Thus an anionic mechanism,  $\text{HOCH}_2\text{O}^-$  being the initiator, seems most likely for the polymerisation of formaldehyde in aqueous solution and this may be represented as follows:



It has been established<sup>(9)</sup> that the propagation step is an equilibrium reaction. The equilibrium constant for the propagation step formulated above is

$$K_p = \frac{[\text{CH}_2\text{O}][\text{HO(CH}_2\text{O)}_n\text{CH}_2\text{O}^-]}{[\text{HO(CH}_2\text{O)}_{n+1}\text{CH}_2\text{O}^-]} = K_1 \cdot K_2 = 2.05 \times 10^{-5}$$

where  $K_1 = 10^{-4}$  (see above)

$$\text{and } K_2 = \frac{[\text{HOCH}_2\text{OH}][\text{HO(CH}_2\text{O)}_n\text{H}]}{[\text{H}_2\text{O}][\text{HO(CH}_2\text{O)}_{n+1}\text{H}]} = 0.205^{(11)}$$



The polyoxymethylene glycols with DP<sub>n</sub> greater than 6 are insoluble in water and therefore as the polymerisation proceeds all material precipitates which has a D.P. greater than this. The polymerisation of the precipitated oligomeric compounds to higher homologues (DP = 6-100) is considered to occur through equilibria similar to those above. Because the propagation reaction is an equilibrium reaction it is possible to derive values for the Heat of Polymerisation and the Entropy of Polymerisation from the pressure of formaldehyde in equilibrium with the polymer. The thermodynamic properties of polyoxymethylene are discussed in Chapter 3.

The properties of the polymers that can be obtained from the polymerisation of formaldehyde in aqueous solution are summarised in Table 1, 1.

TABLE 1.1

Polyoxymethylene Glycols, HO(CH<sub>2</sub>O)<sub>n</sub>H. (P.O.M.)

Name or Type	DP. = n	Melting Range
Oligomers	2 - 8	80 - 120°C
Paraformaldehyde	6 - 100	120 - 170°C
α P.O.M.	100 - 300	170 - 180°C
β P.O.M.	100 - 300	165 - 170°C

(2) Polymerisation in non-aqueous solvents

Formaldehyde may be polymerised in a variety of non-aqueous solvents, including diethylether, chloroform, hexane, A variety of catalysts, including those in Table 1.2, are capable of initiating the reaction

TABLE 1.2

Formaldehyde Polymerisation Catalysts.

Water

Organic Acids and bases

Lewis acids

Amines

Phosphines, Arsines and Stibines

Organometallic compounds

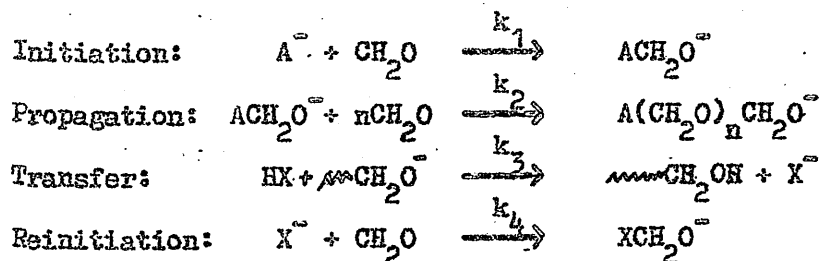
Carbonyls of Fe, Co, Ni.

The nature of the catalysts and the high rates of reaction at low temperatures ( $-80^{\circ}\text{C}$ ) again suggest that an ionic mechanism is operative and as in many ionic reactions of this type the difficulty of achieving reproducibility due to sensitivity to impurities has made kinetic and mechanistic studies difficult.

Anionic Polymerization

Mejzlik<sup>(12)</sup> and his co-workers have studied the kinetics of the polymerization of formaldehyde in diethyl ether solution. They found the order of the reaction with respect to monomer to vary between 2 and 3, and the catalyst exponent to be in the range of 0.5 to 0.8. The molecular weight of the polymer, as measured by intrinsic viscosity, was independent of the catalyst concentration and it was deduced that the reaction is a chain process. Water and methanol were found to be chain transfer agents having no effect on the rate of the reaction. On the other hand carbon dioxide, formic acid and acetic acid are retarders.

Vesely and Mejzlik<sup>(13)</sup> rationalised the above observations as follows. The reaction is an anionic chain reaction involving, initially, the dissociation of the catalyst ion pair into free ions:



Denoting the total anion concentration by  $(O^-)_0$ , they define an overall equilibrium constant,  $K$ , by the relationship

$$K = \frac{(O^-)_0(B^+)}{(Cat)_0}$$

When  $(Cat)_0 \gg K$  ;  $(O^-)_0 = K^{0.5} (Cat)_0^{0.5}$  .

By assuming a steady state concentration of  $(O^-)_0$ , an overall rate equation was derived:

$$-d(CH_2O)/dt = \frac{k_2 K^{0.5} (Cat)_0^{0.5} (CH_2O)}{1 + (k_3/k_4)(HX)/(CH_2O)}$$

The maximum order with respect to monomer predicted by this equation is 2, when  $(k_3/k_4)(HX)/(CH_2O) \gg 1$ . This equation does not, therefore, adequately account for observed orders in the range 2 - 3. However, by using the Bjerrum equation relating dielectric constant to dissociation constant, Vesely and Mejzlik obtained the relationship

$$K = K_0 M^{2.3}$$

between the dissociation constant and the concentration of monomer.

This relationship takes account of the polarity of the monomer.

Substitution for  $K$  in the rate equation gives

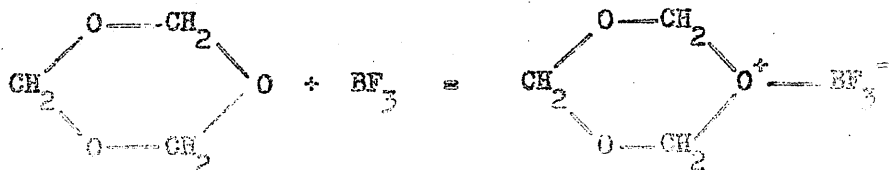
$$-d(CH_2O)/dt = \frac{k_2 K_0^{0.5} (Cat)_0^{0.5} (CH_2O)^{2.2}}{1 + (k_3/k_4)(HX)/(CH_2O)}$$

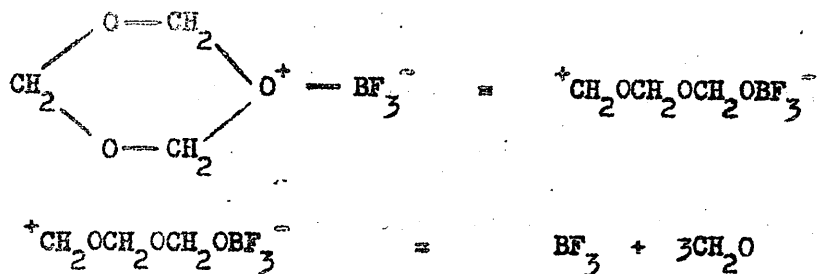
This equation predicts a maximum order of reaction with respect to monomer of 3.2 and thus adequately accounts for the observed orders.

The polymers produced in non-aqueous solvents by the anionic mechanism and in the absence of chain transfer agents have high degrees of polymerisation ( $DP. > 10^3$ ). The properties of these materials are in marked contrast to those of the aqueous polymers. At molecular weights greater than 10,000 polyoxymethylene shows useful mechanical properties and it was probably the realisation of this fact that led to the large development programme undertaken by the Du Pont Company which culminated in the commercial production of Delrin<sup>(14)</sup>.

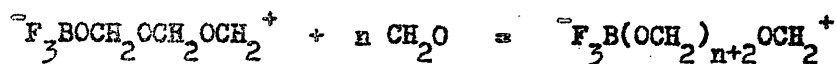
#### Cationic Polymerisation

The marked catalytic activity of Lewis and protonic acids in the polymerisation of formaldehyde suggests that a cationic mechanism can operate. Further evidence for this suggestion can be adduced from the fact that trioxane, the stable cyclic trimer of formaldehyde, can be polymerised to high molecular polyoxymethylene at low temperatures by boron trifluoride. Preliminary kinetic observations by Kern and Jaacks<sup>(15)</sup> suggest that after an initial induction period during which the trioxane ring, opened following electrophilic attack by boron trifluoride, depolymerises to an equilibrium concentration of formaldehyde which then polymerises by a cationic chain reaction, thus:





Polymerisation:



The reaction accelerates throughout its course and this, it was suggested, is due to the alternative initiation reaction,



becoming increasingly important. The acceleration could also be explained by the fact that there is no termination reaction.

Hammick and Boeree (16) reported that the vacuum sublimation of trioxane led to a polyoxymethylene, which they named epsilon-polyoxymethylene. It is clear now, however, (17) that polymerisation is catalysed by acid impurities and that the reaction is cationic. The facility with which the polymerisation occurs in the sublimate is due to the favourable geometry of the trioxane crystal lattice (18).

(B) Bulk Polymerisation of Formaldehyde

Liquid formaldehyde polymerises at rates determined by its purity and temperature. The polymerisation of substantially anhydrous liquid formaldehyde to a solid polymer at  $-20^{\circ}\text{C}$  was first described by Kekule (19). Staudinger noted that the polymers produced in this way were tough, transparent and film forming and he called them eu-polyoxymethylene. The potential usefulness suggested by the resin like character of these polymers is off set by their poor thermal stability. Staudinger believed that his eu-polymer had an average DP. in the region of 5,000. No kinetic studies of the bulk polymerisation of formaldehyde have been made.

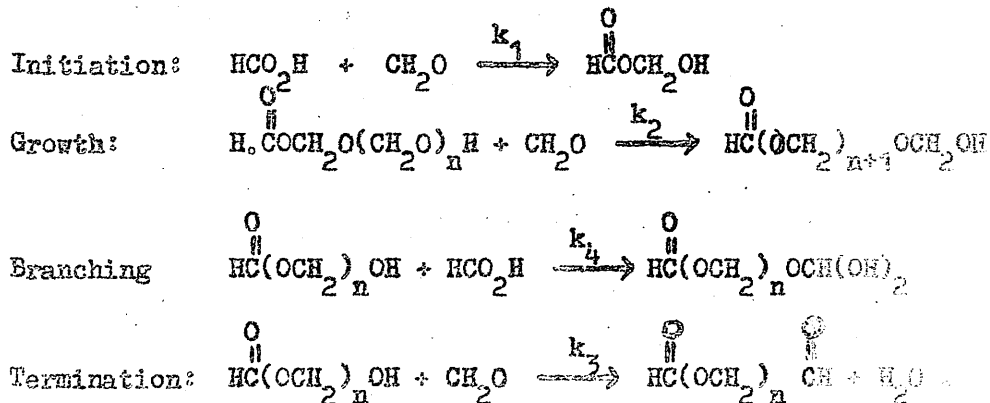
(C) Polymerisation of Caseous Formaldehyde

Work on the polymerisation of gaseous formaldehyde has recently been reviewed by Bevington (20). Gaseous formaldehyde rapidly polymerises on the walls of the containing vessel at temperatures below  $80^{\circ}\text{C}$  above which the polymerisation rate is negligible. Once again it is difficult to achieve reproducibility, although this can be overcome to some extent by careful experimentation. (21) Early workers (22) established that the reaction is heterogeneous and sensitive to impurities both in the gas phase and on the walls of the apparatus.

Later, Carruthers and Norrish<sup>(23)</sup> established that water, formic acid and acetic acid catalyze the reaction. The rate of reaction which is a branching chain reaction is given by

$$-d(\text{CH}_2\text{O})/dt = k_1 k_2 p_c p_m^2 / (k_3 p_m + k_4 p_c);$$

in which  $p_c$  and  $p_m$  are the partial pressures of catalyst and monomer respectively. This rate expression is derived from the scheme of reactions proposed by Carruthers and Norrish



Norrish and Bevington, using  $\text{HCl}$ ,  $\text{SnCl}_4$  and  $\text{BF}_3$  as catalysts established an alternative rate expression<sup>(24)</sup>

$$-d(\text{CH}_2\text{O})/dt = APcPm / (k''p_m + k'p_c);$$

Where  $A$  = the area of the cooled surface on which polymerization occurred. While the termination reaction in the above scheme apparently

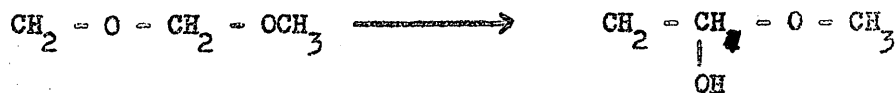


rationalises the observations they note that water which should be produced in appreciable amounts is not found in the system. There is, therefore, no evidence for the formation of a C-C bond in the polymer chain-end structure nor for the feasibility of this reaction.

Tentatively, the authors suggest the reaction may be ionic.

The Structure of the Polymer.

Staudinger distinguished two types of structure that could be derived from the polymerisation of formaldehyde the carbohydrate type, -CH(OH)CH(OH)- and the oxymethylene type. That the polymers produced under the conditions discussed above were of the latter type Staudinger deduced from the evidence provided by their degradation. The polyoxymethylene glycols produce quantitative yields of monomer and water on thermal degradation, whereas if they were of the carbohydrate type they would be expected to char. A small number of (C-C) bonds were found to be present in samples of a polyoxymethylene glycol dimethyl ether derivative which had been heated in boiling water (25) but these were assumed to have arisen in a topochemical rearrangement reaction:



and to be unlikely to occur under normal polymerisation conditions.

This conclusion has recently been confirmed<sup>(26)</sup>.

All the chemical evidence points to the conclusion that polyoxymethylene is a linear polymer and this has been amply confirmed by modern physical methods. It is not proposed to discuss these here but rather to outline briefly the results obtained. The linearity of the polymer molecule is reflected in the high degree of crystallinity of samples of all molecular weights. Indeed, because it is crystalline in nature polyoxymethylene was one of the first macromolecules to be studied by X-ray diffraction techniques by Staudinger's school<sup>(27)</sup>.

It has recently been established that the polymer can be obtained in hexagonal and orthorhombic crystal modifications<sup>(28)</sup>.

The polymer chain is helical with its axis parallel to the *c*-axis of the crystal. The helix is obtained if each O-C-O-C- unit takes up a gauche (staggered, but non-planar) configuration by rotating  $120^\circ$  in the same sense about each successive C-O bond. If the angle is slightly different from  $120^\circ$  in each case a more extended helix is obtained and this is reflected in the variable results found for the identity period, defined as the number of monomer units and turns

(m/n) which occur in each crystal repeat unit. The crystallographic information is summarised in Table 1.3.

TABLE 1.3.

Crystal Structure Data for Polyoxymethylene

Property	Hexagonal	Orthorhombic
Lattice constants ( $\text{\AA}$ )	$a = 4.43; c = 17.3$	$a = 4.46; b = 7.65; c = 3.56$
(m/n)	$9/4^{(27)}; 9/5^{(29)}; 38/21^{(30)}$	$2/1^{(28)}$
Density; ( $\text{g. cc.}^{-1}$ ) (100% crystallinity)	1.492	1.54
Density ( $\text{g. cc.}^{-1}$ ) (amorphous)		1.25.

Infra red spectroscopic evidence also confirms Staudinger's conclusions. It has been shown <sup>(31)(32)</sup> that polymers produced by polymerisation of liquid formaldehyde ( $\alpha$ -polyoxymethylene), by addition of concentrated sulphuric acid to 40% aqueous formaldehyde solution ( $\beta$ -polyoxymethylene) and a sample of commercial paraformaldehyde have essentially the same structure. The formulation of the polymer in terms of hydrogen-bonded formaldehyde <sup>(33)</sup> and  $\text{CH(OH)CH(OH)}$  is ruled out on the basis of the spectrum of the  $\alpha$ -polymer. The spectra show strong bands at 3.2 and 10.7 microns.

due to C=O stretching; at 3.4 microns due to C-H stretching and at 2.9 microns a broad band due to O-H stretching. The hydroxyl band maximum is found at  $3320\text{ cm}^{-1}$  in paraformaldehyde and at  $3450\text{ cm}^{-1}$  in the  $\beta$ -polymer. The different frequencies of the band maxima probably reflect different hydrogen-bonding conditions.

The intensity of the -OH band varies with the molecular weight of the sample being very intense in paraformaldehyde and less intense in the high molecular weight polyoxymethylene glycols. That the high molecular weight polymers do in fact contain chain-end hydroxyl groups is difficult to prove by classical analysis. Indeed Walker<sup>(34)</sup> suggested that the high molecular weight polymers probably had a cyclic structure. When high molecular weight polyoxymethylene glycols are treated with acetic anhydride the OH bands in the infra red spectrum at  $3450\text{ cm}^{-1}$  are replaced by a small ester carbonyl peak at  $1750\text{ cm}^{-1}$ , thus confirming Staudinger's earlier conclusion that the high molecular weight polymers were higher homologues of the oligomeric polyoxymethylene glycols. The usefulness of the infra red technique will be further discussed in Chapter 2 when the problem of characterising a given polymer sample arises.

## The Degradation of Polyoxymethylenes.

### Introduction

The hydrolytic degradation of paraformaldehyde and high molecular weight polyoxymethylene diacetates provided Staudinger with vital information for his macromolecular theory. In these early studies the relative stabilities of the polyoxymethylenes glycols and their diacetate and dimethyl ether derivatives were noted. The thermal stability was found to decrease in the order dimethyl ether, diacetates and glycols. The isolation and characterization of the more stable diacetate and dimethyl ether derivatives with DP up to a 100 firmly established the polymeric nature of the less stable parent glycols. The information on the relative stabilities of the derivatives was incidental to the main objective which was an understanding of the structure of these materials.

Polyoxymethylene was suggested as a model compound for cellulose<sup>(35)</sup> which at that time was attracting considerable attention among organic chemists. The suggestion was based more on physical similarities such as crystallinity and fibre forming properties than on any more obvious chemical analogy than the same empirical molecular formula. In a similar way polystyrene was suggested as a model for natural rubber. The development of polystyrene as a plastic material in its own right was not followed by a similar development of polyoxymethylene the latter being dismissed as being too thermally labile to be of any practical use as a plastic material. Indeed, as

recently as 1952 Bevington,<sup>(36)</sup> reviewing the polymerisation of aldehydes, was prompted to write: "High polymers of aldehydes are of no importance as fibres, plastics or rubbers because they depolymerise readily". While the ready depolymerisation of polyoxymethylenes is unquestionable it is interesting to note that Bevington's statement is no longer completely true. The reason for this will emerge from the discussion which follows:

A new and much broader interest in the degradation reactions of high polymers has been stimulated by the growth of the plastics industry and the associated need for an understanding of the relationship between their macromolecular structure and stability in the various environments in which they are used. Fundamental knowledge of the processes occurring in the deterioration of high polymers may suggest how best to stabilise existing materials and also how to design materials for new applications. The progress made in understanding the mechanism of high polymer degradation reactions is reflected in the number of monographs on the subject (37)(38)(39)(40)(41).

High polymers do not always behave as our knowledge of model compounds of low molecular weight might lead us to expect.

This has been shown to be due as much to the macromolecular environment<sup>(42)</sup> as to the effect of structural abnormalities,<sup>(43)</sup> such as branching and weak links, incorporated into the polymer molecule at random and in low concentrations.

The deterioration of a plastic material in use is chemically complex and can be regarded as the result of the combined effects of heat, light, oxygen and other chemical agencies. In order to make any progress towards a fundamental understanding of the deterioration processes it is important to identify and isolate the various reactions that a given macromolecule can undergo. Thus, for example, in order to establish some measure of the thermal stability of a given polymer the thermal reaction is isolated by carrying out the study in high vacuum or a chemically inert atmosphere.

The first systematic attempt to study the degradation of high molecular weight polyoxymethylene was reported by Kern and Cherdron.<sup>(44)</sup> They discussed the thermal and thermo-oxidative degradation of polymers having hydroxyl, and methoxyl chain-end structures. They distinguished four possible reactions:

- (a) Thermal depolymerisation from the chain-ends.
- (b) Thermal chain-scission at temperatures greater than 270° followed by depolymerisation.
- (c) Thermal oxidation.
- (d) Hydrolytic degradation by secondary products of oxidation.

(a) Thermal degradation

High molecular weight polyoxymethylene glycols depolymerise at conveniently measurable rates at temperatures above 125°C. Comparatively low molecular weight materials, like paraformaldehyde, depolymerise at comparable rates below 100°C. The thermal depolymerisation of polyoxymethylene glycol in the temperature range from room temperature up, through the crystalline melting point at 180°C, to 270°C is chain-end initiated. Evidence for this can be adduced from the fact that the higher molecular weight material depolymerises less readily, and is apparently more stable, having fewer chain-ends at which depolymerisation can be initiated. Further, polyoxymethylene dimethyl ethers are thermally stable in high vacuum up to 270°C. The thermal stability of the whole molecule up to 270°C is thus determined solely by the nature of the chain-end.

The post-polymerisation acetylation of anionically polymerised high molecular weight polyoxymethylene is the basis of the stabilisation of the DuPont product Delrin.<sup>(14)</sup> The stability of Celcon produced by the American Celanese Company is due to the incorporation of (C-C) bonds in the polymer by co-polymerisation of trioxane with suitable comonomers such as dioxolane. The depolymerisation process is unable to pass through dioxolane units.

Kern and Cherdron reported that for a paraformaldehyde with DP = 40 the depolymerisation reaction is first order in the temperature range 90 - 150°C and has an activation energy of 10 K.cals. No more quantitative detail than this is given.



(b) Thermal Chain Scission.

The above authors also showed that a polyoxymethylene dimethyl ether ( $DP = 3 \times 10^2$ ) degrades to monomer in a first order process in the temperature range  $280 - 350^\circ\text{C}$ . The activation energy given is 28 K. cal. It was suggested that the main chain is undergoing scission in this temperature range and therefore  $270^\circ\text{C}$  represents an upper stability limit determined by the strength of the main chain C-O-C ether links. No experimental evidence for the linearity between molecular weight and rate of monomer production to be expected for a molecule undergoing random chain scission followed by rapid depolymerisation is reported.

(c) Thermal Oxidation.

Kern and Cherdron established that the thermal oxidation of polyoxymethylene does not occur at temperatures below  $160^\circ\text{C}$  to any significant extent. They suggested that oxidation of crystalline polyoxymethylene does not occur and the threshold of  $160^\circ\text{C}$  represents the point at which the crystal lattice is beginning to break up. The onset of melting occurs at about  $125^\circ\text{C}$  and is complete at  $178 - 180^\circ\text{C}$ . The major product of oxidation is monomer and very little true polymer oxidation occurs at this temperature. The photo-oxidation follows a different course and will be discussed in Chapter 7.

(d) Hydrolytic Degradation

The hydrolysis of heterochain polymers is one degradation reaction which distinguishes their chemistry from that of the carbon-chain vinyl polymers. The acid hydrolysis of polyoxymethylene is a random chain-scission reaction and leads to rapid depolymerisation. Alkaline hydrolysis involves only the chain-end. The kinetics of the depolymerisation of the soluble polyoxymethylene glycols (45) reflect the fact that there are two hydrolysis mechanisms as well as a purely thermal mechanism leading to depolymerisation and an overall rate constant, k, can be defined in terms of the individual rate constants for these processes, thus

$$k = k_a(H_3O^+) + k_b(OH^-) + k_w$$

$$k_a = 3.001 \text{ l.mole.}^{-1} \text{ min}^{-1}; \quad k_b = 3.5 \times 10^{-7} \text{ l.mole.}^{-1};$$

$$k_w = 6.4 \times 10^{-3} \text{ min}^{-1} \text{ at } 20^\circ\text{C.}$$

Kern and Cherdron observed that the thermal oxidation accelerates and this they attributed to hydrolysis by formic acid produced by the oxidation of formaldehyde. The hydrolysis produced more chain ends at which depolymerisation can occur and hence the reaction is accelerated.

Aims of this work.

When the work to be described in this thesis was undertaken Kern and Cherdron's paper<sup>(44)</sup> represented the only reported attempt to systematise the study of polyoxymethylene degradation.

Their paper is far from a detailed study of any of the reactions, and it was the need for a more thorough examination of the quantitative aspects of the thermal reaction in particular that prompted our work.

## CHAPTER 2

### EXPERIMENTAL

#### 2.1. Introduction

The subject matter of this chapter is strictly limited to a description of the apparatus and techniques applied in this study of the degradation of polyformaldehyde. Where a technique may give results which are equivocal it is described and the critique postponed until the results obtained arise for discussion.

#### 2.2 Preparation of Polymers

In order to study the effect of different modes of preparation on the degradation behaviour of polyoxymethylene several samples were used. Some were prepared by ourselves and others were made available to us by workers in the laboratories of the Distillers Company and BX Plastics Limited.

##### Sample 1 - (A/BULK/RI)

2 g. of DIST/3244/87 (see sample 6 below) were washed with distilled water, with AR acetone and finally dried in vacuum at 70°C for one day. The polymer was then heated to 200°C in vacuum and the monomer produced was trapped at -196°C. Raising the temperature to -80°C the monomer was distilled into a

preflamed cylindrical tube (heavy wall "Pyrex", 20 mm. bore x 10 cm.) held at  $-196^{\circ}\text{C}$ . The tube was then isolated from the rest of the apparatus by sealing at a constriction and brought to  $-80^{\circ}\text{C}$  at which temperature it was held for one day ( $^{\circ}\text{DRIKOLD}^{\circ}$  powder). A contraction ( $\int \text{CH}_2\text{O} = 0.91$  at  $-80^{\circ}\text{C}$   $\int \text{POM} = 1.4$ ) occurred indicating that polymerisation was proceeding but it was very much slower than the literature, referred to in Chapter 1, led us to expect. After one day the tube was opened under vacuum (break seal) and the unpolymerised monomer distilled to a trap. The polymerisation tube was then warmed to room temperature and pumped for two days after which time the monomer pressure was negligibly small (less than  $10^{-2}$  mm. after one hour isolated from the pumps). The polymer (1.72 g.; 86% yield), a white opaque, resin-like mass was dissolved in 95% aqueous perfluoroacetone hydrate at  $25^{\circ}\text{C}$  and reprecipitated as a powder in a large volume of AR acetone held at  $0^{\circ}\text{C}$ .

Sample 2- (A/TRIOXANE/R2)

10 g. of B.D.H. Trioxane was sublimed under high vacuum (Trioxane vapour pressure = 12.7 mm. Hg. at  $20^{\circ}\text{C}$ ) and trapped at  $-196^{\circ}\text{C}$  in a "Pyrex" bulb (radius 5 cm.). After washing the sublimate with AR acetone to extract trioxane 3.64 g. of polymer were obtained.

Sample 3 - (B/TRIOXANE/R2)

1.5 g. of sample 2 were dissolved in 95% aqueous perfluoroacetone hydrate and reprecipitated in the same way as Sample 1. (99% recovery).

Sample 4 - (RN/20/ED/17/P-BX)

Trioxane was polymerised in ethylene dichloride solution at + 50°C using boron-trifluoride etherate as catalyst.

Sample 5 - (RN/20/22/P - BX)

Very pure gaseous formaldehyde produced by the pyrolysis of cyclohexyl hemiformal in the temperature range 125° - 160°C was polymerised by dissolving in it heptane containing 90 p.p.m. of  $\text{Ph}_3\text{P}$  as catalyst.

Sample 6 - (RN/20/22/OAC - BX)

Sample 5 was acetylated by refluxing in a 5:1 mixture of acetic anhydride and pyridine for one hour followed by soxhlet extraction with ethanol for twenty four hours. Samples 4, 5 and 6 were supplied by BX Plastics Limited.

Sample 7 - (DIST/3244/87/P)

Pure gaseous formaldehyde was passed at the rate of

20 g/hr into toluene containing .022% tributylamine for three hours.

Sample 8 - (Dist/3244/87/OAc)

Sample 7 was acetylated in a similar manner to sample 6.

Samples 7 and 8 were supplied by the Distillers Research Laboratory, and because they were 20-30 times larger than any of the others they were used almost exclusively for the detailed study of most of the degradation variables.

2.3 Characterisation of the Polymers

2.3.1. Viscometry

A polymer is most conveniently characterised in terms of its solution properties and osmometry, light scattering, viscometry and ultracentrifugal techniques have yielded information about weight and number-average molecular weights, dispersion and the dimensions of polymer molecules in solution. Hitherto, the lack of a room-temperature solvent for the polymer has unquestionably delayed progress in the characterisation of polyoxymethylene by the above techniques and alternative procedures have had to be adopted (see 2.3.2.)

It has been found (see chapter 6) that perfluoroacetone hydrate (P.F.A.H.) at its M.pt. ( $43-44^{\circ}\text{C}$ ) and as an aqueous solution, at concentrations greater than 77%, will dissolve the polymer to give a 1% solution in 10-20 minutes at  $25^{\circ}\text{C}$ . Polymer solutions were prepared in situ in the viscometer shown in figure 1.

The capillary, A, was made of Veridia precision bore tubing

( $r = 0.25$  m.m.;  $l = 10.8$  cms.; flow-time for distilled water = 21.3

secs. at  $20^{\circ}\text{C}$ ). The sintered glass disc, C, was made from a sawn-off

"Pyrex" filter stick (10 m.m., porosity 2 type 4100). The following

procedure gave a standard deviation of 1.2% as determined from

ten runs using 90% aqueous P.F.A.H.. The weighed polymer sample

was placed in compartment B an accurately measured amount of solvent

was added and the time noted. Mixing was achieved by blowing air

through silica gel tube, D, attached to socket 1 with socket 2 stoppered.

To measure the flow time for a given solution socket 1 was stoppered,

tube D was attached to Socket 3 and a sample of the solution was forced

up into bulb E by pumping air through tube D. Tubes 1 and 3 were

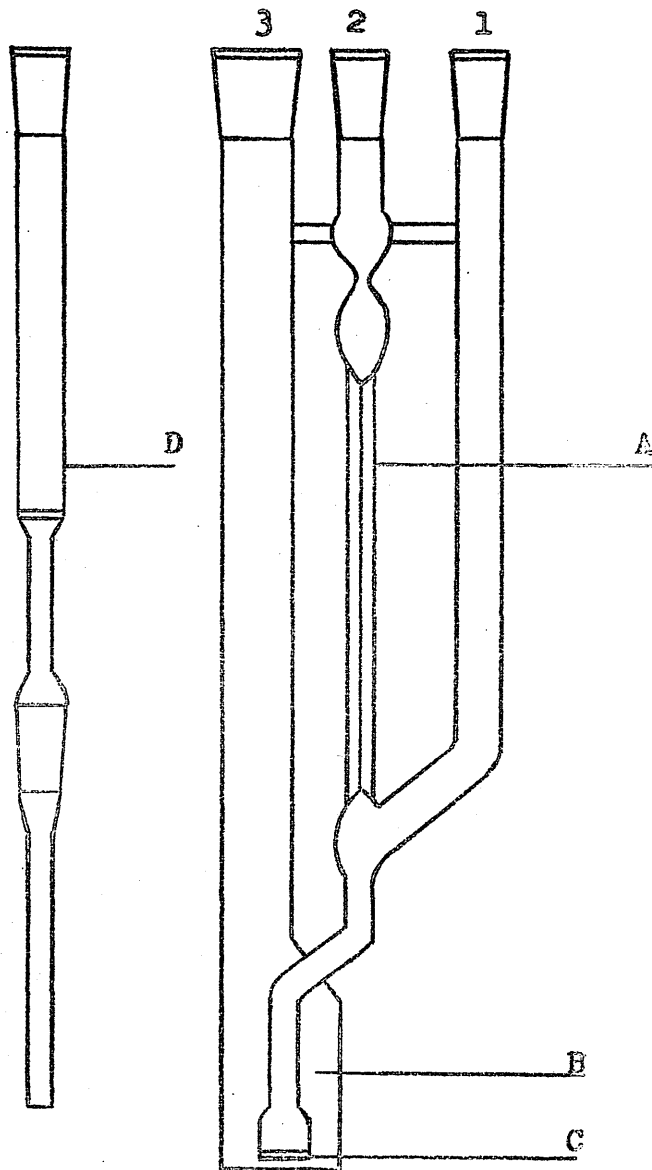
then opened to the atmosphere and quickly connected by a piece of

polythene tubing in order to minimise evaporation losses and

contamination from atmospheric water vapour. (Flow-time,  $t$ , was



FIGURE 1.



Viscometer. (Scale  $\frac{1}{2}$ ).

measured by a "Smiths" stop watch to  $\pm 0.2$  sec.. The solution was diluted by known amounts of solvent added to compartment B. After mixing and temperature equilibration the flow-time for the diluted sample was determined. Normally five dilutions were made and the intrinsic viscosity,  $[\eta]$ , given by

$$[\eta] = \text{Limit (as } c \rightarrow 0) \text{ of } \left( \frac{t-t_0}{t_0} \right) / C ,$$

determined by extrapolating the plot of reduced viscosity to zero concentration. The usual procedures for maintaining glassware clean were carried out after each determination of intrinsic viscosity. All measurements were made at controlled temperature ( $\pm 0.005^\circ\text{C}$ ) in a stirred water thermostat (20 litre capacity, heated by a Robinson 250 W bulb (2" x 8") which was regulated by a Jumo contact thermometer and Sunvic electronic relay type EA4.

### 2.3.2. Infra Red End group analysis

By determining the ratio of the absorbance at 2.9  $\mu$ , due to O - H stretching, to the absorbance at 2.54  $\mu$ , due to the C-O-C stretching overtone, for a cold-pressed film it is possible to get a measure of the number-average molecular weight of a given polymer sample if the chain-end structures are hydroxyl groups. The Du Pont workers<sup>(47)</sup> derived the following relationship

$$\bar{M}_n = 15,700 \frac{\text{absorbance at } 2.54}{\text{absorbance at } 2.9 \mu}$$

The factor of 15,700 is based on independent osmotic pressure measurements and the assumption that each molecule has two hydroxyl chain-ends. The method was thoroughly examined. ~~Beer's~~ Lambert's Law was confirmed for both the O-H and C-O-C absorbances (Fig. 2). The effect of varying the pressure and time of pressing was also examined. The pressure determined the transparency of the film produced. Optimum precision ( $\pm 10\%$ ) was achieved if the following procedure was adopted.

15-20 mg. of powdered polymer, preferably just dried under high vacuum if the sample is a raw polymer, were pressed under vacuum ( $10^{-1}$  m.m. Hg.) at 10 tons per sq. in. by hydraulic press (Research and Industrial Instruments), for not less than 20 minutes. The transparent film produced in this way was then placed in a film holder and its infra-red spectrum was run on a Perkin Elmer spectrometer (Model 13, NaCl optics). The spectrum shown in Fig. 3 is typical. A varying base line is always obtained in the spectra of solids. This is due primarily to scattering of the incident radiation by solid particles with diameter comparable to the

FIGURE 2.

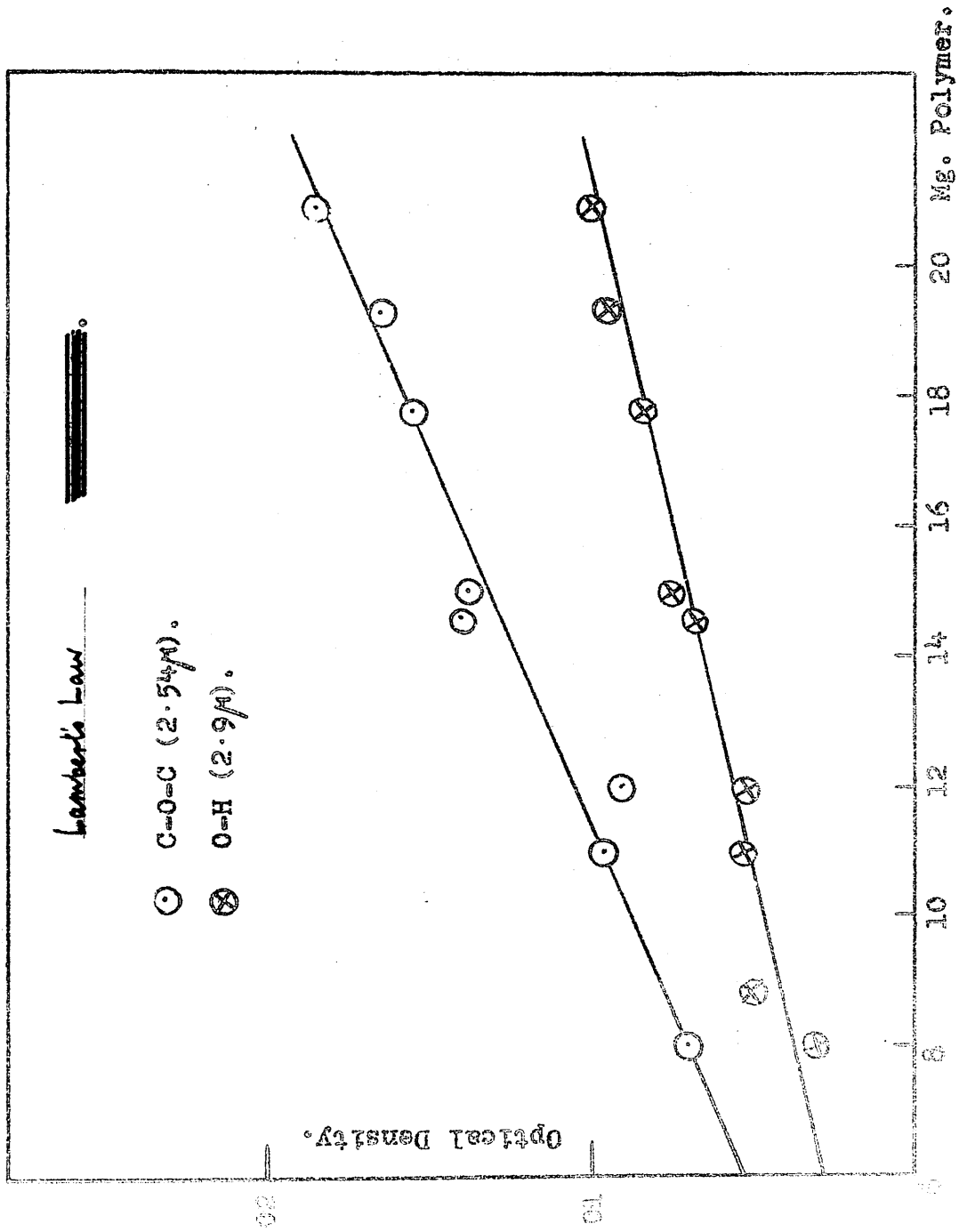
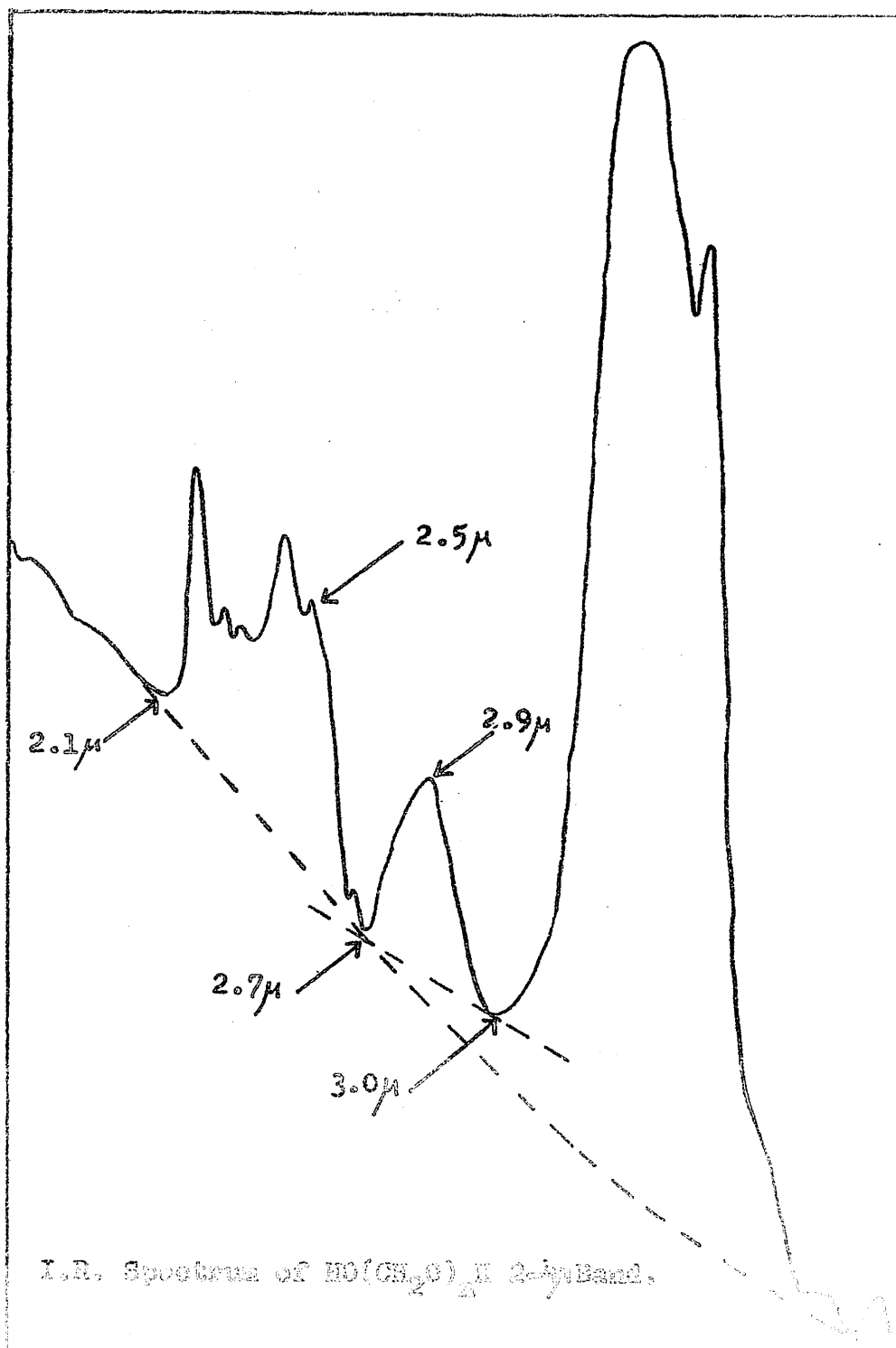


FIGURE 3.



30

wavelength of the incident radiation. In order to standardize the measurement of absorbance a base-line for the 2.5  $\mu$  band was drawn by connecting the minima at 2.1 and 2.7  $\mu$  and for the 2.9  $\mu$  band by connecting the minima at 2.7 and 3.0  $\mu$ <sup>(47)</sup>. The 2.9  $\mu$  band is broad and the band maximum was found to vary from 2.83  $\mu$  to 2.87  $\mu$ . Peak heights were used as a measure of absorbance because little improvement in precision was obtained by measuring the area under each peak. A similar procedure was adopted to characterize acetylated samples. The ratio of absorbance at 2.54  $\mu$  to the absorbance at 5.72  $\mu$  due to carbonyl stretching being used as a measure of molecular weight.

#### 2.4. Degradation Apparatus and Techniques.

##### 2.4.1. Introduction.

There are several approaches to the measurement of thermal degradation rates in high vacuum. In open systems, where the volatile products are pumped away from the reaction zone throughout the reaction, the instantaneous rate of reaction can be determined either by measuring the weight of the degrading polymer continuously or by measuring the transient pressure of the gaseous products as they are pumped away from the reaction zone.

This latter approach was adopted by Grassie and Melville who

developed the dynamic molecular still, (48) the modified form of which (49) was used in this work.

In closed systems, where the volatile products are allowed to accumulate as the reaction proceeds, the rate and extent of reaction are derived from pressure readings, either on a Bourdon gauge (50) or directly with a mercury monometer, taken at intervals throughout the reaction.

The open high vacuum system is the method preferred for the determination of rates of volatilisation because side reactions, pressure effects and ceiling-temperature effects, all of which have to be considered when using the closed system technique, are minimised.

#### 2.4.2. The Dynamic Molecular Still (D.M.S.)

The layout of the degradation apparatus is shown schematically in fig. 4. The still, S, the Pirani gauge, P, and the associated electrical circuits are shown in detail in fig. 5.

##### 2.4.2. (a) The Pirani gauge and the measurement of Rates of volatilisation.

Weighed polymer samples are placed in the weighed demountable copper tray which is then screwed to the copper heating block. The still is evacuated and at "zero pressure" ( $10^{-4}$  -  $10^{-5}$  m.m. Hg.) the Pirani bridge is balanced at a voltage,  $V_0$ , which is determined

Schematic Layout of Apparatus.

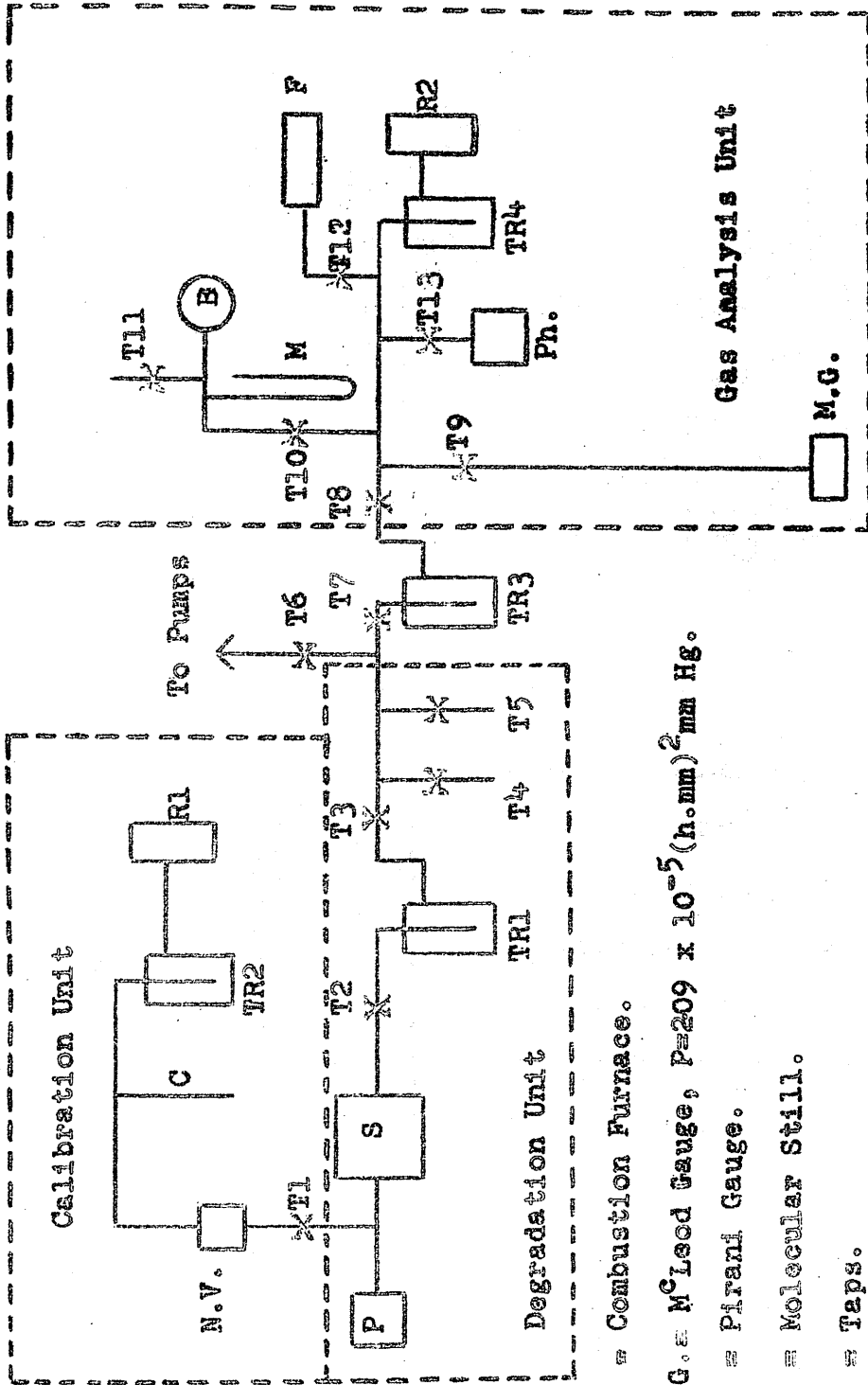


FIGURE 4.

F = Combustion Furnace.

M.G. = McLeod Gauge,  $P=209 \times 10^{-5} \text{ (h.mm)}^2 \text{ mm Hg.}$

P = Pirani Gauge.

S = Molecular Still.

T<sub>n</sub> = Taps.

C = 1 Ml. Graduated Tube. (Pyrex).

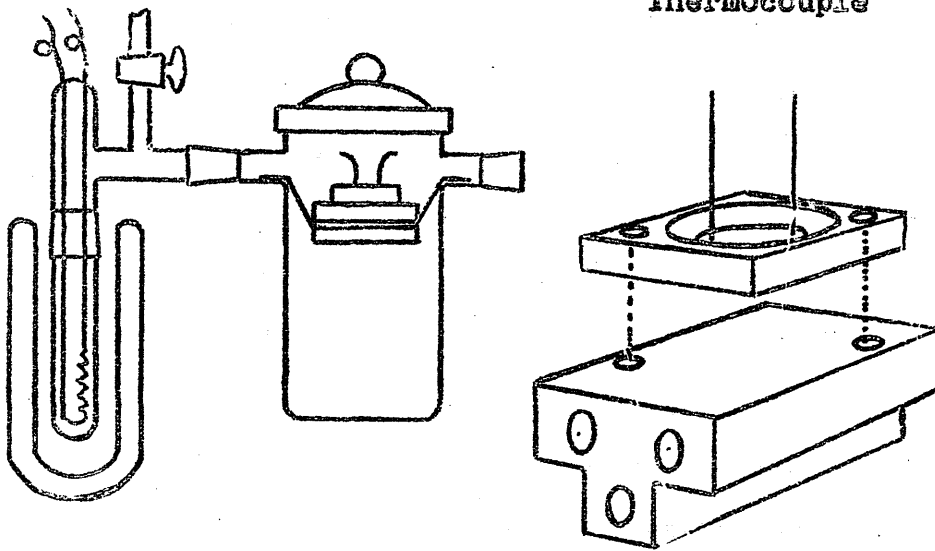
R = Reaction Tubes.

Ph. = Photolysis Apparatus.

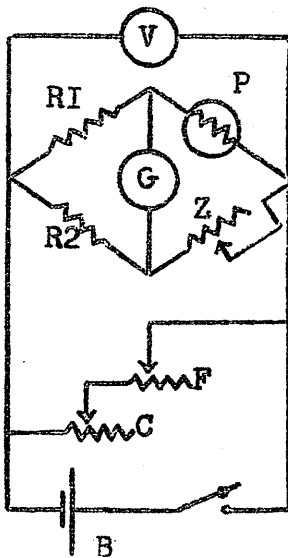
M = Manometer.



FIGURE 5



Thermocouple



R1 = 485 Ohms.

R2 = 510 Ohms.

P = Pirani gauge, 50 Ohms

B = Battery, 2 Volts.

C = Coarse control, 0-250 Ohms.

F = Fine control, 0-50 Ohms.

Z = Zero control, 0-50 Ohms.

V = Voltmeter, Sangamo-Weston,  
0-2Volts.

G = Pye "Spot" Galvanometer.

primarily by the required manometric sensitivity. The measurement of pressure by the Pirani hot-wire manometer depends on the fact that if the pressure of a gas in thermal equilibrium with a hot-wire is increased the temperature of the wire falls due to the increased conduction of heat away from the wire by the gas. The resistance of the wire falls and the bridge goes out of balance. The out of balance current can be used as a measure of the change in pressure or alternatively the bridge can be rebalanced by increasing the applied voltage which is then a measure of the new pressure. The latter procedure works over a wide range of pressure provided the molecular heat conduction varies with pressure. The parameters determining optimum performance have been discussed.<sup>(51)</sup> The gauge shown in fig. 5. was constructed from a 50  $\Omega$  piece of "osram" tungsten filament which was extended to 7.4 cms. and cold pressed between the beater ends of the supporting copper wires (20 gauge). The relationship between bridge voltage,  $V$ , at balance at a pressure,  $p$ , is derived as follows:

When the bridge is balanced the heat input to the pirani filament equals the sum of the conductive and radiative heat losses.

$$\text{Energy input to wire} = i^2 R = \left(\frac{V}{R}\right)^2 R = k_1 V^2$$

$$\text{Energy loss} = T_E [k_2 + k_3 f(p)],$$

where  $T_E$  = temperature excess of wire

$f(p)$  is a function of pressure

$T_E k_2$  = radiative heat loss;  $T_E k_3 f(p)$  = conductive heat loss.

At equilibrium

$$k_1 V^2 = T_E [k_2 + k_3 f(p)]$$

at  $p = 0$   $k_1 V_0^2 = T_E k_2$

$$k_1 V^2 = \frac{k_1 V_0^2}{k_2} [k_2 + k_3 f(p)]$$

$$= k_1 V_0^2 + \frac{k_1 k_3 V_0^2}{k_2} f(p)$$

$$\frac{V^2 - V_0^2}{V_0^2} = \frac{k_3}{k_2} f(p)$$

$(k_3/k_2)$  is determined by the gas.

$f(p) = K (V^2/V_0^2 - 1)$ ,  $K = k_2/k_3$ , is accurately linear up

to about 0.1 m.m. Hg. The temperature excess of the wire,  $T_E$ ,

i.e. the difference in temperature between the wire and the gauge

jacket, appears in the above derivation and for this reason the gauge

must be thermostatted. For convenience  $0^\circ\text{C}$  was chosen and a Dewar

flask of melting ice provided adequate thermostating. The

temperature dependence of the Pirani response was found to be

$dV/dT = -.006 \text{ V}/^\circ\text{C}$ . For this work  $V_0 = 0.500 \text{ Volt}$  was chosen

for two reasons. First it provided for adequate manometric

sensitivity and secondly the computation of  $(V^2/V_0^2 - 1)$  from

observed bridge voltage was facilitated.

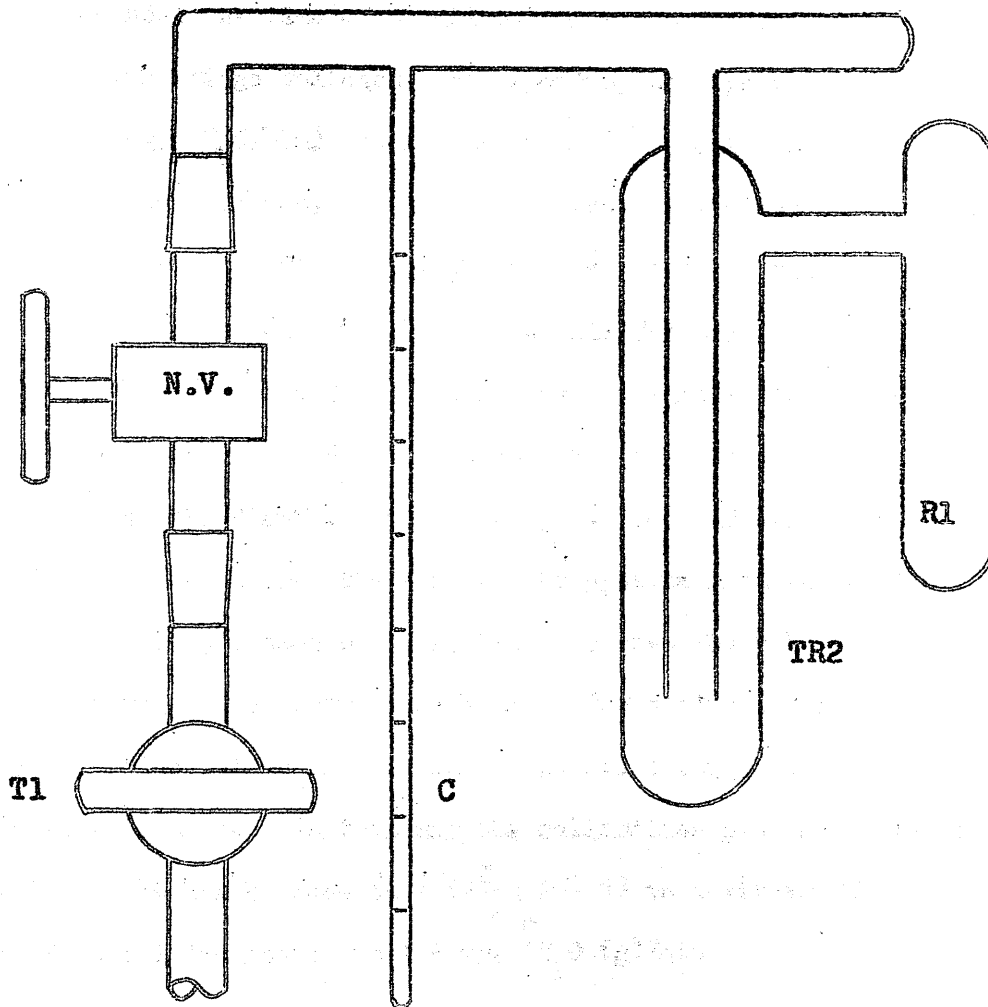
#### 2.4.2. (b) Calibration of the Pirani gauge

If the volatiles produced in thermal degradation are molecularly pumped at a constant rate to trap TR1 (Fig. 4) the transient pressure to which they give rise in the still is proportional to the rate of volatilisation and thus up to a transient pressure of 0.1 m.m. Hg. a linear relationship between rate of volatilisation and  $(V^2/V_0^2 - 1)$  should be observed. This relationship has been confirmed for many volatiles and it was confirmed for gaseous formaldehyde by the procedure described below.

The calibration unit shown schematically in fig. 4 is shown in detail in fig. 6. lg. of a high molecular weight polyoxymethylene was placed in reaction tube, R1, which was then sealed off. The unit was then pumped for one day. The trap, TR2, and calibrated tube, C, were flamed and tap, T1, and needle valve, NV, were closed. Some polymer was degraded at 180°C and the monomer produced trapped in TR2 at -196°C. When sufficient monomer had been prepared it was distilled at -80°C to C held at -196°C. When an adequate amount had been trapped in C TR2 was raised to room temperature and the unit was pumped again.

For a calibration run tube C was held at -80°C in an acetone /CO<sub>2</sub> mixture contained in a transparent Dewar flask.

FIGURE 6.

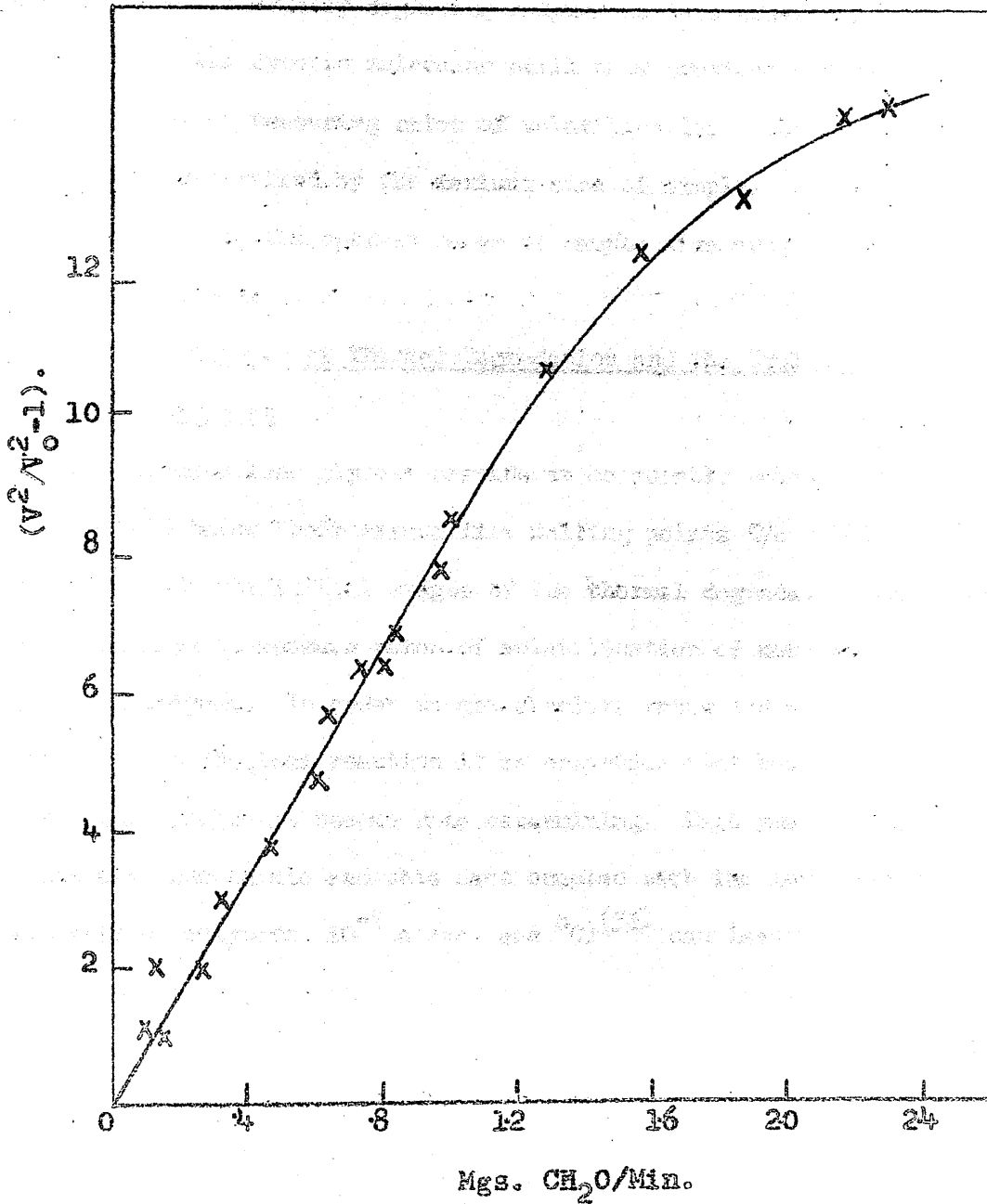


CALIBRATION UNIT.

A voltage,  $V$ , was applied to the Pirani bridge and the needle valve,  $NV$ , adjusted until the bridge was balanced. Equilibrium conditions were attained in less than a minute and the bridge was kept in balance throughout the time of a calibration run by adjusting the valve. For high bridge voltages, corresponding to high rates of flow (1 - 1.5 mg.  $CH_2O$ /min), 30 minutes was an adequate time to give a precise calibration. A calibration run was stopped by closing Tap,  $T1$ , and switching off the bridge current. About 2 minutes were allowed to ensure complete distillation of all monomer to trap,  $TR1$ , Taps,  $T2$  and  $T6$ , were closed and the monomer was distilled from trap,  $TR1$ , to a heavy walled 2m.m. bore Pyrex capillary tube attached to tap,  $T4$ . When the distillation was complete the capillary tube was sealed off and removed from the line and brought to room temperature. It was then weighed, broken open, heated to remove the polymerised monomer and reweighed at room temperature. The difference in the two weights is the weight of the monomer passed through the still in the calibration run. In this way the calibration plot shown in fig. 7 was obtained. It can be seen that  $(V^2/V_0^2 - 1)$  is a linear function of rate of volatilisation up to 1.5 mg.  $CH_2O$  (g)/min.

FIGURE 7.

Pirani Calibration Plot.



If the minimum significant change in Pirani bridge voltage is taken as 20 mV then the minimum detectable rate of monomer production from a thermally degrading polymer in this apparatus is 10  $\mu\text{g./min.}$  The dynamic molecular still thus provides a very sensitive means of measuring rates of volatilisation. The ultimate sensitivity is determined by the maximum size of sample. The factors determining the optimum range of sample size are discussed in the next section.

2.4.2.(c) The Kinetics of Thermal Degradation and the Evaluation of Activation Energies.

Polyoxymethylene glycols degrade at measurable rates some 30 to 40°C below their crystalline melting points (76 - 180°C). In order to study the initial stages of the thermal degradation reaction in detail we have to measure rates of volatilisation of monomer from a solid polymer. In order to get absolute rates and activation energies for the chemical reaction it is essential that heat and mass transfer should not become rate determining. Depolymerisation reactions are endothermic and this fact coupled with the low thermal conductivity of polymers ( $10^{-4}$  cal/cm. sec °C)<sup>(52)</sup> can lead to a cooling of the sample and a drop in the rate of reaction.

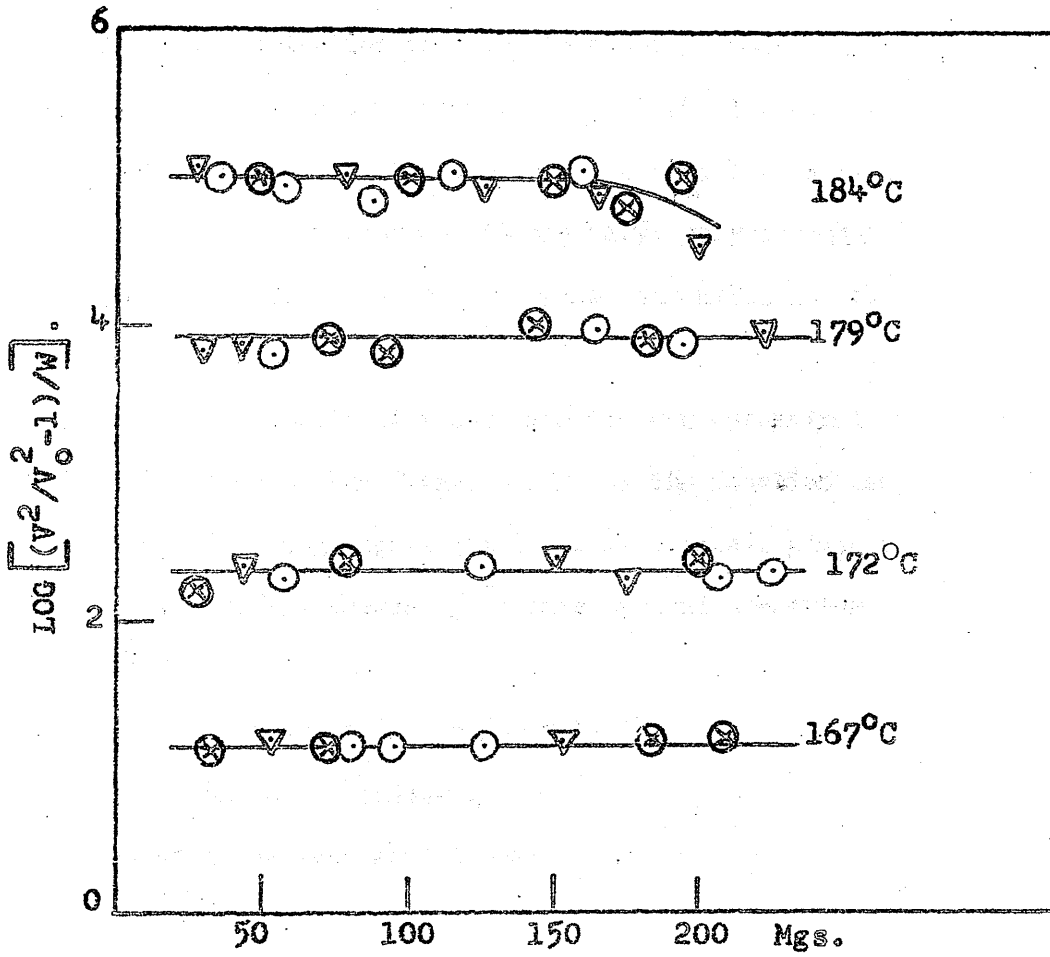


In polyoxymethylene this factor is potentially the more serious at high temperatures because, like polythene, its thermal conductivity decreases as temperature increases.<sup>(53)</sup> The rate of diffusion of monomer out of a solid crystalline polymer depends on the geometry and size of the particles and also the external pressure. If heat and mass transfer are rate controlling an increase in sample size leads to a fall in specific rate, defined as the rate per gram. By the same token it can be concluded that they are not rate determining in the region where specific rate is independent of the weight of the polymer sample. This point was thoroughly examined in the case of poly(methyl-methacrylate) degradation by Grassie and Melville<sup>(48)</sup> and a similar examination was undertaken in this study.

To ensure uniform heating each polymer sample was covered by 10 - 12 g. of 60 mesh copper powder (Hopkins and Williams). Figure 8 shows log (specific initial rate) versus sample weight,  $w$ , for a series of temperatures. This figure is based on the specific initial rates, expressed as  $(v^2/v_0^2 - 1)/w$ , of a series of different weights of the same polymer. The polymer was sieved and particle sizes from 80 up to 40 mesh were found to be present and in order to assess the effect of particle size on specific rate several runs with samples having particle sizes 40, 60 and 80 mesh were made and no change in specific initial rate greater than

FIGURE 8.

○ 40   ⊗ 60   ▽ 80 Mesh.



LOG(specific initial rate) Vs. Wt. for sample 7.

5% was observed. It can be seen from figure 8 that despite the fact that we are dealing with a solid polymer heat and mass transfer present no serious drawback to the measurement of rates of volatilisation of formaldehyde from degrading polyoxymethylene. This may be due to the fact that the polymer is crystalline and, because the polymerisation reaction is heterogeneous, the chain ends, where the depolymerisation reaction is initiated, are at the surface of the crystallites. Geometrically, then, the polymer is in complete contrast to the vinyl polymers which are usually amorphous with the polymer chains entangled and chain-ends buried in the polymer mass.

The initial rate of volatilisation was determined by noting the voltage on the Pirani bridge as the reaction temperature was reached. Plotting  $\log$  (initial specific rate), given by  $\log [(V^2/V_0^2 - 1)/w]$ , versus  $1/T^\circ K$  gave typical Arrhenius plots of slope  $\theta$ .

The energy of activation  $E_a$ , is given by

$$E_a = 4.575 \tan \theta$$

This equation is derived as follows:

For an  $n^{\text{th}}$  order reaction

$$\text{Rate} = k(w)^n = A. e^{-E_a/RT} (w)^n$$

if the Arrhenius law holds,

$$\ln (\text{Rate}) = \ln A \cdot (w)^n - E_a/RT$$

$$\ln \frac{\text{Rate}_1 A_2 W_2^n}{\text{Rate}_2 A_1 W_1^n} = \frac{E_a}{R} \left( \frac{1}{T_2} - \frac{1}{T_1} \right) \quad (1)$$

Assuming that over the small range of degradation under consideration

$A_1 = A_2$ ;  $W_1 = W_2$  equation (1) becomes

$$\ln \frac{(\text{Rate}_1)}{(\text{Rate}_2)} = \frac{E_a}{R} \left( \frac{1}{T_2} - \frac{1}{T_1} \right) \quad (2)$$

$$E_a = \frac{1.987}{0.4343} \cdot \log \frac{(R_1/R_2)}{(1/T_2 - 1/T_1)} = 4.575 \tan \theta$$

where  $\theta$  is the slope of  $\log_{10} (\text{Rate})$  versus  $1/T^\circ\text{K}$  plot.

Activation energies were also determined by noting the Pirani voltage and temperature as the heating blocks cooled after a run. Accurate temperature measurement is essential in determining activation energies and this was achieved by using Copper-constantan thermocouples (Fig. 5). The cold junction was immersed in a tube, (1 cm. bore) filled with silicone oil, which was placed in a Dewar flask containing melting ice. The temperature readings are accurate

to  $\pm 0.2^{\circ}\text{C}$ .

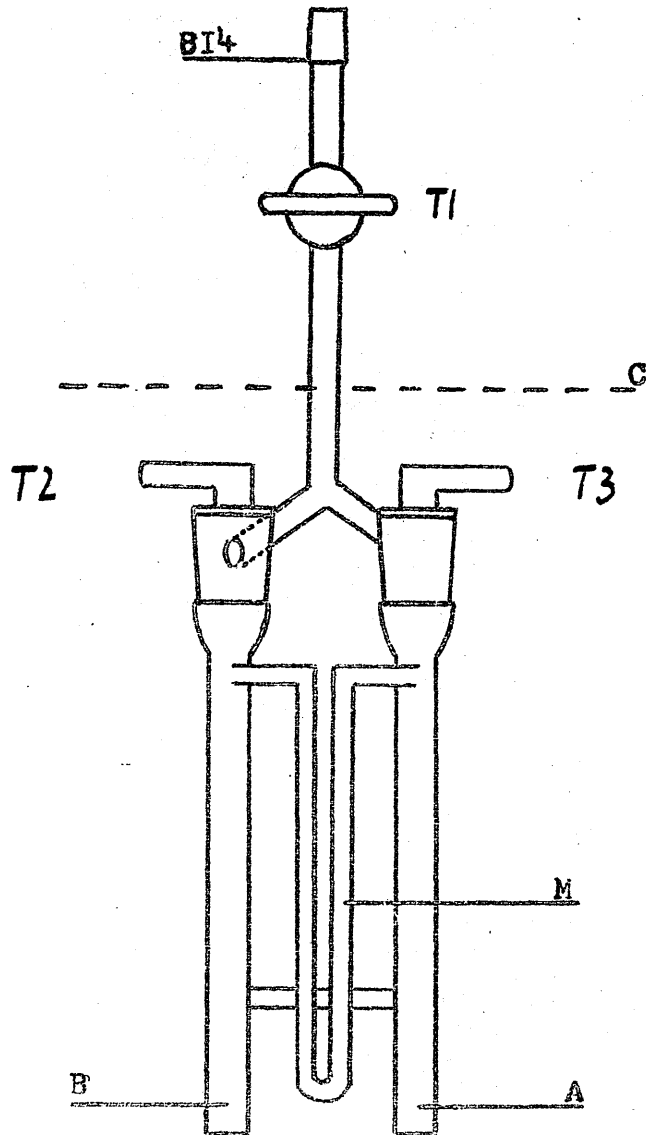
To determine the extent of reaction the weight of residual polymer was determined by weighing the demountable copper tray after an appropriate cooling time. Alternatively, the rate versus time curve was plotted on large graph paper and integrated by planimeter. This procedure is more tedious and was used mostly as a check on mass balances. The extent of the reaction was checked by distilling the monomer produced from Trap, TR1, to a heavy wall 2 m.m. bore capillary tube attached to tap, T4, sealing off the tube and carrying out the weighing procedure described in 2.3.2. (b) above.

#### 2.4.2. (d) Vacuum Manometric Apparatus

Since formaldehyde is a gas (B.pt.  $-19^{\circ}\text{C}$ ) it is possible to follow the course of the degradation of very small amounts of polymer very precisely by allowing the monomer to accumulate in a closed evacuated system and measuring its pressure directly by a manometer.

The apparatus shown in figure 9 was constructed from Pyrex tubing, Springham high vacuum single pump stopcocks and 2.8 m.m. bore capillary tubing. The volume of A was determined by filling the compartment with mercury and part of a manometer to a point which was noted and weighing the mercury. A suitable amount

FIGURE 9.



VACUUM MANOMETRIC APPARATUS.

SCALE 3:1

of mercury for the manometer was established. An expression relating the "zero - pressure" volume,  $V_0$ , of A to the volume when the compartment contains a gas at pressure  $h$  cms. Hg. was determined as

$$V = (V_0 + 0.0675 h) \text{ c.c.},$$

where  $h$  is the difference in height of the mercury columns and  $V_0 = 43.36$  c.c.

All pressures were converted to pressures,  $P_0$ , in volume,  $V_0$ , using the following Boyles Law expression

$$P_0 = \frac{h F(\rho) (V_0 + 0.0675 h)}{V_0 T} .298,$$

where  $h$  = height of mercury column at temperature  $T^\circ\text{K}$ .

$$F(\rho) = \int_{\text{Hg}} (298^\circ\text{K}) / \int_{\text{Hg}} (T^\circ\text{K})$$

converts the  $h$  values to standard pressures at the given temperature  $T^\circ\text{K}$  and takes account of the small change in the density of mercury,  $\rho_{\text{Hg}}$ , with temperature. The coefficient of cubical expansion of glass is considered to be negligible.

At  $184^\circ\text{C}$  a height of 2.09 cms. Hg corresponds to 100% depolymerisation of 1 mg. of polymer. The apparatus is therefore very sensitive and since  $h$  can be measured to  $\pm .01$  m.m. by cathetometer (Precision Tool and Instrument Co.) the technique is almost as sensitive as the dynamic molecular still.

Procedure for measuring Rates of Degradation

1 - 10 mg. of polymer were placed in compartment A and covered with an accurately weighed 4g Cu powder. The required amount of mercury (22.4 g.) was placed in compartment B. The taps were greased with silicone high vacuum grease (Edwards High Vacuum Ltd.) and the apparatus was evacuated. The manometer tube was flamed. The mercury was thoroughly degassed by freezing in liquid nitrogen and thawing, twice. Taps T1, T2, T3, were closed, the apparatus removed from the vacuum line. The mercury was allowed to flow into the manometer and then the whole apparatus, up to line C, was placed in a stirred thermostat tank containing silicone oil (Hopkins and Williams type MS 550). The thermostat comprised two concentric cylindrical Pyrex glass tanks, the inner one had a capacity of 10 litres the outer 15 litres. The inner tank sat on four cork rings placed in the bottom of the outer tank. The oil was placed in the inner tank and the annular air space provided thermal lagging. The tank was heated by a 500 W fused silica immersion heater (Thermal Syndicate Ltd.) fed by a Variac transformer which was operated continuously. Temperature control was effected by a similar heater, 250 W, switched by a Sunvic EA4 electronic relay activated by a Jumo contact thermometer. At 184°C temperature control was  $\pm 0.1^\circ\text{C}$ , as measured by Copper-constantan



thermocouple.

It was found that polymer samples can be brought to high reaction temperatures very quickly by immersing the apparatus in the tank held at the appropriate temperature. Thus, a 10 mg. polymer sample in the form of a cold-pressed disc without copper powder melted ( $180^{\circ}\text{C}$ ) 3 minutes after the apparatus was immersed in the tank at  $190^{\circ}\text{C}$ . However, fully 5 to 7 minutes were usually required for the tank to return to thermal equilibrium there being a drop of about  $1\text{C}^{\circ}$  after immersion of the manometric apparatus.

The leak rate of the apparatus was checked in blank runs and also by observing the pressure for 1 to 2 hours after the calculated  $P_{\infty}$ , corresponding to 100% reaction, had been achieved. The leak was always negligible. An exhaustive test showed that this apparatus began to leak slowly only after 4 days continuous immersion in the silicone oil bath at  $200^{\circ}\text{C}$ . Care in greasing the taps was of prime importance and the use of single pump taps is an essential design feature for the successful operation of the apparatus under these conditions.

The  $P_{\infty}$  values observed in this apparatus were found to be within  $\pm 0.2$  to  $\pm 0.5\%$  of the value calculated for 100% gaseous monomer behaving as an ideal gas.

### Catalysis and Inhibition Experiments

The vacuum manometric apparatus was also used in a series of experiments designed to determine the effect of various substances on the rate of the thermal degradation. The polymer sample was ground with the substance being considered and then placed in compartment A. The procedure described above was followed, the oil tank temperature chosen was 184°C. The choice of 184°C was determined primarily by the need to get the "catalyst" or "inhibitor" as intimately mixed with the polymer sample as possible and this is more likely to occur with the molten polymer.

The effect of the substances listed in Table 2.1 on the rate of the thermal reaction at 184°C was examined.

TABLE 2.1

KCl

NaOCH<sub>3</sub>

NaOCOCH<sub>3</sub>

Ph<sub>3</sub> C Cl

D.P.P.H. (~~Di~~phenyl picryl hydrazyl)

1:4 diamino anthraquinone.

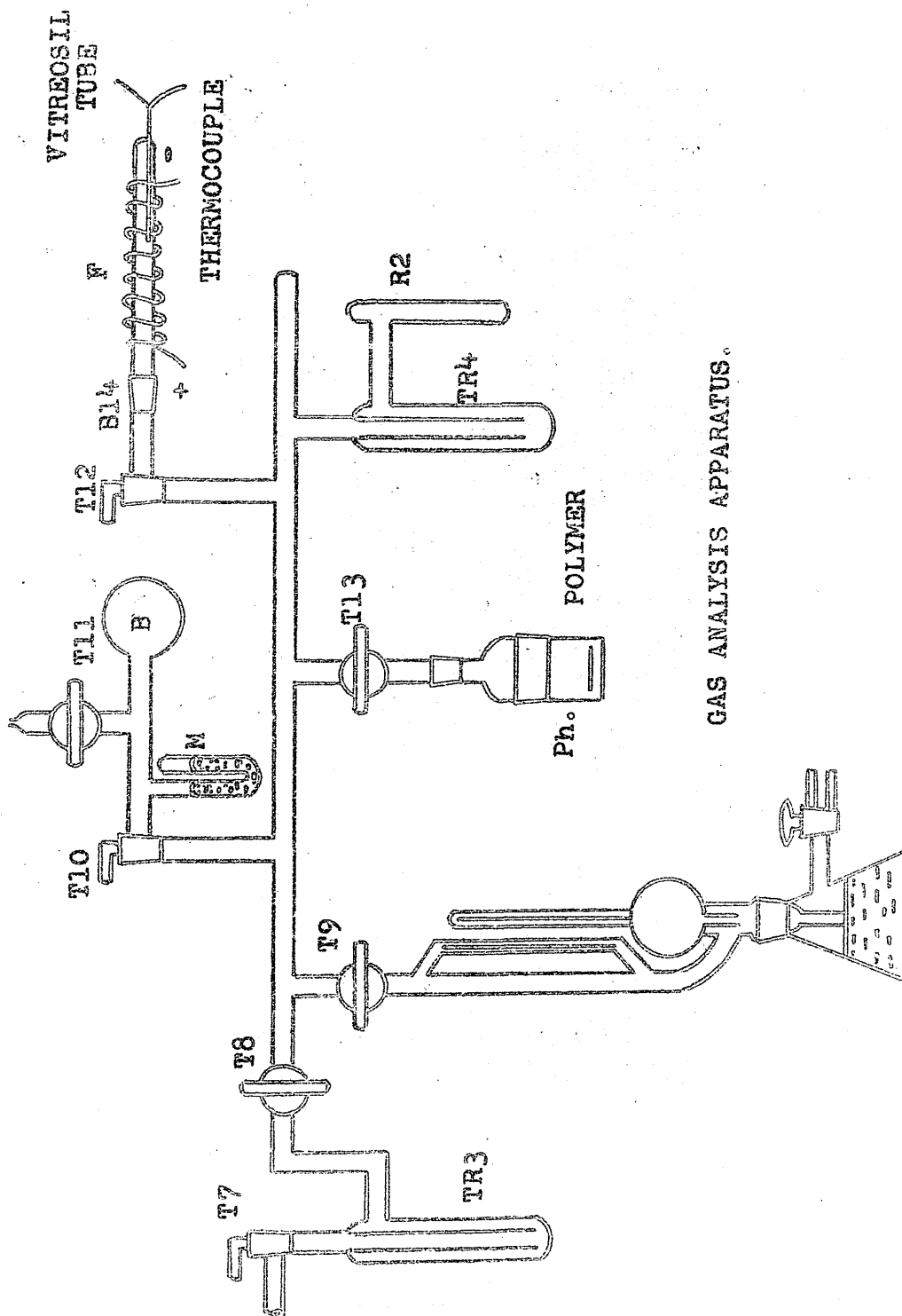
AR reagents were used where available. All the salts were heated in vacuum to 150°C before use. The triphenyl chloromethane was recrystallised from anhydrous diethyl ether. The D.P.P.H. was used as received (Aldrich Chemical Co.) (M. pt. 137°C). The 1:4 diaminoanthraquinone was received from Dr. Grassie.

### 2.5 Gas Analysis Apparatus.

As will be shown later (Chapter 5) a discussion of the mechanism of the chain-end initiated thermal depolymerisation of polyoxymethylene glycols led us to consider product analysis in more detail. In particular the possibility that hydrogen might occur among the products was considered. If it did occur it would almost certainly not contribute more than 0.1% to the total weight of reaction products since all the earlier work clearly suggests that the reaction gives quantitative yields of monomer and water. Clearly a micromethod of analysis is required and the apparatus, shown schematically in Figure 4 and in more detail in Figure 10, was used.

This apparatus provides for the measurement of very small pressures ( $10^{-5}$  to  $5 \times 10^{-2}$  m.m. Hg.) of non-condensable gases and also for their combustion in the silica furnace, F. Both copper oxide and iodine pentoxide were used as oxidising agents.

FIGURE 10.



CuO (B.D.H. Microanalytical Reagent) at  $300 \pm 5^\circ\text{C}$  will oxidise CO and  $\text{H}_2$  and at  $350^\circ\text{C}$   $\text{CH}_4$  as well.  $\text{I}_2\text{O}_5$  (B.D.H. Microanalytical) selectively oxidises CO at  $120 - 150^\circ\text{C}$ .<sup>(54)</sup> In order to analyse the products of the vacuum photolysis of the polymer ( $\text{CH}_2\text{O}$ ,  $\text{H}_2$ , CO) a fused-silica cell (Thermal Syndicate) was attached at tap, T13.

#### Calibration of the Apparatus.

The apparatus was calibrated for quantitative work as follows. With all taps except T11 and T13 open the apparatus was evacuated to  $10^{-6}$  m.m. T8 and T10 were then closed,  $\text{N}_2$  was introduced into section B via T11 and its pressure noted on the manometer, M. T10 was then opened and the new pressure of  $\text{N}_2$  noted. This procedure was repeated at two other initial pressures. The volume of the whole apparatus was then calculated using Boyle's Law and the volume,  $V_0$ , of section B, which had been determined before it was attached to the apparatus as

$$V = V_0 + 0.42 p; \quad \text{where } V_0 = 47.44 \text{ mls. and } p = \text{cms. Hg.}$$

$V_0$  is the "zero pressure" volume of section B and  $p$  is the pressure of  $\text{N}_2$  in cms. Hg. as read on M. The total volume of the apparatus, with T8, T10, and T13 closed, was found to be in the region of 400 mls. It varied from run to run because the reaction tube, R2, was renewed each time.

The reaction tube, R2, was heated in a Wood's metal bath, controlled by an Ether "Transitrol" temperature controller. The combustion furnace, F, was heated by a nichrome wire wound round the thermocouple and insulated from it by asbestos paper. The temperature of the furnace was adequately controlled ( $\pm 2^{\circ}\text{C}$ ) by a Variac transformer.

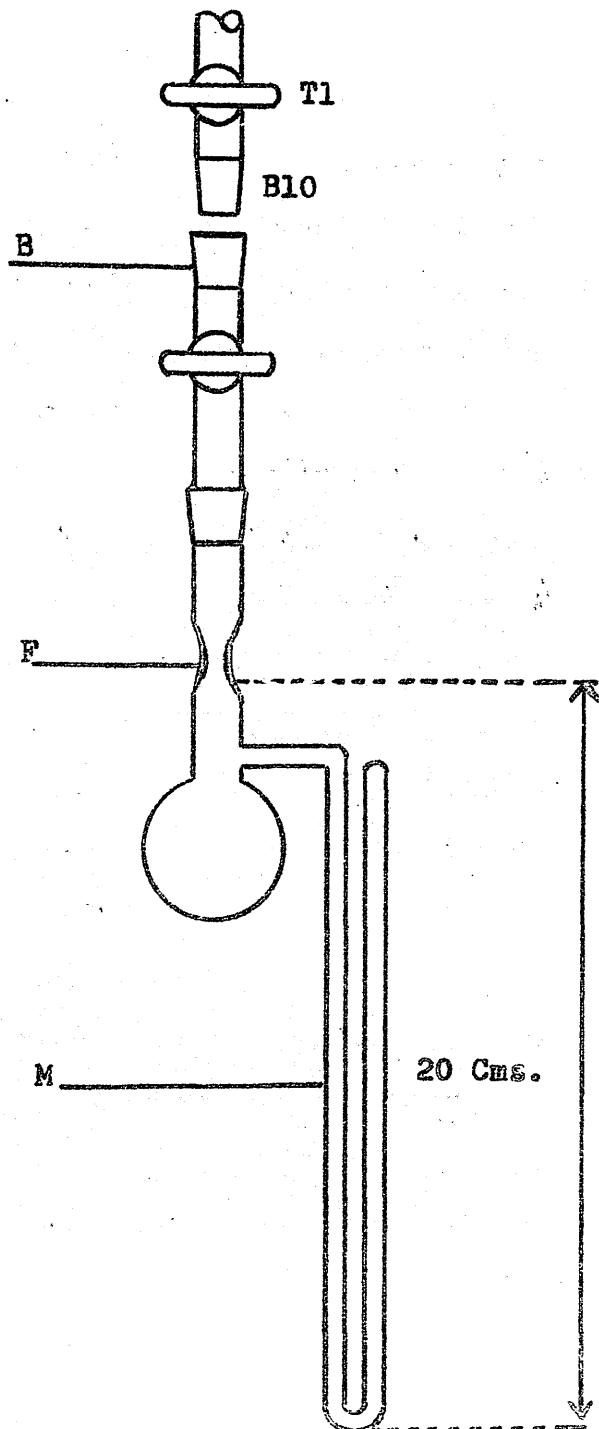
With trap, TR4, held at liquid  $\text{N}_2$  temperature ( $-196^{\circ}\text{C}$ ) the only gases which will register a pressure in the McLeod gauge are  $\text{H}_2$ ,  $\text{CO}$ ,  $\text{CH}_4$  and  $\text{C}_2$  hydrocarbons. In order to identify the non-condensables produced in a reaction it is necessary to oxidise them and then measure the pressure at  $-80^{\circ}\text{C}$  after oxidation. If only  $\text{H}_2$  is present in the non-condensable fraction of the products no pressure will be observed at  $-80^{\circ}\text{C}$  whereas  $\text{CO}$ ,  $\text{CH}_4$  will yield equivalent pressures of  $\text{CO}_2$  at  $-80^{\circ}\text{C}$  and  $\text{C}_2$  hydrocarbons will yield twice the equivalent pressure of  $\text{CO}_2$  at  $-80^{\circ}\text{C}$ .  $\text{CO}$  and  $\text{CH}_4$  can be differentiated by the selective oxidation of the former by  $\text{I}_2\text{O}_5$  at  $120^{\circ} - 150^{\circ}\text{C}$ . The presence of  $\text{CH}_2\text{O}$  among the products causes a slight complication because it has a partial vapour pressure of about 21 m.m. Hg. at  $-80^{\circ}\text{C}$  and would lead to errors in the interpretation of the pressures at  $-80^{\circ}\text{C}$  in terms of  $\text{CO}_2$  produced in the combustion. Similarly any  $\text{CO}_2$  produced in the polymer degradation reaction would cause ambiguity. This complication is remedied as follows.

After the polymer degradation, thermal or photolytic, has been stopped T8, which is kept closed during the degradation, is opened to trap, TR3, T7 having been previously closed. The drop in pressure of non-condensables is noted. The trap TR4 is then brought to room-temperature and all material condensable at  $-196^{\circ}\text{C}$  is transferred to TR3 held at  $-196^{\circ}\text{C}$ . When the transfer is complete TR4 is again brought to  $-196^{\circ}\text{C}$  and T8 is closed. The pressure of non-condensable material is again noted, the percentage lost by opening T8 calculated and the oxidation carried out. The oxidation with CuO at  $300^{\circ}\text{C}$  was very efficient usually taking about 30 minutes; with  $\text{I}_2\text{O}_5$  at  $140^{\circ}\text{C}$  the oxidation usually took 45 to 60 minutes. The oxidation was judged complete when the pressure reached a steady value which invariably corresponded to the initial pressure obtaining at the beginning of the degradation run. Since all runs were not less than 3 hours in duration a satisfactory leak-rate and also thorough degassing of the apparatus, polymer and oxidising agent had to be ensured. Each run was usually preceded by at least one full day's pumping and overnight degassing.

## 2.6 Equilibration Apparatus

In order to measure the pressure of monomer in equilibrium with polymer at a given temperature the apparatus shown in Figure 11 was used. The required amount of mercury was added to the bulb and

FIGURE 11.



EQUILIBRIUM APPARATUS.



the whole assembly was evacuated. The manometer tube, M, was flamed several times. The mercury was thoroughly degassed [see section 2.4.2. (d)], tap, T1, was closed and the assembly removed from the vacuum line at joint B. The mercury was then transferred under vacuum to the manometer, M. The vacuum was released and as quickly as possible the required amount of polymer was placed in the bulb. The apparatus was again evacuated and pumped continuously for two days. For a further 4 hours the polymer was pumped at 40°C to ensure complete degassing. One sample (Chapter 3, sample B) was 50% degraded at 170° while still being pumped. When all pretreatment of the sample was complete the apparatus was sealed off at the constriction, F. The apparatus was then submerged in the silicone oil thermostat tank, described in section 2.4.2. (d), held at the equilibration temperature. The pressure of monomer was measured periodically and the system was considered to have reached equilibrium if the pressure remained constant for two days. A routine time of 5 days at each temperature was adopted. The highest temperature was selected first and the temperature dropped periodically throughout the experiment. Because of the time scale involved in this experiment three equilibration tubes were prepared and run at the same time. The pressure was read, with the thermostat stirrer switched off, by Cathetometer (Precision Tool and Instrument Co. Ltd.). All pressure readings were converted to m.m. Hg. at 20°C.

## 2.7 Measurement of Polymer density

The density of polymer powders was determined by a pycnometric method using a 0.5% solution of 'Teepol' in distilled water. The procedure adopted was as follows.

50 - 60 mg. of polymer powder were accurately weighed into a calibrated pycnometer (Vol. = 10.0399 mls at 25°C), and about 5 mls. of the 'Teepol' solution placed in the pycnometer. When the powder had been wetted it sank to the bottom of the pycnometer and the pycnometer was then filled and placed in a water thermostat bath controlled at 25° ± .005°C. After 2 hours in the thermostat the surface of the pycnometer was carefully dried and the pycnometer weighed. The polymer density at 25°C,  $\rho_p^{25^\circ}$ , was calculated from

$$\rho_p^{25^\circ} = W_p / (V_o - WT / \rho_T^{25^\circ}),$$

where  $W_p$  = weight of the polymer  
 $V_o$  = volume of the pycnometer (10.0399 mls.)  
 $WT$  = weight of 'Teepol' solution  
 $\rho_T^{25^\circ}$  = density of 'Teepol' solution = 0.99626<sub>5</sub>  
at 25°C.

$$(\rho_{H_2O} = 0.99707_3).$$

## 2.8 Photochemical Techniques

Polymer samples in the form of cold-pressed films (15-20 mg.), suitable for infra-red examination (section 2.3.2.), were irradiated with ultra-violet light either in air or in high vacuum in a fused silica cell attached to tap, T13 (Fig. 10). Two light sources were used.

(a) 30-Watt Hanovia "Chromatolite" lamp.

More than 85% of the output of the low pressure mercury arc employed in this lamp is due to the resonance line at 2537 Å. About a further 10% of the output is due to the 1849 Å, resonance line but since this wavelength is effectively absorbed by 1 cm. of air the lamp is for practical purposes regarded as a source of monochromatic 2537 Å radiation.

(b) 125-Watt Osram - MB lamp.

All the light below 3200 Å produced by the medium pressure mercury arc employed in this lamp is absorbed by the lead glass envelope and of the remaining ultraviolet output the 3650 - 3663 Å lines comprise the major part. Several visible lines are also emitted.

The two sources were used to compare the effect on the polymer of 3650 - 3663 Å radiation with that produced by 2537 Å

radiation. The output of each lamp was determined by N.A. Weir.<sup>(55)</sup>

The relevant information is given in Table 2.2.

TABLE 2.2.

Output of Ultraviolet light sources

<u>Lamp</u>	<u><math>\lambda(\text{\AA})</math></u>	<u>Output</u>
Hanovia	2537	$3.1 \times 10^{-9}$
Osram	3650	$2.5 \times 10^{-8}$
	3663	$4.6 \times 10^{-9}$
	4046	$9.65 \times 10^{-9}$
	4077	$9.65 \times 10^{-9}$
	4339	$5.7 \times 10^{-9}$
	4357	$3.16 \times 10^{-9}$

2.9 Preparation of Perfluoroacetone hydrate.

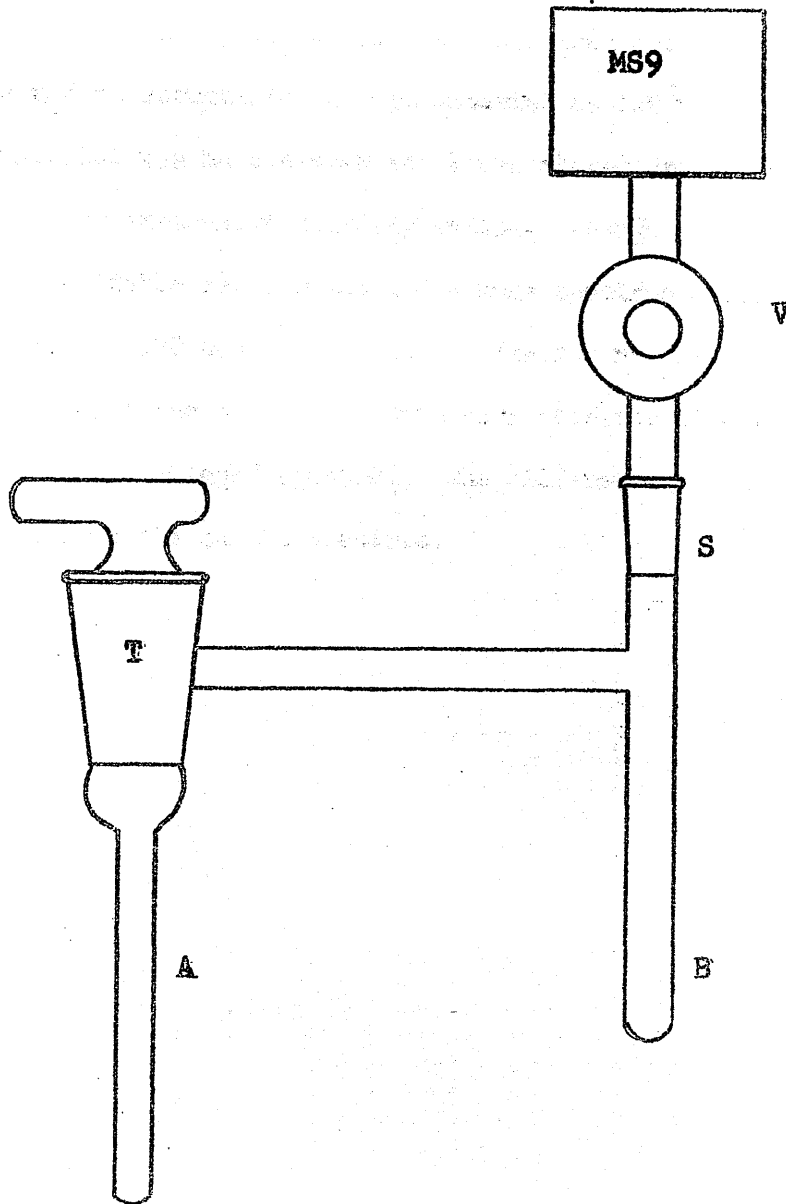
Gaseous perfluoroacetone (B.pt.  $-28^{\circ}\text{C}$ ) (Chemicals Procurement Laboratories, Inc. New York.) was bubbled into ice cold distilled water contained in a train of three 1 litre capacity round bottomed flasks. The hydration of the gaseous ketone is a smooth, efficient and exothermic reaction giving quantitative yield of the pure hydrate,  $(\text{CF}_3)_2\text{C}(\text{OH})_2$  (M. pt.  $43 - 44^{\circ}\text{C}$ .) The pure hydrate has not been characterised before and is discussed in Appendix I.

The purity of a given sample was determined by making up a 1% aqueous solution of the solid in distilled water and titrating 25 ml. portions to a potentiometrically determined end-point with standard N/10 NaOH (B.D.H. Volumetric Solution).

#### 2.10 Mass Spectrometric product analysis.

The volatile products of thermal degradation of samples 6 (DIST/3244/87-P) and sample 7 (DIST/3244/87-OAc) produced at temperatures in the range 100 - 190°C were introduced directly into the sample inlet system of an AEI-MS9 double focussing mass spectrometer using the apparatus shown in Figure 12. 1 - 5 mg. of polymer were placed in tube A; tap, T was greased and placed in position and the whole apparatus evacuated via socket, S. The apparatus was pumped at  $10^{-5}$  mm. Hg. for 30 minutes, tap T was closed, the apparatus removed from the vacuum-line and attached to the B14 inlet cone of the spectrometer. The spectrometer inlet valve V, was opened to the spectrometer vacuum system and the apparatus up to tap T was pumped to  $10^{-6}$  -  $10^{-7}$  m.m. Hg. The tube A was then immersed in a Wood's metal bath which had previously been brought to the degradation temperature. The following procedure for sampling the volatile products was adopted. With valve, V, closed and tap, T, open a pressure of volatiles was allowed to accumulate. The sensitivity of the

FIGURE 12.



APPARATUS FOR MASS SPECTROMETRIC PRODUCT ANALYSIS.

instrument is such that  $10^{-6}$  -  $10^{-5}$  mm. Hg. of volatiles is adequate for analysis so that, for example, no more than about 5 minutes is required to accumulate enough material at  $100^{\circ}\text{C}$ . When sufficient material had accumulated tap T was closed and valve, V, opened to the instrument sampling system, enough sample was taken to give a suitable ion current and a mass spectrum was run. The mass range 1 - 120 was investigated. Instrument "blanks" were run and all peaks on the sample spectrum were compared with the corresponding peak on the "blank" spectrum. The difference of the two spectra was taken as the sample spectrum.

CHAPTER 3

The Thermodynamic Properties of Polyoxymethylene and their  
relation to the thermal stability of the polymer

3.1 Introduction

The thermodynamic stability of a polymer is determined by the Gibbs Free Energy of polymerisation,  $\Delta G_{gc}^{\circ}$  which is given by

$$\Delta G_{gc}^{\circ} = \Delta H_{gc}^{\circ} - T\Delta S_{gc}^{\circ}, \quad \text{where}$$

$\Delta H_{gc}^{\circ}$  is the heat of polymerisation of gaseous monomer (g) at 1 atmosphere ( $^{\circ}$ ) to condensed (C), crystalline ( $^{\circ}$ ) polymer.

$\Delta S_{gc}^{\circ}$  is the entropy of polymerisation.

Because of the difficulties encountered in evaluating entropies it has become common practise to consider the  $\Delta H$  terms in isolation. Justification for this less rigorous approach can be sought in the fact that, for olefinic compounds, the entropy contribution to the free energy of polymerisation is fairly constant lying in the narrow range of 7 - 10 K cal $^{-1}$  mole $^{-1}$  (56). The variations in  $\Delta G$  for the various olefinic monomers are thus reflected in the  $\Delta H$  values and it is therefore reasonable to use  $\Delta H$  values to establish a thermodynamic scale of polymer stability.



Thus it is generally true that the lower the value of  $\Delta H$  the more readily will a polymer depolymerise. The rate of depolymerisation is also determined by the heat of polymerisation since the activation energy,  $E_d$ , for depropagation is related to  $\Delta H$  by the expression  $E_d = E_p - \Delta H$ , where  $E_p$  is the activation energy for the polymerisation propagation reaction. Since  $E_p$  values are low, 3 - 5 K.cals mole<sup>-1</sup> for radical polymerisation reactions, the value of  $E_d$  will in general be largely determined by that of  $\Delta H$ .

For vinyl polymers it has been established that, generally, those which give high yields of monomer on thermal degradation have heats of polymerisation around 10 K. cal. mole<sup>-1</sup> and those which give little or no monomer have heats of polymerisation around 20 k. cal. mole<sup>-1</sup>. Because the depolymerisation reactions of vinyl polymers are free-radical processes exceptions to the above generalisations, based on  $\Delta H$  value, arise in situations where the free radical intermediates are resonance stabilised and hence less reactive in transfer reactions which tend to reduce the yield of monomer. A good example is provided by polystyrene ( $\Delta H = 17$  K. cal. mole<sup>-1</sup>) which yields about 65% monomer although its  $\Delta H$  value would suggest that the monomer yield would be low.

The same sort of generalisation should be applicable to a discussion of the stability of carbonyl polymers. It is reasonable to argue, therefore, that the quantitative yield of monomer obtained in the thermal degradation of polyoxymethylene is due to the fact that  $\Delta H^{\circ}_{gc}$  has a low value. The exact value of this quantity is in doubt and it merits some discussion.

### 3.2. The Heat of Polymerisation of gaseous Formaldehyde - $\Delta H^{\circ}_{gc}$ .

#### 3.2.1. Introduction

No accurate calorimetric determination of  $-\Delta H^{\circ}_{gc}$  for the polymerisation of formaldehyde has been reported. There are several ways of estimating this quantity (Sect. 3.2.2.). In the case of polyoxymethylenes with hydroxyl chain-ends  $\Delta H^{\circ}_{gc}$  can be determined from the pressure of monomer in equilibrium with the polymer (Sect. 3.2.3.).

#### 3.2.2. Estimation of $\Delta H$ for polymerisation of formaldehyde.

Three quite independent estimates of  $\Delta H$  can be made.

(a) A lower limit to the heat of polymerisation is given by the heat of solution of gaseous formaldehyde in polar solvents which was determined fairly accurately by Walker<sup>(57)</sup> who found the values shown in Table 3.1.

TABLE 3.1

Heat of Solution of Gaseous Formaldehyde

<u>Solvent</u>	<u><math>-\Delta H, \text{K. cal} \text{ mole}^{-1}</math></u>
H <sub>2</sub> O	14.8
CH <sub>3</sub> OH	15.0
nC <sub>3</sub> H <sub>7</sub> OH	14.2
nC <sub>4</sub> H <sub>9</sub> OH	14.9

Average 14.7

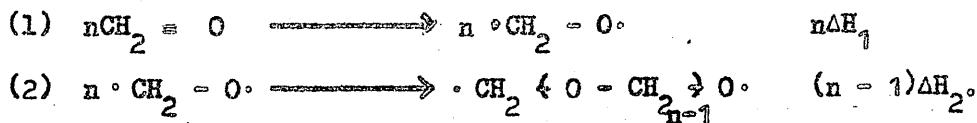
The solution of formaldehyde in these solvents leads to the formation of semiformals, HO-CH<sub>2</sub>-OR, where R = H; CH<sub>3</sub>; C<sub>3</sub>H<sub>7</sub>; C<sub>4</sub>H<sub>9</sub>; and since this involves opening the carbonyl double bond, a process which must occur in the polymerisation of formaldehyde, Walker agreed that a value in the region of 15 k. cal represents a reasonable estimate of the heat of polymerisation.

(b) An estimate of  $\Delta H_{\text{gc}}^{\circ}$  can also be made from existing thermochemical data since it represents the difference between the heat of combustion of polymer,  $\Delta H_{\text{c}}^{\text{POM}}$ , and the heat of combustion of monomer,  $\Delta H_{\text{c}}^{\text{CHO}}$ . Generally, the values obtained from combustion data are less reliable than those measured directly because the calculation involves the difference between the two large heats of combustion. Where these heats of

combustion are very precise a reasonably accurate value for  $\Delta H$  is obtained. Thus, using the data quoted by Dainton<sup>(58)</sup>, we have

$$\begin{aligned} -\Delta H^{\circ}_{gc'} &= \Delta H^{\circ}_{c, POM} - \Delta H^{\circ}_{c, CH_2O} \\ &= -120.05 + 134.4 \pm 0.3 \\ \therefore \underline{-\Delta H^{\circ}_{gc'} = 14.3 \pm 0.3 \text{ k. cal. mole}^{-1}}. \end{aligned}$$

(c) Though it is now accepted that formaldehyde does not polymerise by a free radical mechanism the following procedure is a justifiable device for obtaining yet another estimate for  $\Delta H^{\circ}_{gc'}$ . Thus, if the polymerisation of formaldehyde were to proceed through the biradical  $\cdot CH_2 - O \cdot$ , a value for the heat of polymerisation could be obtained from the value of  $D(C - O)$  and the energy required to form the biradical. The polymerisation can be represented as follows



If  $n$  is large chain-end effects can be ignored and the heat of polymerisation is given by

$$\Delta H_p = \Delta H_1 + \Delta H_2$$

The energy for process (1),  $\Delta H_1$ , can be calculated from the

band frequency of the  ${}^3A_2 \leftarrow {}^1A_1$  singlet-triplet transition in the ultraviolet absorption spectrum of gaseous formaldehyde, which is given as  $3900 \text{ \AA}$  <sup>(59)</sup> and which is equivalent to an energy of  $73.3 \text{ k. cal. mole}^{-1}$ .  $\Delta H_2 = D(C-O)$ , the bond dissociation energy of the acetal C - O linkage which has a value in the region of  $84.3 \text{ K. cal. mole}^{-1}$ . <sup>(60)</sup> Thus

$$\Delta H_p = 73.3 - 84.3 = -11 \text{ k. cal. mole}^{-1}.$$

This value is for the gas phase polymerisation and to get  $\Delta H^{\circ} \text{gc}^{\circ}$  we have to add the heat of vaporisation,  $\Delta H_v$ , and also the heat of fusion  $\Delta H_m$ , of the polymer. The heat of vaporisation,  $\Delta H_v$ , is readily calculated from the cohesive energy density, C.E.D., defined as the amount of heat required to vaporise unit volume, of the polymer which has been estimated <sup>(61)</sup> as  $124 \text{ cal. c.c.}$  assuming a density of  $1.42 \text{ gcc.}^{-1}$  for the polymer. The cohesive energy density is given

by 
$$\text{C.E.D.} = (\Delta H_v - RT) \text{ cal.c.c.}^{-1} = 124$$

$$\therefore \Delta H_v = 2620 + RT \text{ cal. mole}^{-1}.$$

At  $453^{\circ}\text{K}$ , the melting point of the polymer,  $\Delta H_v = 3.5 \text{ k. cal. mole}^{-1}$ .

$\Delta H_m$ , the heat of fusion is given by Incue <sup>(62)</sup> as  $1.59 \text{ k. cal. mole}^{-1}$ .

Thus  $-\Delta H^{\circ} \text{gc}^{\circ} = 11.0 + \Delta H_v + \Delta H_m = 11 + 3.5 + 1.6 = 16.1$

$\text{k. cal. mole}^{-1}$ . The small (about  $5 \text{ cal. mole}^{-1}$ ) change in heat

capacity of the polymer between  $300^{\circ}\text{K}$  and its melting point is

ignored. This calculation is crude but it does result in good agreement with the other estimates of the heat of polymerisation. It is interesting to note that the  $^3A_2 \leftarrow ^1A_1$  transition in formaldehyde is "forbidden" and this coupled with the fact that the energy of the process is high is most probably why formaldehyde does not normally polymerise by a free radical mechanism.

### 3.2.3. Experimental Determination of $-\Delta H^{\circ}_{gc}$ .

$-\Delta H^{\circ}_{gc}$  can be evaluated from equilibrium measurements.

This approach is possible in the case of polyoxymethylene with hydroxyl chain ends since it is one of the few polymers which can be brought to thermodynamic equilibrium with its monomer. In this sense polyoxymethylene glycols are analogous to living polymers like poly( $\alpha$ -methylstyrene) synthesised anionically using  $Na^+$  naphthenide in tetrahydrofuran. Stable active centres are required for polymer-monomer equilibrium and while it is clear that in the case of poly( $\alpha$ -methylstyrene) the active centre is the intimate ion-pair (polymer) $^- Na^+$  the nature of the active centre in polyoxymethylene is less clear, though it is probably molecular, in Dainton's view. (58)

By measuring the pressure of formaldehyde in equilibrium with polyoxymethylene Dainton (58) obtained values of

$\Delta H^{\circ}_{gc}$  and  $\Delta S^{\circ}_{gc}$  as follows

$$-\Delta H^{\circ}_{gc} = 12.35 \pm 0.045 \text{ k. cal. mole}^{-1}$$

$$-\Delta S^{\circ}_{gc} = 31.02 \pm 0.13 \text{ Gibbs mole}^{-1}$$

These values were corrected to 25°C using the measured specific heat of the polymer and monomer, giving

$$-\Delta H^{\circ}_{gc} (25^{\circ}\text{C}) = 12.24 \pm 0.08 \text{ k. cal. mole}^{-1}$$

$$-\Delta S^{\circ}_{gc} (25^{\circ}\text{C}) = 30.66 \pm 0.22 \text{ Gibbs mole}^{-1}$$

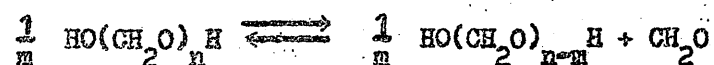
The correction is a small one.

More recently Dainton<sup>(63)</sup> has obtained a value of  $\Delta S^{\circ}_{gc} = 41.8 \pm 0.2 \text{ Gibbs mole}^{-1}$  from heat capacity measurements in the temperature range 20 - 300°K. This value for  $-\Delta S^{\circ}_{gc}$ , it was argued, is more reliable and in good agreement with the calculated value<sup>(63)</sup>. The need for further equilibrium studies arises from the unacceptable discrepancy of 11.2 entropy units between the two determinations of  $\Delta S^{\circ}_{gc}$ . Possible explanations for the discrepancy have been discussed by ~~Evans~~ Ivin<sup>(64)</sup>

One discrepancy between the two studies which has not been noted is that different polymers were used. Thus for the equilibrium study<sup>(58)</sup> a- and eu-polyoxymethylenes were used whereas for the heat capacity measurements<sup>(63)</sup> high molecular weight Delrin was used.

For several reasons it seemed worthwhile to measure the pressure of monomer in equilibrium with polyoxymethylene. Firstly, some light might be thrown on the discrepancy between the two entropy values noted by Dainton<sup>(63)</sup>. Secondly, the  $-\Delta H^{\circ}gc^{\circ}$  value for high molecular weight material might suggest why these materials are more thermally stable than Staudinger's polymers. Also, since  $E_d = E_p - \Delta H_p$  some check on the order of magnitude of the activation energy for depolymerisation is possible if  $\Delta H_p$  is known and  $E_p$  has a "normal" value of around 3 - 5 k. cal. mole<sup>-1</sup>. Since it was the largest, sample **7** was used exclusively for this work.

The equilibrium between monomer and polymer <



is governed by the equilibrium constant,  $K_p$ , given by

$$K_p = \frac{\left\{ \text{HO}(\text{CH}_2\text{O})_{n-m} \right\}^{1/m} \left\{ \text{CH}_2\text{O} \right\}}{\left\{ \text{HO}(\text{CH}_2\text{O})_n \text{H} \right\}^{1/m}} = \left\{ \text{CH}_2\text{O} \right\} = p_{\text{CH}_2\text{O}}$$

i.e.  $K_p = p_{\text{CH}_2\text{O}}$

since the activities,  $\{ \dots \}$ , of the solid phases are taken conventionally as unity. The fugacity of formaldehyde can be equated with its pressure if it is assumed that it behaves ideally in the temperature range of the equilibrium measurements. The free energy of polymerisation  $-\Delta G^{\circ}gc^{\circ}$ , is given by the van't Hoff



Isotherm,

$$-\Delta G^{\circ}_{gc} = RT \ln K_p = RT \ln p_{CH_2O}.$$

The heat of polymerisation,  $-\Delta H^{\circ}_{gc}$ , is obtained by integration of the van't Hoff Isochore,

$$d/dT (\ln K_p) = \frac{\Delta H}{RT^2} \quad (1)$$

Equation (1) can be integrated directly if it assumed that  $\Delta H$  is independent of temperature in the temperature range of the equilibrium measurements. As noted above, the error in this assumption is small (about 1%).

The integrated form of equation (1) is

$$\ln K_p = C - \frac{\Delta H}{RT}$$

Figure 13 shows typical plots of  $\log p_{CH_2O}$  versus  $1/T^{\circ}K$ .

Curve A was obtained for undegraded polymer (sample 7 chap. 2., Section 2.2.). Each point is the average of three equilibrium pressure readings measured in three separate equilibration tubes which were immersed in the thermostat tank together. Curve B was obtained for 200 mg. of sample 7 after approximately 50% degradation at  $170^{\circ}C$ . All the relevant data are summarised in Tables 3.2. and 3.3.

Figure 13.

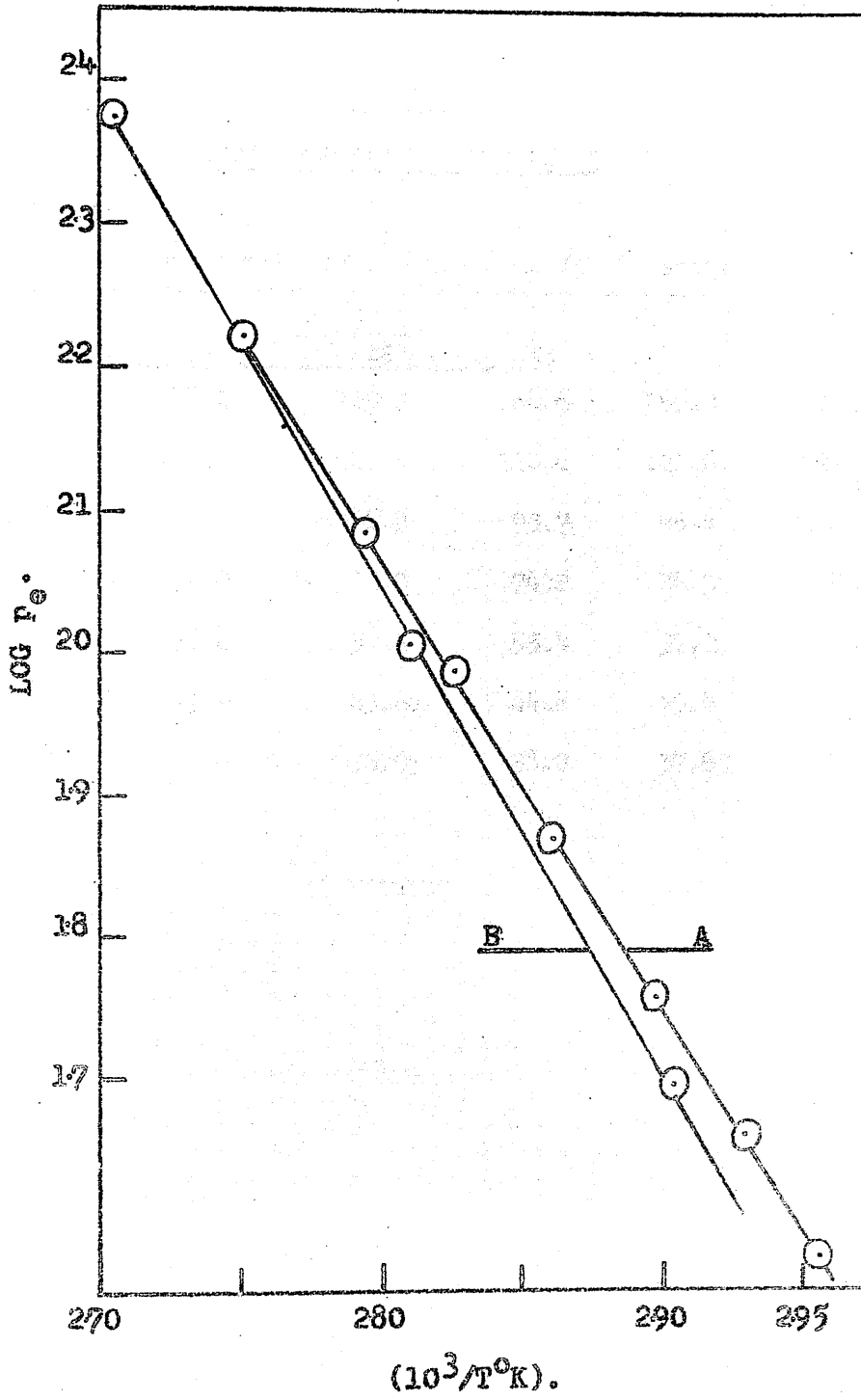


TABLE 3.2.

DATA FOR CURVE A FIGURE 13

Temperature (°C)	Equilibrium Pressures, pe, mm.Hg.			Average $\bar{p}_e \log \bar{p}_e 10^3/T^{\circ}K$		
	Tube	A1	A2	A3		
91.2		168.2	165.2	164.6	166.0	2.220 2.749
85.0		122.7	121.4	120.8	121.6	2.085 2.792
81.0		97.1	96.3	95.7	96.4	1.985 2.824
76.5		74.8	73.9	74.2	74.3	1.871 2.860
72.2		58.6	57.4	55.4	57.2	1.757 2.896
68.5		45.9	45.67	44.6	45.4	1.657 2.928
65.4		37.8	36.93	38.0	37.6	1.575 2.954

TABLE 3.2.

DATA FOR CURVE B, FIGURE 13

<u>Temp (<sup>o</sup>C)</u>	<u>pc. mm. Hg.</u>	<u>log. pc</u>	<u>10<sup>3</sup>/T<sup>o</sup>.</u>
71.3	49.6	1.695	2.904
82.7	100.9	2.004	2.811
88.4	144.9	2.161	2.764
96.5	227.5	2.357	2.705

The relationship between equilibrium pressure,  $p_e$ , and absolute temperature was derived for each curve and the following expressions were obtained.

$$\log p_e (A) = 10.871 - 3.147 (10^3/T)$$

$$\text{and } \log p_e (B) = 11.374 - 3.34 (10^3/T)$$

The gradients of the curves gave  $-\Delta H^{\circ}_{gc}$  values, as follows

$$-\Delta H^{\circ}_{gc} (A) = 14.32 \text{ k. cal. mole}^{-1}$$

$$-\Delta H^{\circ}_{gc} (B) = 14.84 \text{ k. cal. mole}^{-1}$$

Values for  $-\Delta S^{\circ}_{gc}$ , the entropy of polymerisation, were derived as follows:

$$\Delta G = \Delta H - T\Delta S = -RT \ln K_p$$

$$\Delta S = \frac{\Delta H}{T} + R \ln K_p$$

$$\Delta S^{\circ}_{gc} (A) = \frac{-14.32}{298} + 4.56 [10.871 - 3.147(10^3/298)]$$

$$-\Delta S^{\circ}_{gc} (A) = 46.6 \text{ Gibbs mole}^{-1}$$

and

$$\Delta S^{\circ}_{gc} (B) = \frac{-14.84}{298} + 4.56 [11.374 - 3.34(10^3/298)]$$

$$-\Delta S^{\circ}_{gc} (B) = 49.0 \text{ Gibbs mole}^{-1}$$

Recently, unpublished Du Pont work was referred to by Walker<sup>(65)</sup> and from the equilibrium pressures given the following information has been calculated for the two samples discussed. These will be designated (C) and (D) here. Sample (C) is a partially amorphous high molecular weight polyoxymethylene and sample (D) is a 100% crystalline sample.

(C)  $\log p_e (C) = 10.966 - 3.166(10^3/T)$   
 $-\Delta H^{\circ}_{gc} (C) = 14.3 \text{ k. cal. mole}^{-1}$   
 $-\Delta S^{\circ}_{gc} (C) = 46.5 \text{ Gibbs mole}^{-1}$

(D)  $\log p_e (D) = 12.486 - 3.766(10^3/T)$   
 $-\Delta H^{\circ}_{gc} (D) = 17.0 \text{ k. cal. mole}^{-1}$   
 $-\Delta S^{\circ}_{gc} (D) = 57.7 \text{ Gibbs mole}^{-1}$

For comparison, it is interesting to include a similar set of data obtained recently by Iwasa and Imoto for  $\alpha$ -polyoxymethylene (66).

(E) ( $\alpha$ -POM)

$\log p_e (E) = 12.02 - 3.57(10^3/T)$   
 $-\Delta H^{\circ}_{gc} (E) = 16.3 \text{ k. cal. mole}^{-1}$   
 $-\Delta S^{\circ}_{gc} (E) = 41.8 \text{ Gibbs mole}^{-1}$

3.3 The Ceiling Temperature of Polyoxymethylene

The thermodynamic ceiling temperature,  $T_c$ , of a polymer is defined as that temperature at which the free energy of polymerisation is zero.  $T_c$  is therefore the highest temperature at which the polymer is thermodynamically stable. Since  $-\Delta G^{\circ}_{gc} = RT \ln p_e (CH_2O)$ , it is clear that, in a closed system, polymerisation will occur only if the pressure of formaldehyde exceeds the equilibrium pressure at the given temperature. From figure 13 the equilibrium pressure of formaldehyde at  $100^{\circ}C$  is 650 mm. Hg and no polymerisation will

be observed at pressures below this value, thus Norrish and Carruthers (67) noted that in the presence of formic acid, a powerful polymerisation catalyst, no polymerisation occurred at 100°C and a formaldehyde pressure of 300 m.m. Hg.

The ceiling temperatures for samples (A) to (E) (Sect. 3.2.3.) are readily calculated by putting  $p_e = 1$  atmosphere (760 m.m. Hg.). The results are given in Table 3.4.

TABLE 3.4.

Thermodynamic Ceiling Temperatures for Polyoxymethylenes

SAMPLE	$\log p_e$ (Equilibrium pressure)	$T_c$ (°C).
A	$\log p_e = 10.871 - 3.147(10^3/T)$	121
B	$\log p_e = 11.374 - 3.34(10^3/T)$	120
C	$\log p_e = 10.966 - 3.166(10^3/T)$	118
D	$\log p_e = 12.486 - 3.766(10^3/T)$	119
E	$\log p_e = 12.02 - 3.57(10^3/T)$	118

3.4 Discussion

It is clear from Table 3.5 that  $-\Delta H_{gc}^{\circ}$  must lie in the range 14 - 16 k. cal.. The experimental results show good agreement. However, in the light of the general picture provided by the information summarised in Table 3.5., entries (5) and (9) are anomalous. That the anomaly, in the case of entry (5), arises from the choice of low molecular weight material for the earlier

TABLE 3.5

	<u><math>-\Delta H^{\circ}_{gc}</math></u>	<u><math>-\Delta S^{\circ}_{gc}</math></u>	<u>Reference</u>
(1) Estimate (a)	14.7	-	Table 3.1 and (57)
(2) " (b)	14.3	-	Sect. 3.2.2. (b)
(3) " (c)	16.1	-	" " (c)
(4) Cp measurements	-	41.65	(63)
(5) $\alpha$ ; eu-POM	12.24	30.66	(58)
(6) (A)	14.32	46.6	Table 3.2
(7) (B)	14.84	49.0	Table 3.3.
(8) (C)	14.3	46.5	(65)
(9) (D)	17.0	57.5	(65)
(10) (E)	16.3	41.8	(66)
(11) Calculated	-	43.1	(63)



equilibrium study<sup>(58)</sup> has already been suggested (Sect. 3.2.3.) and this seems to be borne out by the results which we have obtained with the high molecular weight material. The thermodynamic functions can be regarded as being independent of chain length only at high degrees of polymerisation. Thus, for  $\alpha$ -methylstyrene,  $\Delta H_{1c} = 8.424 - 18.58/n$  for  $n = 11$  to  $46$  at  $25^\circ\text{C}$ ,<sup>(68)</sup> where  $n$  is the degree of polymerisation. The effect of chain length on  $-\Delta H_{gc}^\circ$  for formaldehyde polymerisation is unknown but if  $\overline{DP} > 100$  the effect should be small. That the discrepancy in the entropy is due to a molecular weight effect is much less plausible and some other explanation must be sought.

The difference between the results for samples (C) and (D) [Entries (8) and (9) Table 3.5] is attributed by Walker<sup>(65)</sup> to the difference in crystallinity between the two samples, the latter being 100% crystalline. The improbably large  $-\Delta S_{gc}^\circ$  associated with this sample suggests that true thermodynamic equilibrium has not been achieved in this case, at least in the low temperature region ( $50-75^\circ\text{C}$ ). If true equilibrium has not been achieved at the lower temperatures the  $\log p_e$  versus  $1/T^\circ\text{K}$  curve has an exaggerated slope and this is reflected both in  $\Delta H$  and  $\Delta S$  but particularly in the latter. Despite the possibility that because of its high crystallinity sample (D) may not have reached true equilibrium the value of  $\Delta H_{gc}^\circ$  obtained is still a useful indication of its

stability relative to the other samples. The higher value of  $-\Delta H^{\circ} \text{gc}^{\circ}$  for the partially degraded sample (B) (entry (7) table 3.5.) suggests that it is more stable than the undegraded sample (A) (entry (6) Table 3.5). Kinetic evidence for this suggestion will be presented in Chapter 4. It was also found that the density and hence the crystallinity, based on  $\rho_{\text{amorphous}} = 1.25$  and  $\rho_{\text{crystal}} = 1.506^{(69)}$ , had increased as a result of degradation. Though the increase in crystallinity was marginal (76 to 81%) it seems to be in accord with Walker's suggestion that crystallinity confers stability on the polymer. Further evidence for this suggestion can be adduced from the fact that a marked increase in the rate of the thermal degradation reaction is observed in the temperature range  $125 - 130^{\circ}\text{C}$  in which the onset of premelting occurs<sup>(70)</sup>. That true equilibrium is not achieved by highly crystalline samples is made more plausible by the fact that all the plots of  $\log p_e$  versus  $1/T^{\circ}\text{K}$  merged and the ceiling temperature for all the polymers listed in Table 3.411e in the region of  $120^{\circ}\text{C}$ . It can therefore be argued that these polymers are thermodynamically identical in the region of the ceiling temperature but that metastability due to kinetic factors and crystallinity makes some apparently more thermodynamically stable than others.

In vinyl polymers where there are no stable active centres through which polymer-monomer equilibrium can be established metastability is fully developed and the polymers are kinetically stable above their thermodynamic ceiling temperatures,  $T_c$ . The introduction of active centres at temperatures above  $T_c$  leads in most cases to rapid depolymerisation. In the case of polyoxymethylene the active centres are not destroyed in an efficient polymerisation termination reaction as they are in most free radical polymerisations and in order to achieve metastability comparable to that of the vinyl polymers a post polymerisation step is necessary. Thus if ether chain-ends are introduced into the polymer it remains stable in high vacuum up to  $270^{\circ}\text{C}$ , which is some  $150^{\circ}$  above its ceiling temperature. In complete contrast, the hydroxyl chain-ended polymers are completely depolymerised at  $130^{\circ}\text{C}$  although at a comparatively low rate.

It is clear that thermodynamic considerations alone do not always give a true indication of the stability of a polymer with respect to depolymerisation and that a complete discussion requires kinetic information as well.

CHAPTER 4

The Thermal Depolymerisation of Polyoxymethylene

4.1 General Introduction

The mechanisms of the thermal degradation of a variety of polymers are now fairly well understood<sup>(37-41)</sup>. Perhaps the most useful generalisation which has emerged from earlier work is that the kinetics of polymer chain-scission processes, which include depolymerisation reactions, are most conveniently rationalised in terms of free radical chain reactions involving the four elementary steps (a) initiation, (b) depropagation, (c) transfer and (d) termination. To establish the detailed mechanism of depolymerisation, i.e. to establish the part played by each of the four possible elementary reactions under a given set of conditions, information about the following is required

- (1) The products and their relative abundance
- (2) The rates and activation energies of the degradation reactions.
- (3) The molecular weight of the polymer as a function of extent of reaction.

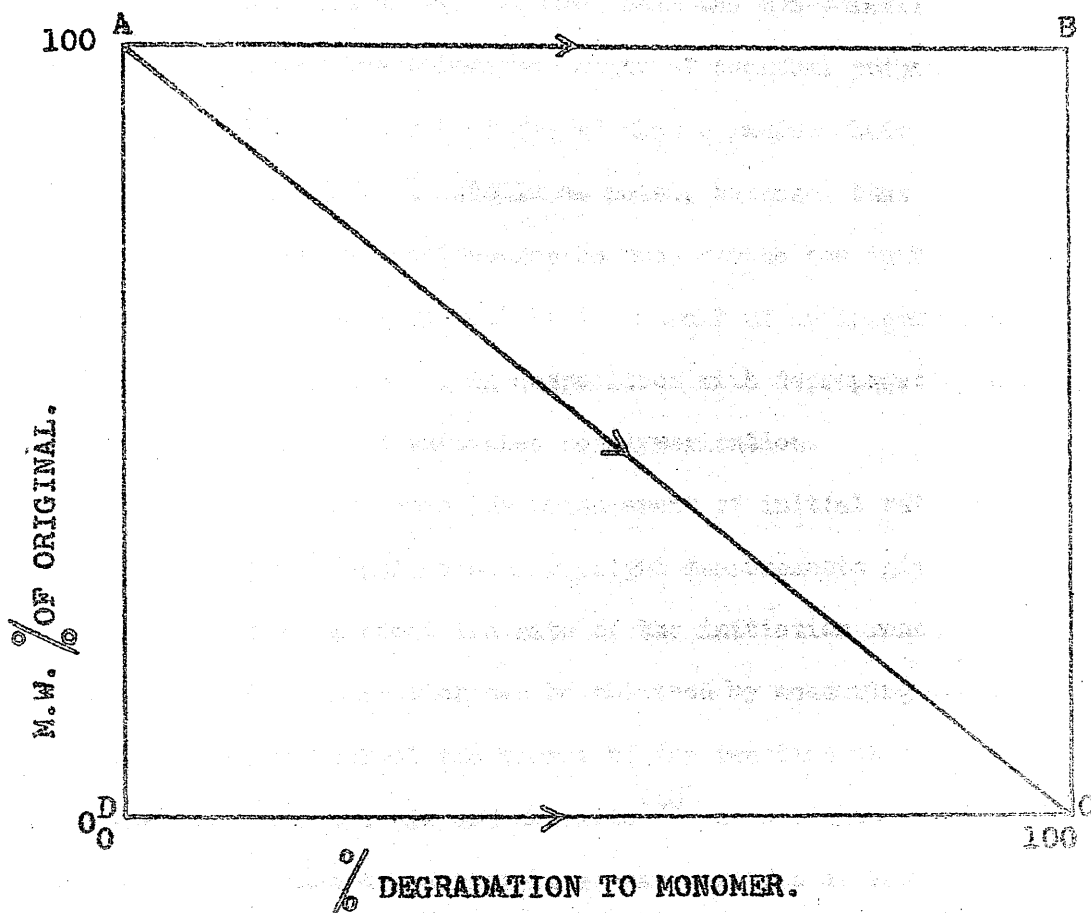
Thus the production of high yields of monomer is a clear indication that the predominant reaction is the "unzipping" of monomer units (depropagation) from active centres produced in an initiation reaction occurring either exclusively at the chain-end or at random along the chain or, conceivably, a combination of these two possibilities. In the case of the thermal degradation of vinyl polymers there is now little doubt that the initiation reaction involves homolytic bond scission and that the propagating species is identical to the free radical which occurs in the polymerisation reaction. Experimental proof of this is provided by the inhibition of the depolymerisation reaction by free-radical inhibitors.

Having established its free radical nature the next step is to establish the molecular site at which the initiation reaction occurs. This is done by measuring the dependence of initial rate on molecular weight. There are three possibilities: initial rate is (a) inversely proportional to, (b) directly proportional to or (c) independent of molecular weight. Possibility (a) arises when the initiation reaction occurs at the chain-end and the zip-length,  $\epsilon$ , of the depropagation reaction is less than the molecular chain length, C.L.; (b) arises when the initiation is random and  $\epsilon \geq C.L.$  and (c) arises either when initiation is random and  $\epsilon \leq C.L.$  or when

initiation occurs at the chain and  $\epsilon \gg C.L.$ . The ambiguity which arises in case (c) is readily resolved by molecular weight measurements. Thus in the case where  $\epsilon \gg C.L.$  the molecular weight of the polymer residue remains virtually unchanged for large extents of reaction and an initial rate independent of molecular weight is a clear indication that the initiation reaction is occurring at the chain-end. The other situation yielding an initial rate independent of molecular weight (random initiation  $\epsilon \leq C.L.$ ) is also clearly distinguished by measuring the molecular weight of the polymer residue. In this case degradation yields two non-volatile polymer fragments, since  $\epsilon \leq C.L.$ , which cause a large drop in the average molecular weight. Clearly if there is independent evidence for chain-end initiation then an initial rate which is independent of molecular weight is an indication that  $\epsilon \gg C.L.$

Grassie and Melville<sup>(48)</sup> summarised the molecular weight changes arising from the various mechanisms that can operate in depolymerisation in the diagram shown in Figure 14. In general, if the molecular weight of the polymer residue follows AC one non-volatile residue is being produced for every original molecule that has been activated in an initiation reaction. If the molecular weight of residual polymer lies in area ABC less than one non-volatile residue is produced. While complete unzipping of every chain which

FIGURE 14.



has been activated can be inferred if the molecular weight of residual polymer lies on AB. If more than one non-volatile residue is produced the molecular weight of residual polymer will be in area ACD and it can be inferred that a random chain scission reaction has occurred. It should be noted, however, that in the latter case the random chain-scission need not be the initiation reaction, it could equally well be the result of an intermolecular transfer reaction occurring in competition with depropagation during the course of chain-end initiated depolymerisation.

As indicated above the measurement of initial rates of degradation coupled with molecular weight measurements gives valuable information about the site of the initiation reaction. Further valuable information can be obtained by measuring the rate of degradation throughout the course of the reaction at a given temperature. Thus Grassie and Melville<sup>(48)</sup> established that only 50% of poly(methylmethacrylate) was degraded at 220°C and that much higher temperatures were required to depolymerise the polymer completely to monomer. This was shown to be due to the presence of two types of chain-end, one rather more stable than the other. Thus the presence of a "chain end spectrum" can be detected by a thorough kinetic examination of the reaction at a variety of temperatures.



How far can the concepts and techniques developed in the attempt to understand the degradation behaviour of vinyl polymers help to rationalise the observed degradation behaviour of the polyoxymethylene class of polymer? Does the presence in the polymer of stable "active centres", as indicated in Chapter 3, remove the necessity for an initiation reaction of the type required in the degradation of vinyl polymers? Is the reaction a chain reaction? What kind of chain reaction is it? In this and the following chapter the thermal degradation of polyoxymethylenes with hydroxyl and acetate chain ends will be discussed in some detail. The kinetics and molecular weight changes are discussed in this Chapter and the mechanism of the reaction is discussed in Chapter 5.

In this chapter it will be shown that the high molecular weight polymers with hydroxyl chain ends are completely degradable at  $130^{\circ}\text{C}$ , detectable degradation occurring in the dynamic molecular still at temperatures in excess of  $100^{\circ}\text{C}$ . The thermal depolymerisation reaction is first-order at all temperatures in excess of  $130^{\circ}\text{C}$  showing a deviation from first order behaviour which occurs later in the reaction the higher the temperature, being very difficult to detect at temperatures above  $200^{\circ}\text{C}$ . The suggestion that this deviation is associated with the crystallinity of the sample is examined in 4.2.3. Other possible explanations are examined in Chapter 5.

In contrast the acetates are much more stable than the parent glycols showing little degradation below 165°C. It will be shown that whereas the polymer with acetate chain-ends shows uniform first order behaviour with an activation energy of 58 k. cal. mole<sup>-1</sup> throughout the reaction the activation energy for volatilisation of monomer from the glycols, prepared in a variety of ways, shows complex behaviour increasing to a maximum of 52 k. cal. mole<sup>-1</sup> as the reaction proceeds.

It will be shown that at temperatures in the range 160 - 175°C the molecular weight of the polymer residue lies in ABC of figure 14 at all extents of reaction studied. From which it can be inferred that the zip-length of the depolymerisation reaction is less than the average molecular chain-length and also that random-chain scission or transfer reactions are playing no detectable part in the reaction.

The ideas and techniques developed in the study of the thermal degradation of vinyl polymers have been used extensively and it is interesting to quote the following in this connections

"The mechanism of the depolymerisation of poly(methyl methacrylate) has been elucidated by measuring the molecular weight of the polymer at stages during the reaction, but a similar method cannot be used for polyformaldehyde owing to the impossibility of measuring molecular weights". (36)

## 4.2 Thermal Depolymerisation Polyoxymethylene glycols and acetates

### Part 1 Kinetics

#### 4.2.1. Introduction

Convincing chemical evidence for the conclusion that the thermal degradation of polyoxymethylene glycols is a chain-end initiated depolymerisation reaction can be found in the literature and was referred to in Chapter 1. However, not all the variables that might influence the degradation behaviour of polyoxymethylenes have been studied. In this section the results obtained in examining some of these variables in the dynamic molecular still will be presented.

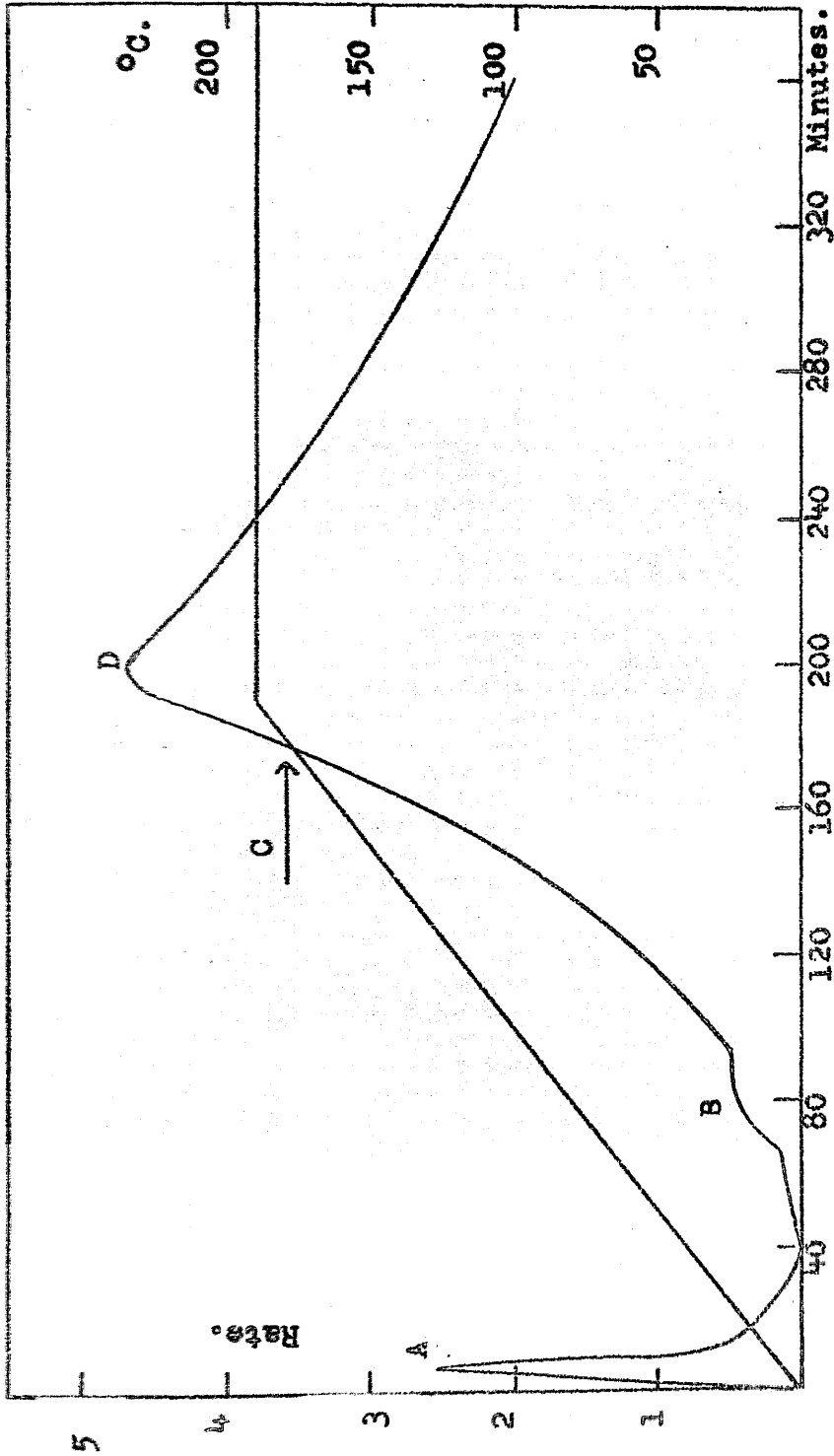
#### 4.2.2. The Degradation Variables

##### 4.2.2. (a) Temperature and the Activation Energy of the Reaction.

The discussion in Chapter 3 led to the conclusion that polyoxymethylene is thermodynamically stable up to a temperature of 120°C, which had been determined as the ceiling temperature of the polymer. It was also pointed out that metastability above the ceiling temperature was a function of the chain-end structure, the polymer being labile if the chain ends were hydroxyl groups and rather more stable if the chain ends were esterified or etherified.

The general features of the thermal degradation of a sample were established by plotting the rate, expressed as  $(V^2/V_0^2 - 1)$ , as determined by the Pirani gauge [see 2.4.2. (a)] against time as the temperature was linearly increased. A typical Pirani curve obtained in this way is shown in Figure 15. Since the temperature is increasing at a constant rate Figure 15 can be read as a derivative thermogravimetric curve in which each peak corresponds to a volatilisation process which differs in activation energy from the others. Two things determine the resolution of such a curve - the difference in activation energy of the processes operating and also the rate of change of temperature. Figure 15 represents a rate of temperature change of  $1.0^\circ/\text{min}$ . The Pirani plot has three distinct features, observed in all degradation experiments. Switching on the heaters always gave a sharp initial peak A which decayed to zero rate before the temperature reached  $50^\circ$ . The initial peak A corresponds to volatilisation of absorbates from the copper block and the heaters since it was not observed if, in a blank experiment, the heaters were switched off at  $50^\circ\text{C}$  and then switched on again when the block reached room temperature. The partially resolved

FIGURE 15  
Typical Pirani Plot.



shoulder, B, was always observed with raw polymers and always occurred in the range 80-100°C. This is probably associated with the transition from the orthorhombic to the hexagonal crystal form which is known to occur in this temperature range<sup>(71)</sup>. The exponential increase in the rate between B and D begins in the temperature range 125°-135°C in which premelting starts<sup>(70)</sup>. C corresponds to the crystalline melting point and is not associated with any discontinuity in this curve which is evidence for the conclusion that the reaction occurring between B and C is the same as that occurring between C and D. This suggests that only the amorphous phase, which is present in increasing amounts from 125°C onwards, is reacting at a detectable rate. D corresponds to the point where the increase in rate due to increasing temperature is overtaken by the more rapid decrease in rate due to degradation and contributes nothing more to the interpretation of the plot than that already given. Besides providing a qualitative picture of the behaviour of polyoxymethylene at temperatures up to the melting point a slow increase in temperature allows initial activation energies for volatilisation to be determined [2.4.2.(C)]. Figure 16 shows the Arrhenius plots obtained with samples S1, S2, S3, S4, S5 and S7. Figure 17 shows the plots obtained with the acetate

FIGURE 16.

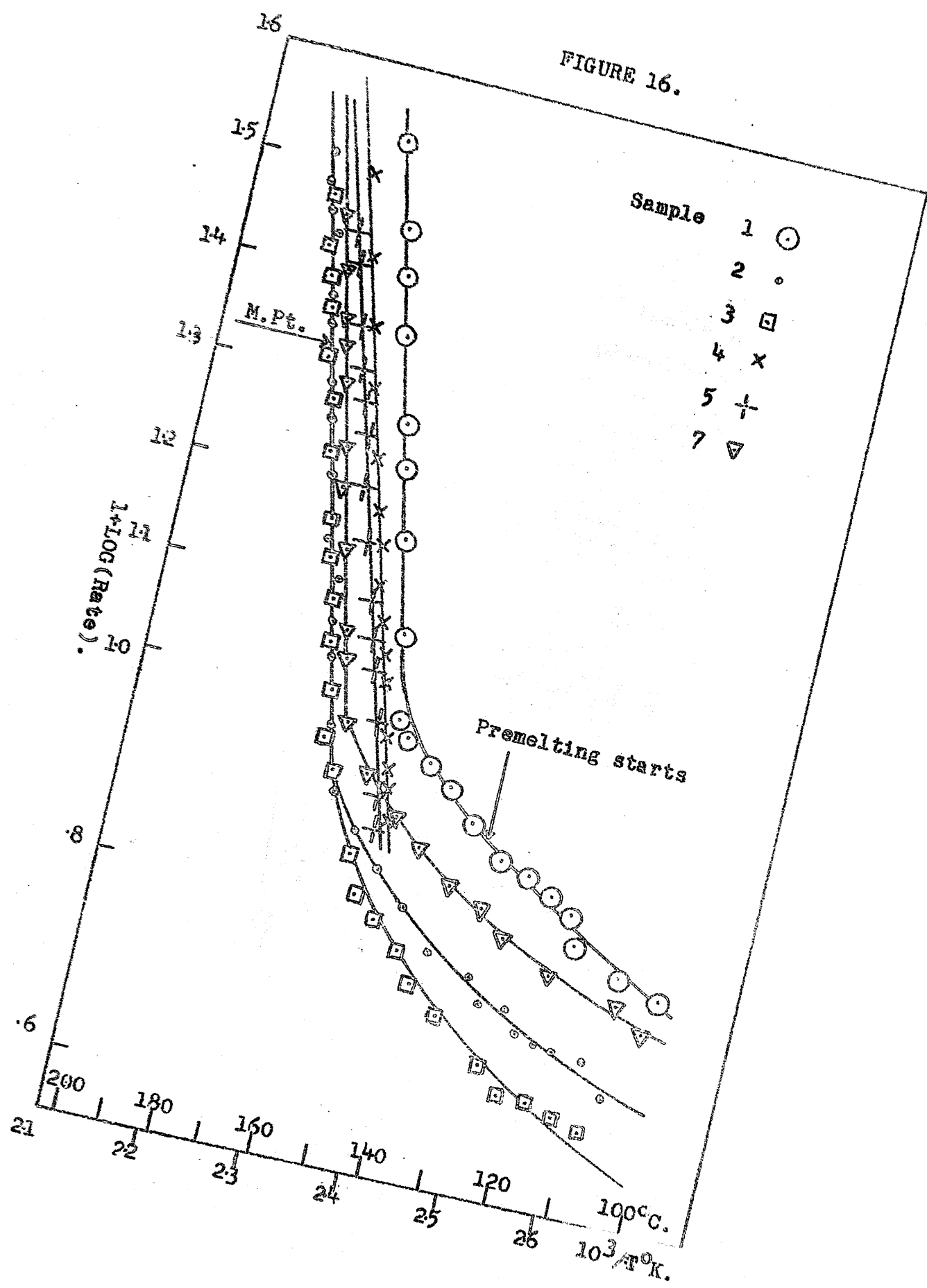
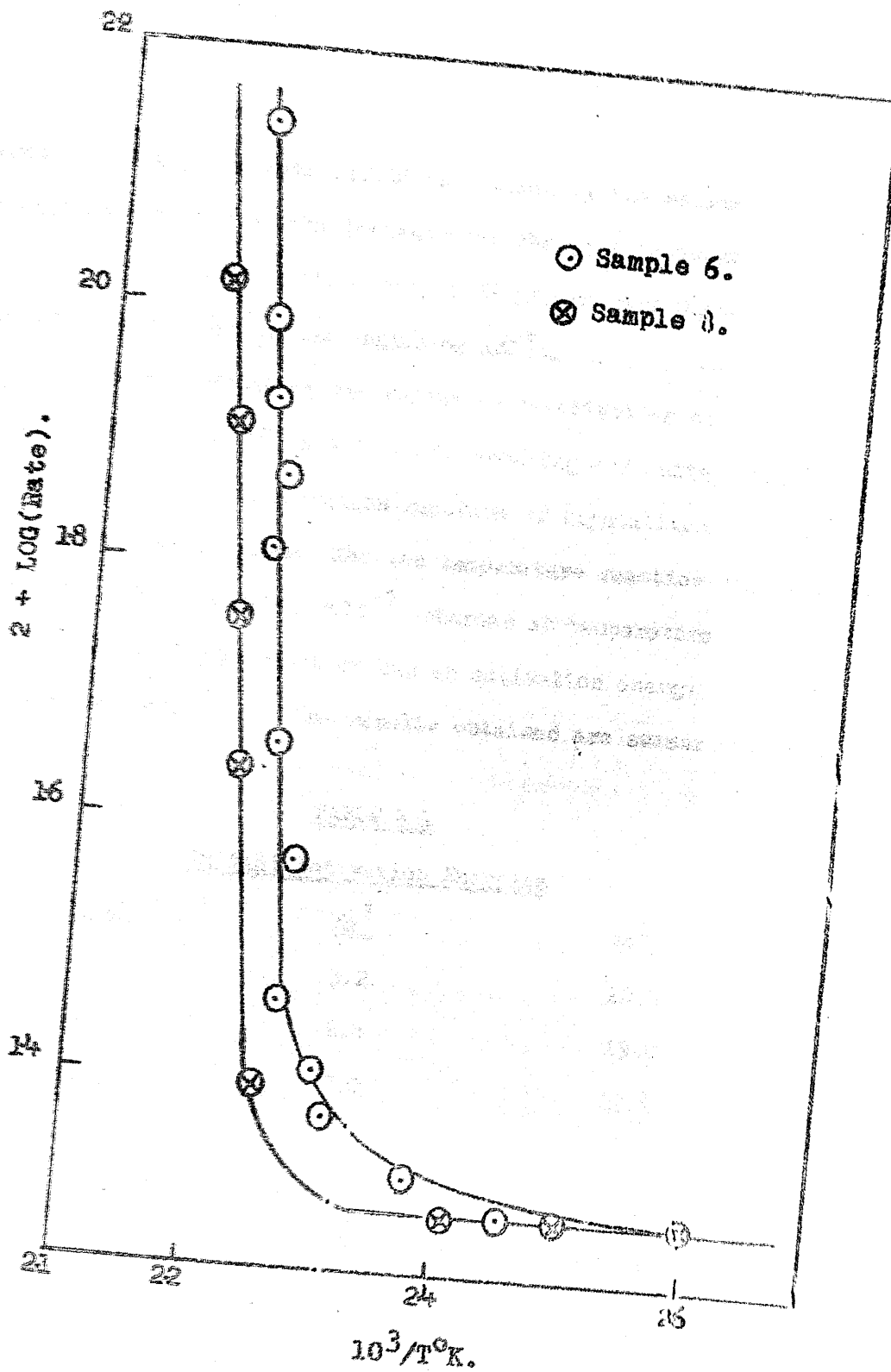


FIGURE 17.





samples S6 and S8. These plots have been derived from specific rates, obtained by dividing the rate at any time by the initial weight. Strictly the rate should be divided by the weight of the residual polymer at the instant that the rate is measured. The error is not serious since only 2-5% polymer has degraded on reaching temperatures in the region of 180°C.

Besides indicating the different reactivities of the sample studied Figure 16 reveals an interesting and quite general characteristic of the degradation reaction of crystalline polyoxymethylene glycols of various origins. The low temperature reaction has an activation energy,  $E_a^1$ , of 5-7 k cal. mole<sup>-1</sup>, whereas at temperatures in excess of 130-140°C the reaction has an activation energy,  $E_a^2$ , of 17-20 k. cal. mole<sup>-1</sup>. The results obtained are summarised in Table 4.1.

TABLE 4.1

<u>Sample</u>	<u><math>E_a^1</math></u>	<u><math>E_a^2</math></u>
1	5.2	20.3
2	6.4	19.0
3	7.0	19.4
4	-	16.7
5	-	17.0
7	6.8	20.6

Clearly, two quite distinct processes, both yielding monomer, are operating. The low value of  $E_a^1$  is consistent with the observation that depolymerisation can occur at low temperatures (Chapter 3). If the depolymerisation reaction is a chain reaction comprising initiation, depropagation and termination the activation energy for initiation must be abnormally low for the reaction to occur at temperatures in the range 60-100°C.

Between 120°C, the ceiling temperature, and 130°C, the temperature at which premelting is setting in, <sup>(70)</sup> the slope of the Arrhenius plot smoothly changes and reaches a value which remains constant though the crystalline melting point (178-179°C) up to about 185°C. This change of slope can be associated with few possibilities. Either the measured activation energy is a composite one and one of its terms has changed markedly with the increase in temperature or there has been a change of mechanism.

The activation energy for monomer production was also measured at various extents of reaction by switching off the heaters, noting Pirani volts and temperature and plotting rate,  $(v^2/v_0^2 - 1)$ , versus  $1/T^{\circ}K$  assuming that negligible degradation occurred between the time the heaters were switched off at the reaction temperature (170-175°C) and the time the rate fell to

zero. The results obtained in this way are summarised in Table 4.2 and are plotted in Figure 18.

TABLE 4.2

Activation energy,  $E_a$ , for monomer production as a function of % degradation to monomer.

<u>Sample</u>	<u>% Degradation</u>	<u>Degradation Temp (<math>^{\circ}</math>C)</u>	<u><math>E_a</math></u>
1.	< 4	168	20.3
	10.6		32.0
	26.1		47.8
	35.2		51.2
	47.7		51.8
2.	< 5	170	19.0
	17.2		24.8
	36.8		49.6
	43.4		49.4
	64.3		49.8
4	< 4	172	16.7
	25.6		34.0
	32.4		36.8
	46.8		45.4
	73.6		49.4

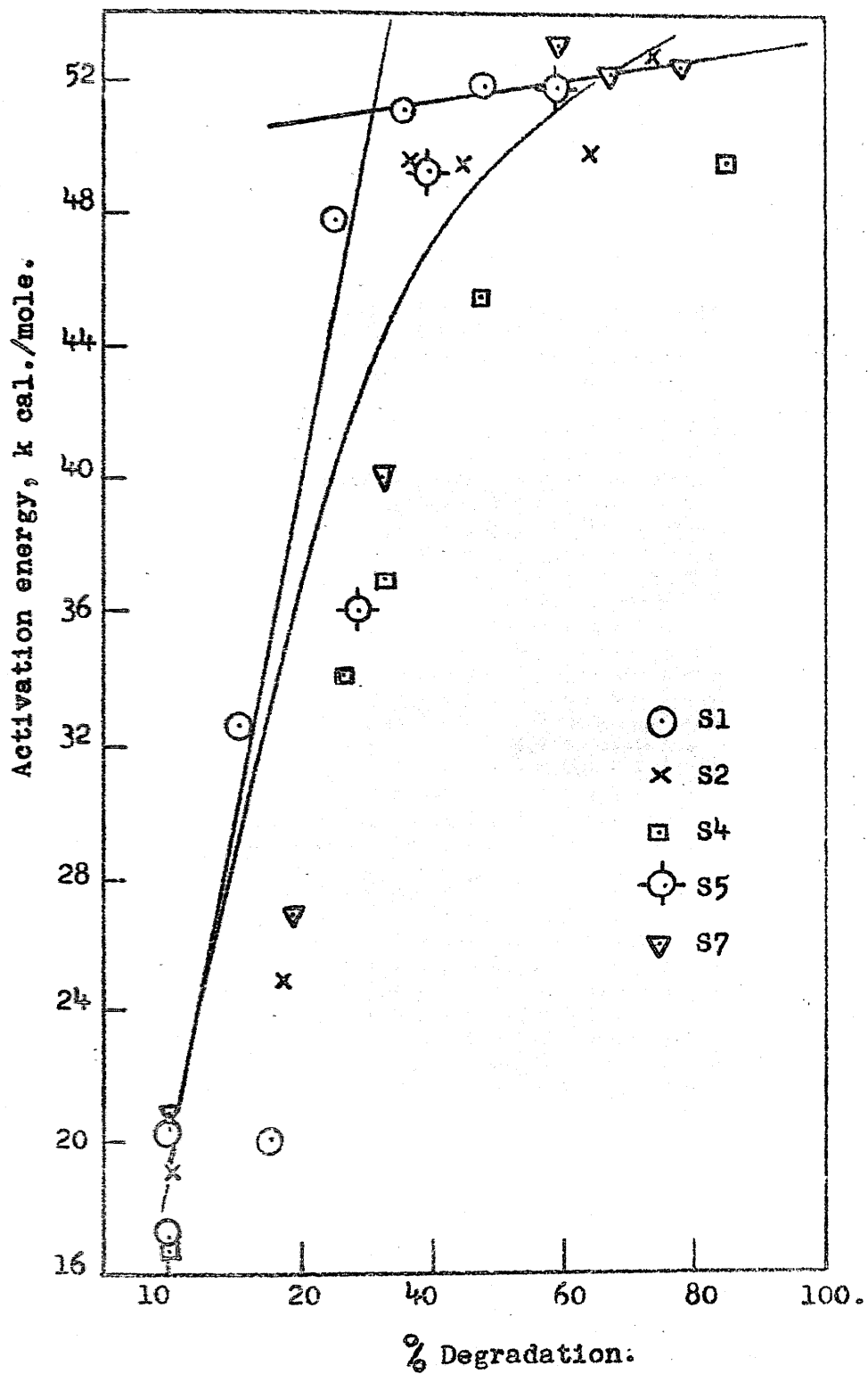
Table 4.2 continued.

5.	6	176	17.0
	15.4		20.2
	28.1		36.0
	39.1		49.2
	58.0		51.8
7.	3	175	20.6
	18.5		26.8
	31.4		40.1
	58.5		53.0
	56.4		52.3
	67.6		52.4

---

While it is clear that the precision of the results plotted in Figure 18 is poor there seems to be a general trend towards an activation energy of about 50 k. cal. mole<sup>-1</sup> as the reaction proceeds beyond 35-40% at temperatures in the range 170-175°C.

FIGURE 18.



It is clear from Fig. 17 that there is no detectable degradation of acetylated polyoxymethylenes below 165°C and that above this temperature the rate of reaction follows the Arrhenius law up to 200°C with an activation energy of 58.1 k. cal. mole<sup>-1</sup>. It was found that at all extents of degradation of the two acetate samples the activation energy, as measured by the "cooling" method described above, lay in the range 59-61 k. cal. mole<sup>-1</sup>. This behaviour is in complete contrast to that of the glycols. The enhanced stability of the esterified polymers is conveniently expressed in terms of the specific rates of depolymerisation at 170°C compared with the same quantity for the parent glycols. The relevant data are given in Table 4.3.

TABLE 4.3

Rate of Depolymerisation of Polyoxymethylene glycols and their acetate derivatives at 170°C.

<u>Sample</u>	<u>Chain-end</u>	<u>Rate (V<sup>2</sup>/Vo<sup>2</sup>-1)</u>
5	-OH	4.34
6	-OAc	0.45
7	-OH	2.67
8	-OAc	0.25

#### 4.2.2. (b) Mode of Preparation and Molecular Weight.

The mode of preparation of a polymer determines three important parameters which can markedly influence its degradation behaviour: average molecular weight, the molecular weight distribution and the microstructure of the polymer, e.g. chain-ends, branching, weak links. Whereas the kinetics of the free radical polymerisation of vinyl compounds is sufficiently understood for it to be possible to control readily the molecular weight of vinyl polymers it is clear that our limited understanding of formaldehyde polymerisation (Chapter 1) precludes accurate control in a similar manner. It must be stated, however, that a crude control is possible by ensuring that the monomer is pure and free of transfer agents but in practise this has proved an extremely difficult thing to achieve reproducibly.

Despite these limitations and the fact that they have been produced in different ways it appears that all the unstabilised samples (S1, 2, 3, 4, 5 and 7) with, perhaps, the exception of sample 4, are similar in structure, have the same number of chain-ends per molecule and have molecular weights lying in a fairly narrow range. Evidence for these conclusions is presented in the remaining part of this subsection.

The infra-red spectra of all samples with hydroxyl chain ends were recorded and the infra red number average molecular weight,  $\bar{M}_n$  (I.R.), determined using the technique described in 2.3.2.. All the infrared spectra were qualitatively identical so it can be inferred that the polymers have identical macrostructure. The infra red spectra can give no information about the number of hydroxyl groups per molecule nor whether adsorbed water is contributing to the absorbance in the hydroxyl band. Thus the I.R. evidence alone would make any conclusions based on the relationship between rates of degradation and  $\bar{M}_n$  (I.R.) rather tentative. Despite the inherent ambiguity in the I.R. method an inverse relationship between  $\bar{M}_n$  (I.R.) and specific initial rate at 160°C is obtained as indicated by the results summarised in Table 4.4. and plotted in fig. 19.

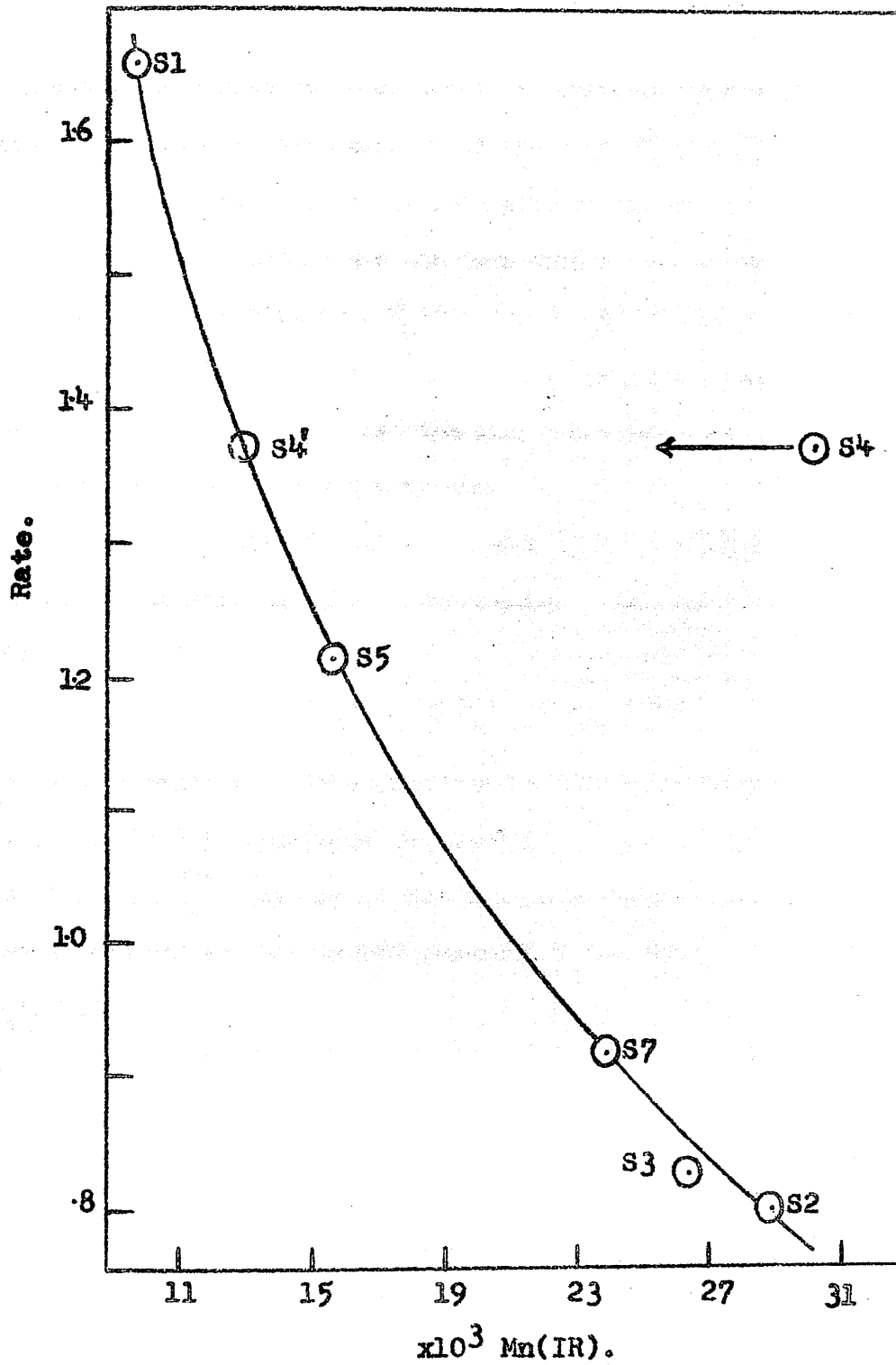
TABLE 4.4.

Specific Initial Rate at 160°C,  $R_i$ , versus  $\bar{M}_n$  (I.R.)

<u>Sample</u>	<u><math>R_i</math>, (<math>v^2/v_0^2 - 1</math>)</u>	<u><math>\bar{M}_n</math> (I.R.) <math>\times 10^3</math></u>
1	1.660	9.89
2	0.802	28.0
3	0.832	26.5
4	1.374	30.0
5	1.217	15.7
7	0.913	24.0



FIGURE 19.



Since five of the six points lie on a smooth curve it can be argued that the only significant difference between these samples is  $\bar{M}_n$  and that they have the same number of hydroxyl chain-ends per molecule. The inverse relationship between R and  $\bar{M}_n$  (I.R.) is consistent with the fact that the reaction is initiated at the hydroxyl chain-ends. Sample 4 is the only anomaly and the fact that it can be brought onto the curve by assuming that  $\bar{M}_n$  (I.R.) is 0.455 of the measured value seems to be plausible evidence for the conclusion that samples 1, 2, 3, 5 and 7 have two hydroxyl chain-ends per molecule and that sample 4 has only one.

Without osmotic  $\bar{M}_n$  values we must rely on solution viscosities to confirm the above conclusions. The Mark-Houwink equation,

$$[\eta] = K \cdot \bar{M}_n^\alpha,$$

allows us to develop a relationship between intrinsic viscosity and  $\bar{M}_n$  (I.R.). Table 4.5 summarises the results. Figure 20 is the plot of  $\log [\eta]_{95\%}^{25^\circ\text{C}}$ , the log of the intrinsic viscosity of the polymer determined at 25°C in 95% aqueous P.F.A.H. (2.3.1.), versus  $\log \bar{M}_n$  (I.R.).

FIGURE 20.

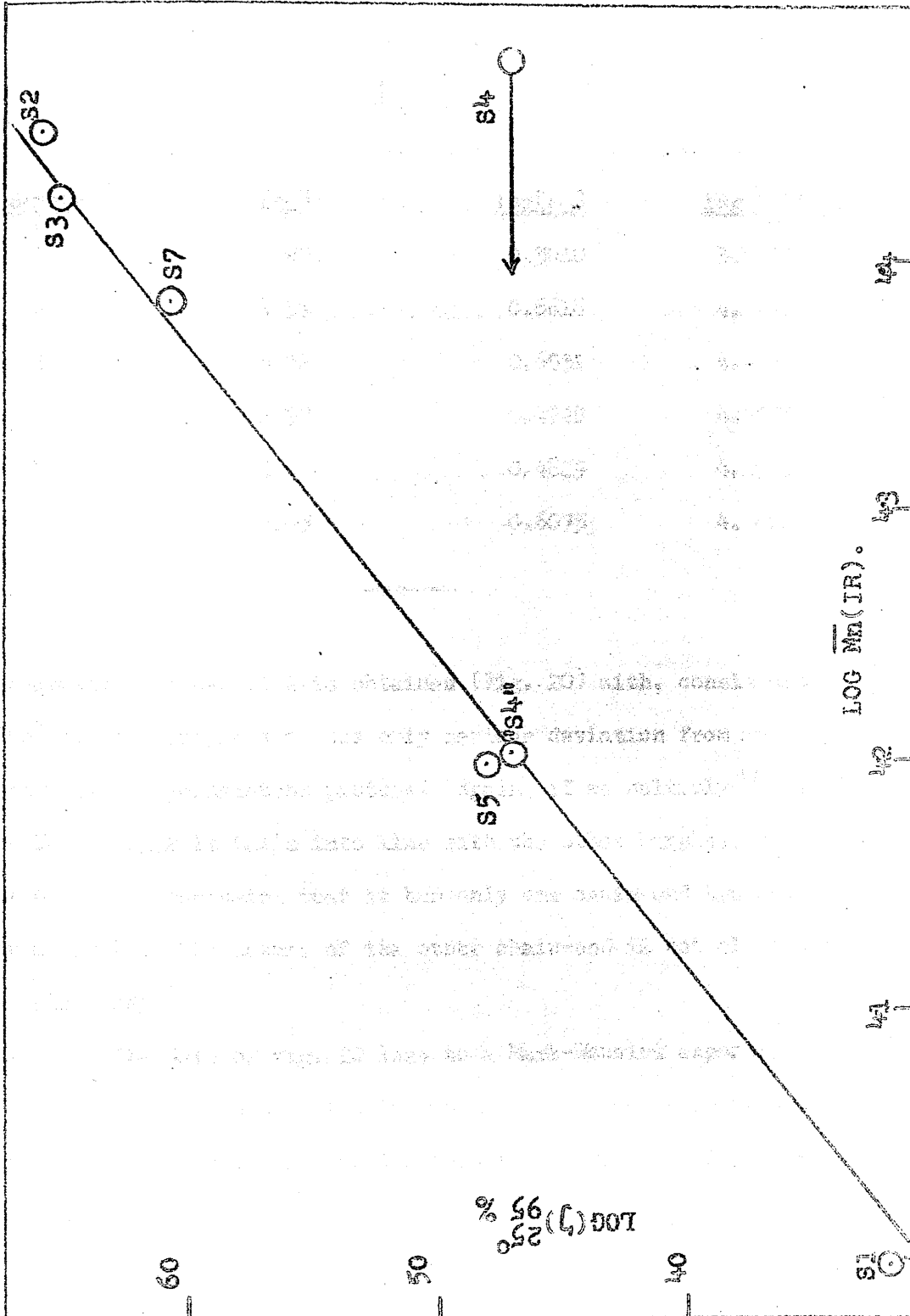


TABLE 4.5.

Data for  $[\eta] = K\bar{M}_n(I.R.)^a$

<u>Sample</u>	<u><math>[\eta]</math></u>	<u><math>\log[\eta]</math></u>	<u><math>\log \bar{M}_n(I.R.)</math></u>
1	2.00	0.3010	3.9952
2	4.59	0.6618	4.4472
3	4.52	0.6551	4.4232
4	2.97	0.4728	4.4771
5	3.04	0.4829	4.1959
7	4.05	0.6075	4.3802

A reasonably linear plot is obtained (Fig. 20) with, consistent with Fig. 19, sample 4 as the only serious deviation from an otherwise self-consistent picture. Again, if we multiply  $\bar{M}_n(I.R.)$  for S4 by 0.532 it falls into line with the other samples, confirming our original conclusion that it has only one chain-end hydroxyl per molecule. The nature of the other chain-end is not elucidated in this study.

The data of fig. 20 lead to a Mark-Houwink exponent,  $a$ , of 0.81, which suggests a fairly extended molecule in solution. The accuracy of this value must remain in doubt. It will be discussed in Chapter 6.

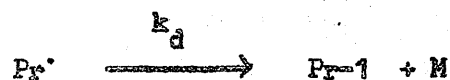
It is interesting to stretch the available data further and consider the value of  $x$  in the expression  $R = K[\bar{M}_n \text{ (I.R.)}]^x$ , where  $R$  is the specific initial rate (160°C.). This can provide useful information as will be seen from the following discussion.

If the reaction is a chain reaction, comprising initiation, depropagation and termination, it can be presented as follows:

Chain-end initiation



Depropagation

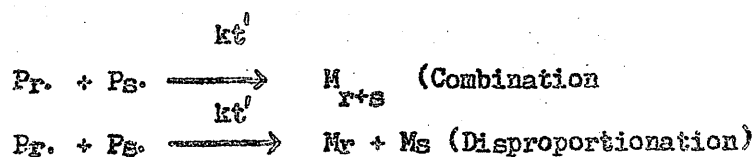


Termination

1st order:



2nd order:



The rate of initiation is proportional to the number of chain-ends which is proportional to  $\bar{M}_n^{-1}$ , therefore

$$\begin{aligned} \text{Rate of initiation} &= k_i A \bar{M}_n^{-1} \\ \text{Rate of depolymerisation} &= k_d \text{ (number of active centres)} \end{aligned}$$

i.e.  $\frac{d(M)}{dt} = \underline{k_d(P)} \dots\dots\dots(1)$

If the active centres, P, are being destroyed in a termination reaction and a steady state concentration of active centres can be assumed, we have

$$\frac{d(P)}{dt} = 0 = k_i A \bar{M}_n^{-1} - k_t (P)^2 \dots\dots(2)$$

if the termination reaction is bimolecular, and

$$\frac{d(P)}{dt} = 0 = k_i A \bar{M}_n^{-1} - k_t^1 (P) \dots\dots(3)$$

if the termination reaction is unimolecular.

Solving (2) and (3) for (P) and substituting in (1) gives

$$\frac{d(M)}{dt} = \frac{k_d k_i^{\frac{1}{2}} A^{\frac{1}{2}} (\bar{M}_n^{-\frac{1}{2}})}{k_t^{\frac{1}{2}}} = K \bar{M}_n^{-\frac{1}{2}}$$

if the termination is bimolecular, and

$$\frac{d(M)}{dt} = \frac{k_d k_i A}{k_t^1} (\bar{M}_n^{-1}) = K^1 \bar{M}_n^{-1}$$

if termination is unimolecular.

There are thus two possibilities for the exponent x in the relationship,  $R = K[\bar{M}_n(I.R.)]^x$ ,  $x = -\frac{1}{2}$  or  $x = -1$ .

The latter value is also obtained if there is no termination reaction and the overall rate is determined by the rate constant for depropagation  $k_d$ , i.e.

$$\frac{d}{dt} (M) = k_d (P) = k_d A \bar{M}_n^{-1}$$

This situation can only arise when  $k_i > k_d$  or when the polymer is living and thus doesn't require the generation of active centres in an initiation reaction. The argument of Chapter 3 led us to the conclusion that polyoxymethylene glycols were living in the sense that it was possible to establish an equilibrium between polymer and monomer in the temperature range 60 - 100°C. The evidence provided by the  $E_a^1$  values (Table 4.1) certainly suggests that  $k_i > k_d$ .

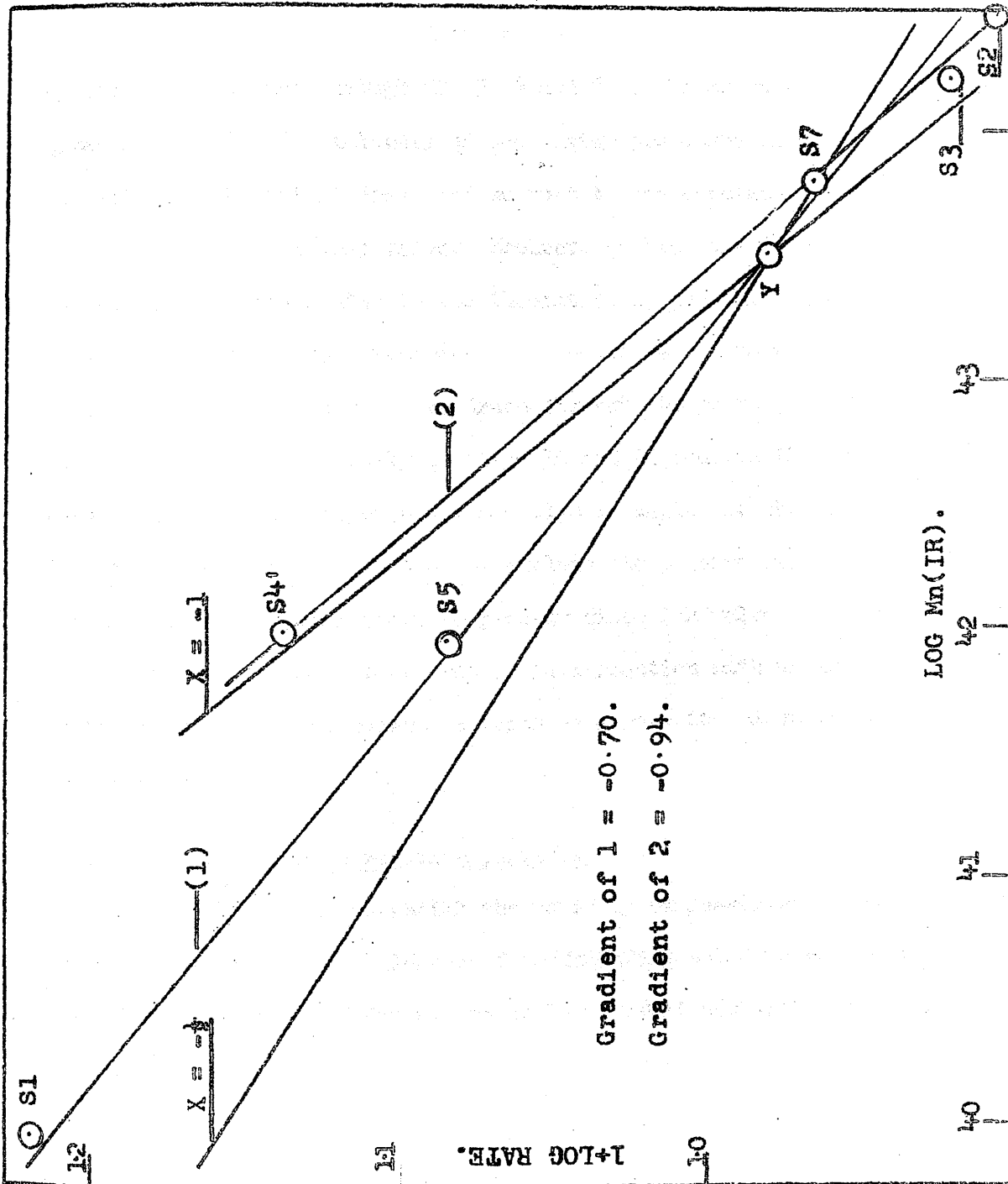
The value of  $x$  is obtained by plotting  $\log R$  versus  $\log \bar{M}_n$  (I.R.). For convenience  $1 + \log R$  is plotted against  $\log \bar{M}_n$  (I.R.) in Fig. 21, the data for which is summarised in Table 4.6.

TABLE 4.6

Data for  $R = K[\bar{M}_n$  (I.R.)]<sup>x</sup>

<u>Sample</u>	<u>1+log R</u>	<u><math>\bar{M}_n</math> (I.R.)x10<sup>3</sup></u>	<u>log <math>\bar{M}_n</math> (I.R.)</u>
1	1.2202	9.89	3.9952
2	0.9041	28.0	4.4472
3	0.9202	26.5	4.4232
4	1.1381	30.0	4.4771
5	1.0853	15.7	4.1959
7	0.9652	24.0	4.3802

FIGURE 21.





Ignoring S4, a value of  $x = -0.7$  is obtained. If a "corrected"  $\bar{M}_n$  (I.R.) for S4, obtained by dividing the measured value by 2, is considered a line through S2, 3, 4 and 7 can be drawn which gives  $x = -0.94$ . The validity of the latter procedure is open to serious doubt but it does lend support to the conclusion that  $x = -1$  is the more likely value. However, at best the data serve to demonstrate that  $x$  lies in the theoretically possible range. As an indication of the precision required to determine  $x$  theoretical lines for  $x = -\frac{1}{2}$  and  $x = -1$  are drawn through the point  $y$ . The data represented graphically in Figs. 19 and 21 confirm that the depolymerisation of polyoxymethylene glycols begins at the chain-end. The imprecise value for  $x$  does not exclude the possibility that the reaction is a molecular stepwise process since its value lies close to  $-1$  which can arise either from a chain-reaction with unimolecular termination or from a process in which depropagation plays the rate determining role.

#### 4.2.2. (c) Weight as a reaction variable.

In order to establish the validity of measuring rates of volatilisation of formaldehyde from degrading solid polyoxymethylene in the Grassie-Melville dynamic molecular still it was shown in section 2.4.2. (c), Figure 8, that over a range of weights up to 200 mg. the

initial specific rate,  $(dw/dt)/w$ , is constant at a given temperature, indicating that the reaction is not limited by heat and mass transfer and thus allowing the initial stages of the reaction to be studied directly [4.2.2. (a) and (b)]. Implicit in Fig. 8 is the conclusion that the weight order of the reaction is unity, i.e.  $dw/dt = kw$ . Sample 7 was used exclusively to establish this point since the limited amounts of the other samples did not permit an exhaustive examination of weight as a reaction variable. There is no reason to doubt the generality of first order behaviour. Recent theoretical work<sup>(72)</sup> suggests that the weight order of chain-end initiated depolymerisation reactions should be unity.

4.2.2. (d) Time as a reaction variable.

Kern and Cherdron reported<sup>(44)</sup> that the thermal depolymerisation of a polyoxymethylene glycol of DP = 40 showed first order behaviour throughout the whole course of the reaction in the temperature range 90-150°C. From this we can deduce that no complicating factors arise in the thermal reaction of low polymers. With the high molecular weight glycols examined in this study the picture is rather different, negative deviations from first order kinetics being observed. In this context a negative deviation is defined as arising when the rate of reaction falls off faster than

predicted by the integrated rate expression. Negative deviations were detected by plotting  $\log_e (\text{Rate}) = \log_e (V^2/V_0^2 - 1)$  against time. For a first order reaction this plot is linear, since

$$\left(\frac{dw}{dt}\right)_t = kw_t \quad \dots\dots (1), \text{ which integrates to}$$

$$w_t = w_0 e^{-kt} \quad \dots\dots (2):$$

Substitution for  $w_t$  in (1) gives

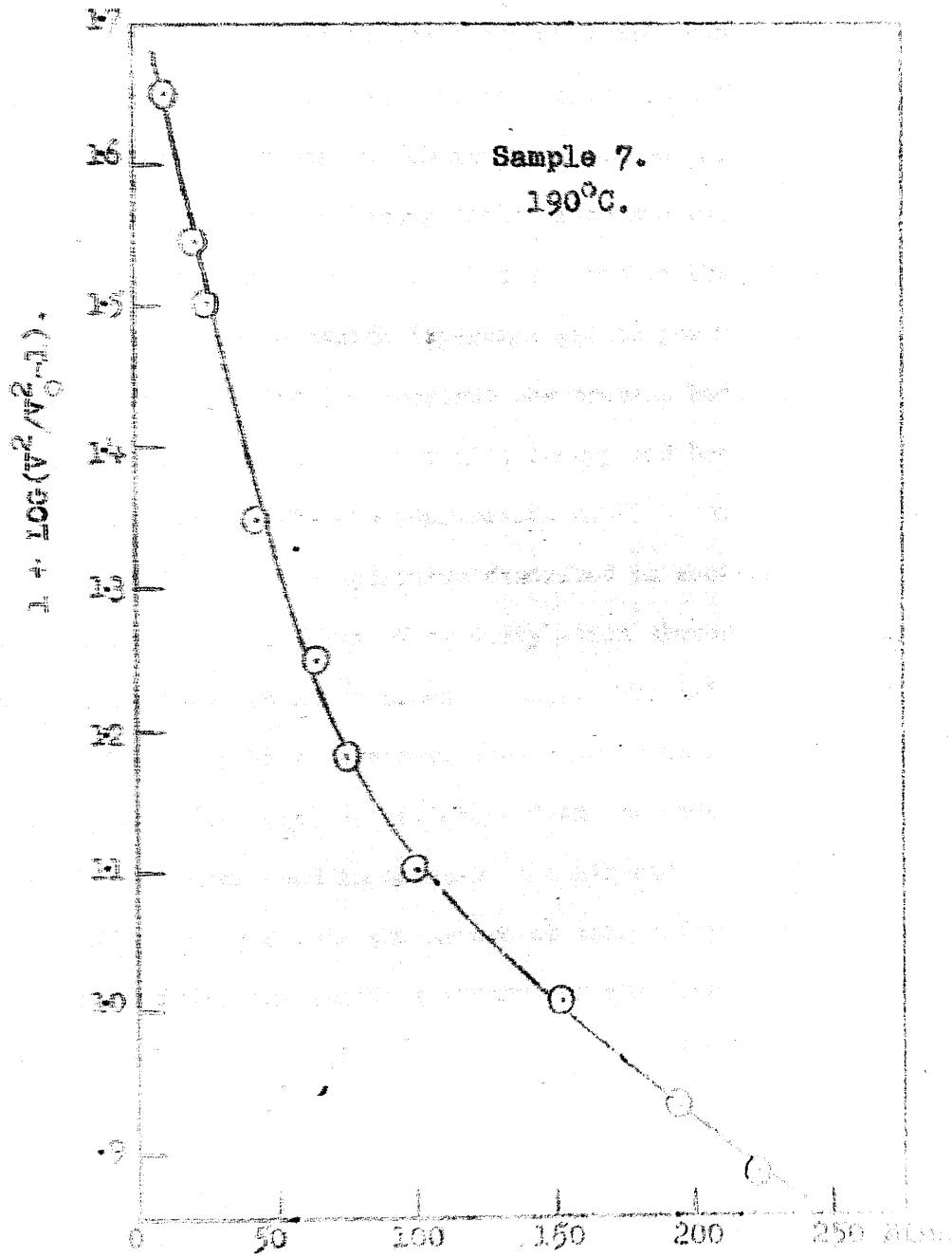
$$\frac{dw}{dt} = kw_0 e^{-kt}$$

$$\text{Hence } \log_e (\text{Rate}) = \log_e \frac{dw}{dt} = \log_e (kw_0) - kt \quad \dots\dots (3)$$

A typical plot of  $\log_e (\text{rate})$  versus time is shown in Figure 22. It is clear that  $k$ , as defined in equation (3) is not a constant. From this we can deduce that either the polymer is becoming more stable as the degradation proceeds, because a stabilising reaction is occurring, or that some molecules are more labile than others.

FIGURE 22.

$1 + \text{Log}(\text{Rate})$  versus time.



The latter possibility was found to be the case in the thermal depolymerisation of poly(methylmethacrylate)<sup>(48)</sup>, the molecules with unsaturated chain-ends being the more reactive. The presence of a "chain-end spectrum" in poly(methylmethacrylate) was associated with an increase in the activation energy of the reaction as the reaction proceeds. The possibility of a "chain-end spectrum" seems to be ruled out in the case of polyoxymethylene glycols since the results of 4.2.2. (b) suggest that all the unacetylated samples (S1, 2, 3, 5, 5, 7) contain at least one active centre (hydroxyl group) per molecule. The possibility that a chain-end spectrum was present had to be explored because an increase in activation energy had been observed [4.2.2. (a), Fig. 18]. 100% depolymerisation of S7 occurred at 130<sup>o</sup>C after 15 days in the apparatus described in section 2.6. Sample 8 which is obtained from S7 by acetylation showed no measureable degradation at 130<sup>o</sup>C after 15 days. The labile chain-end can therefore only be an hydroxyl group and further each molecule has at least one. The negative deviation from 1st order kinetics cannot therefore be explained in terms of a chain-end spectrum.

Further insight into the nature of this effect can be obtained by determining the relative amounts of the "fast" and "slow" phases at a variety of temperatures. A plot of log (% weight of

polymer remaining) versus time shows curvature similar to that of Fig. 22 and a typical plot obtained for sample 7 at 170°C is plotted in Figure 23. If the two lines EF, DC are assumed to represent two concurrent but independent molecular processes differing in energy then the relative amounts of the "fast" (represented by E) and "slow" (D) phases should be independent of temperature. Thus, in the case of poly(methylmethacrylate) the "fast" phase should always correspond to 50% of the sample if the two types of molecules react independently of each other. It is clear from Table 4.7 and Figure 24 that as the reaction temperature is increased the "fast" phase,  $W_F$ , increases. The increase in the ratio ( $W_F/W_S$ ) is clear proof that the negative deviation is not due to the concurrent and independent reaction of two different types of molecule present in fixed amounts in the original sample. The data suggests that two processes are in competition.

FIGURE 23.

Log(% Wt. remaining) vs. time.

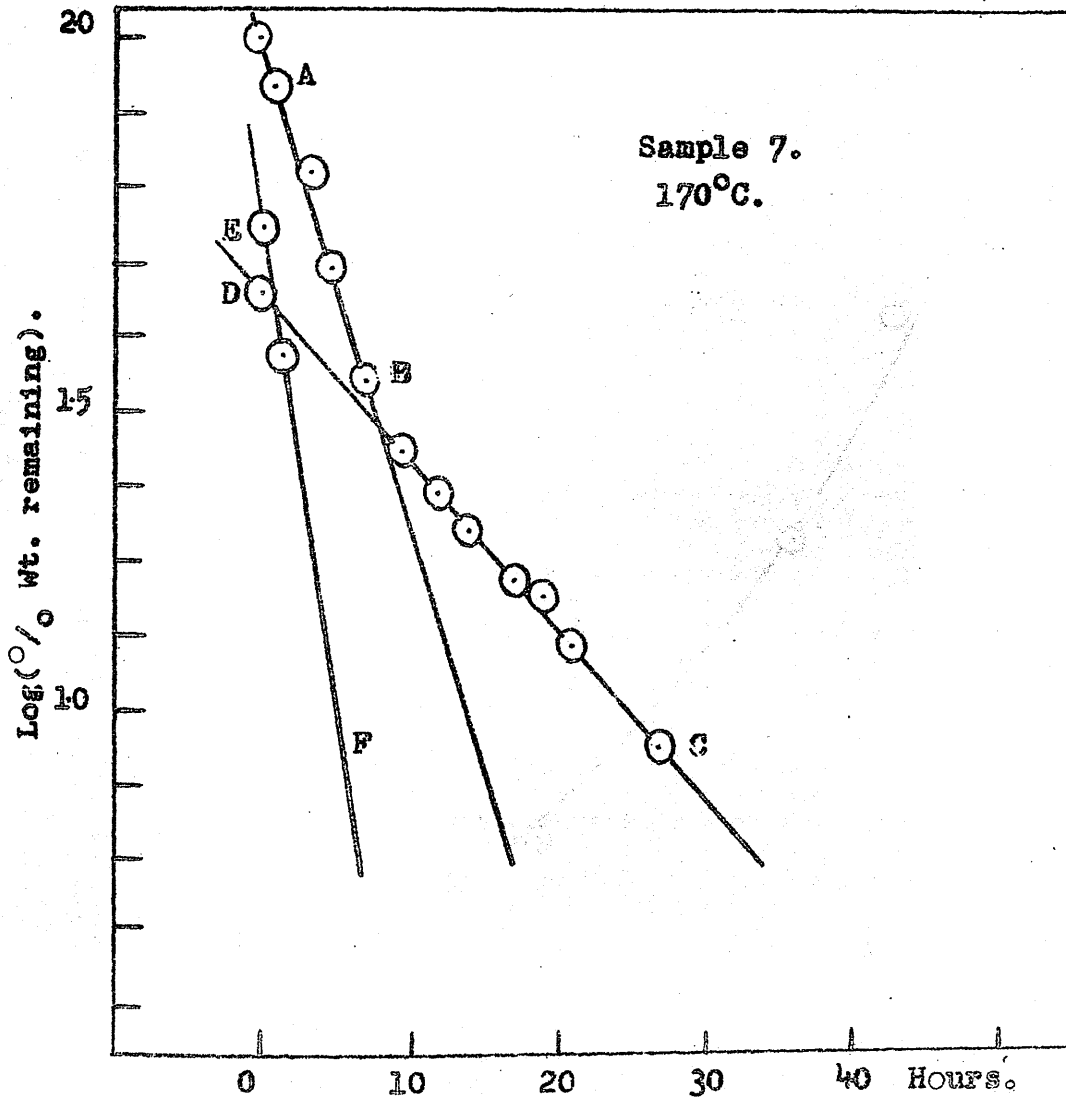


FIGURE 24.

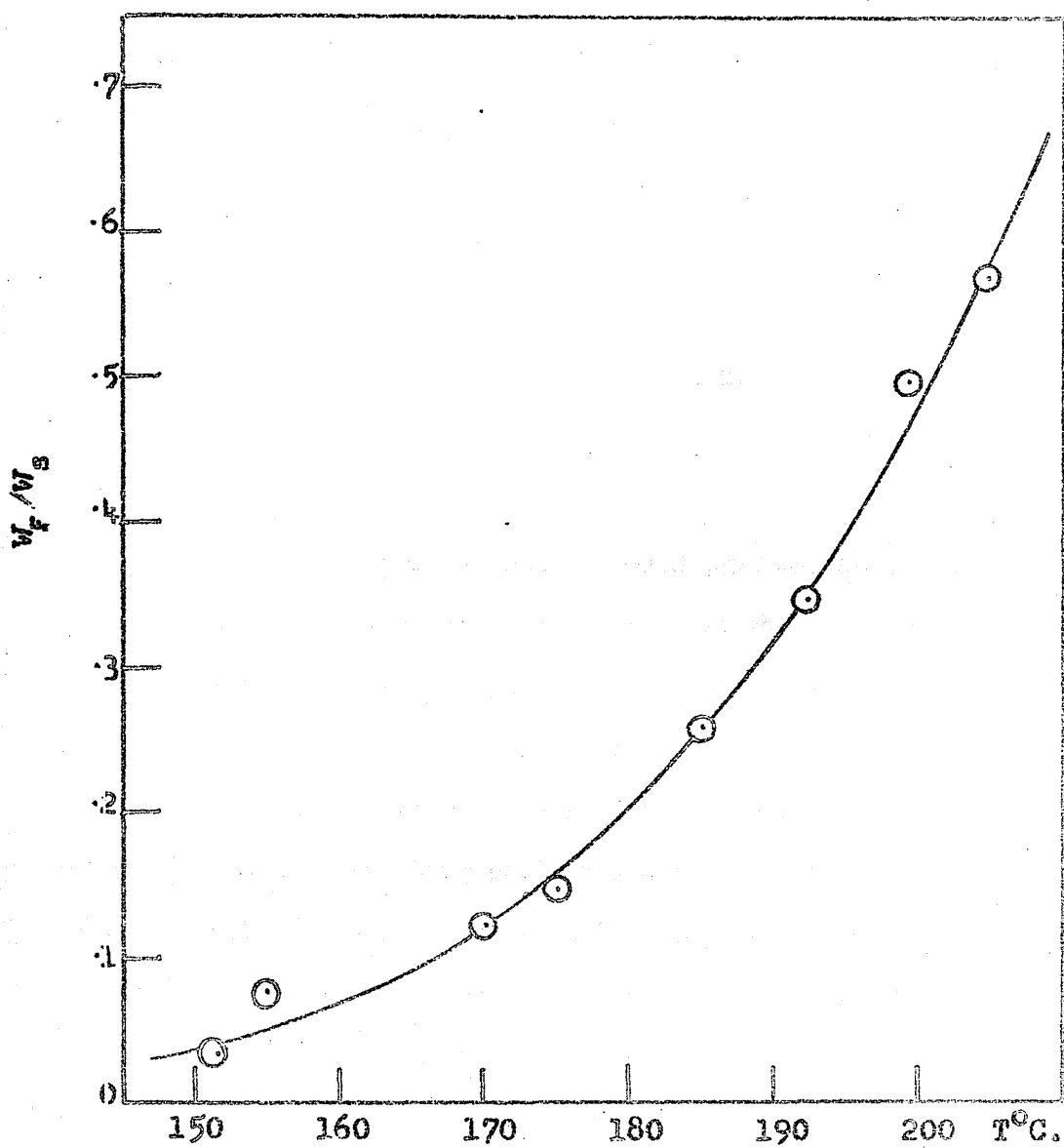




TABLE 4.7  
(WF/WS) versus Temperature for Sample 7

<u>%WT</u>	<u>%WS</u>	<u>WF/WS</u>	<u>T°C</u>
25.9	74.1	0.35	151.5
43.2	56.8	0.76	155.
55.2	44.8	1.23	170.
59.7	40.3	1.48	175
72.6	27.4	2.65	185
77.9	22.1	3.52	192
83.4	16.6	5.04	199.5

Chemical or physical factors could produce the observed effect. One possibility is that at temperatures below the crystalline melting point the amorphous phase of the polymer reacts more readily than the crystalline phase. As the temperature is raised the amount of amorphous phase increases and so (WF/WS) increases. If the amorphous phase is reacting preferentially then the density of the polymer should increase as degradation proceeds. The density of the polymer as a function of percentage degradation is discussed in section 4.2.3.. Another possibility is that a chemical reaction leading to stabilisation of ~~the~~ fraction of the chain-end is in

competition with depolymerisation but because its activation energy is lower than the activation energy for depolymerisation it becomes less significant at higher temperatures. The nature of possible stabilising reactions will be considered in Chapter 5 where the mechanism of depolymerisation will be discussed.

4.2.3. Polymer density as a function of percentage depolymerisation

The experimental evidence presented in 4.2.2. (d) led to the suggestion that amorphous solid polyoxymethylene glycols are less stable than crystalline materials. The evidence presented in Chapter 3 led to a similar suggestion. If the amorphous phase is more reactive than the crystalline phase and depolymerisation is faster <sup>than</sup> the crystalline-amorphous transition at a given temperature then it should be possible to observe an increase in crystallinity as reaction proceeds. Obviously, this hypothesis can only be tested at temperatures below the crystalline melting point (178°C).

The crystallinity,  $X_C$ , of a polymer is defined as the weight fraction of the crystalline phase, i.e.

$$X_C = \frac{W_K}{W_A + W_X} = \frac{W_X}{W_0} \quad \text{where}$$

$W_X$  is the weight of the crystalline phase,

$W_a$  is the weight of the amorphous phase and  $W$  is the weight of the sample. A relationship between  $X_c$  and the observable quantities  $W$  and  $\rho_0$ , the density of the sample can be derived as follows:

Let  $V_A$  and  $V_X$  be the volumes of the amorphous and crystalline phases respectively, then

$$V_A + V_X = V = W/\rho_0 \quad \dots\dots\dots(1)$$

and

$$\rho_X V_X + \rho_A V_A = W \quad \dots\dots\dots(2)$$

where  $\rho_A$  and  $\rho_B$  are the densities of the crystalline and amorphous phases respectively.

From (1)  $V_A = W/\rho_0 - V_X$

Substituting for  $V_A$  in (2) gives

$$\rho_X V_X + \rho_A (W/\rho_0 - V_X) = W$$

$$\therefore V_X (\rho_X - \rho_A) + \rho_A / \rho_0 \cdot W = W$$

$$\therefore V_X = W(1 - \rho_A/\rho_0) / (\rho_X - \rho_A)$$

$$X_C = W_X/W = \rho_X V_X/W$$

$$\therefore X_C = \rho_X (1 - \rho_A/\rho_0) / (\rho_X - \rho_A)$$

$$\therefore X_C = \frac{(1 - \rho_A/\rho_0) \rho_X}{(\rho_X - \rho_A)}$$

As indicated in Chapter 1, Carazzolo and Mammi<sup>(28)</sup> have recently established that P.C.M. can occur in hexagonal and orthorhombic modifications differing in the pitch of the polymer helix and also crystalline density. Table 4.8 summarises the results obtained with sample 7. Four determinations of polymer density, two before and two after 50% depolymerisation at 170°C were made.

X<sub>c</sub> is calculated for both hexagonal and orthorhombic models.

TABLE 4.8

Crystallinity, X<sub>c</sub>, of P.C.M. before and after 50% depolymerisation at 170°C.

$\rho_A = 1.25$	$\rho_x(\text{ORTHO}) = 1.54$	$\rho_x(\text{HEX}) = 1.492$
$\rho_o$	<u>X<sub>c</sub>(ORTHO)</u>	<u>X<sub>c</sub>(HEX)</u>
<u>Before Degradation</u>		
1.458	75.78	87.98
1.461	76.69	89.03
<u>After Degradation</u>		
1.474	80.72	93.71
1.470	79.50	92.29

Clearly the results are not unambiguous and in order to interpret them in terms of our hypothesis that amorphous regions are depolymerising preferentially to give an overall increase in density we have to assume the following. Firstly that the original sample contained only one type of crystalline phase and secondly that the increase in density is not due to thermal annealing. The latter assumption seems reasonable since Hammer, Koch and Whitney<sup>(69)</sup> have shown that for a polymer film ( $\bar{M}_n$  70,000) reversible melting-crystallisation occurs with little change in crystallinity if the film is kept below 181°C. The first of the above assumptions is the most difficult to justify. However, it leads to a serious ambiguity only if the original sample is predominantly hexagonal and if the hexagonal-orthorhombic transition is favoured. Independent evidence for the conclusion that sample 7 was predominantly orthorhombic before degradation is obtained from infra red spectroscopic evidence. Carazzolo and Marni<sup>(28)</sup> and more recently Zamboni and Zerbi<sup>(71)</sup> report that hexagonal and orthorhombic show differences in I.R. absorption particularly in the 7.75 $\mu$  band. The orthorhombic form shows a strong absorption at 7.75 $\mu$  whereas the hexagonal form shows negligible absorption (Fig. 5 and 6 of Ref. 28). It has also been established<sup>(71)</sup> that the orthorhombic-hexagonal transition is

preferred occurring <sup>at</sup> 75-80°C. We can therefore argue that the crystallinity of the sample can only have increased as the result of degradation at 170°C and that if the original sample was predominantly orthorhombic the increase could be as high as 17%. The density results then lend some support to the original hypothesis.

#### 4.2.4. $\bar{M}_n$ as a function of conversion to monomer.

The relationship between  $\bar{M}_n$  (I.R.) and  $[\eta]$  was discussed in 4.2.2. (b) where it was shown that the two available methods of estimating the average molecular weight gave consistent results. The two methods were used to measure the change in molecular weight as a function of conversion to monomer. The results presented in this section are based exclusively on measurements carried out with samples S7 and S8 in the dynamic molecular still (2.4.2.) at three degradation temperatures - 160°, 170° and 175°C. In early experiments only  $\bar{M}_n$  (I.R.) was measured but later, when the viscosity method had been developed, the  $\bar{M}_n$  (I.R.) was measured first and the cold pressed disc then weighed and dissolved in 95% aqueous P.F.A.H. and  $[\eta]$  measured (2.3.1.). The results obtained are summarised in Table 4.9 and Figs. 25 and 26.

FIGURE 25.

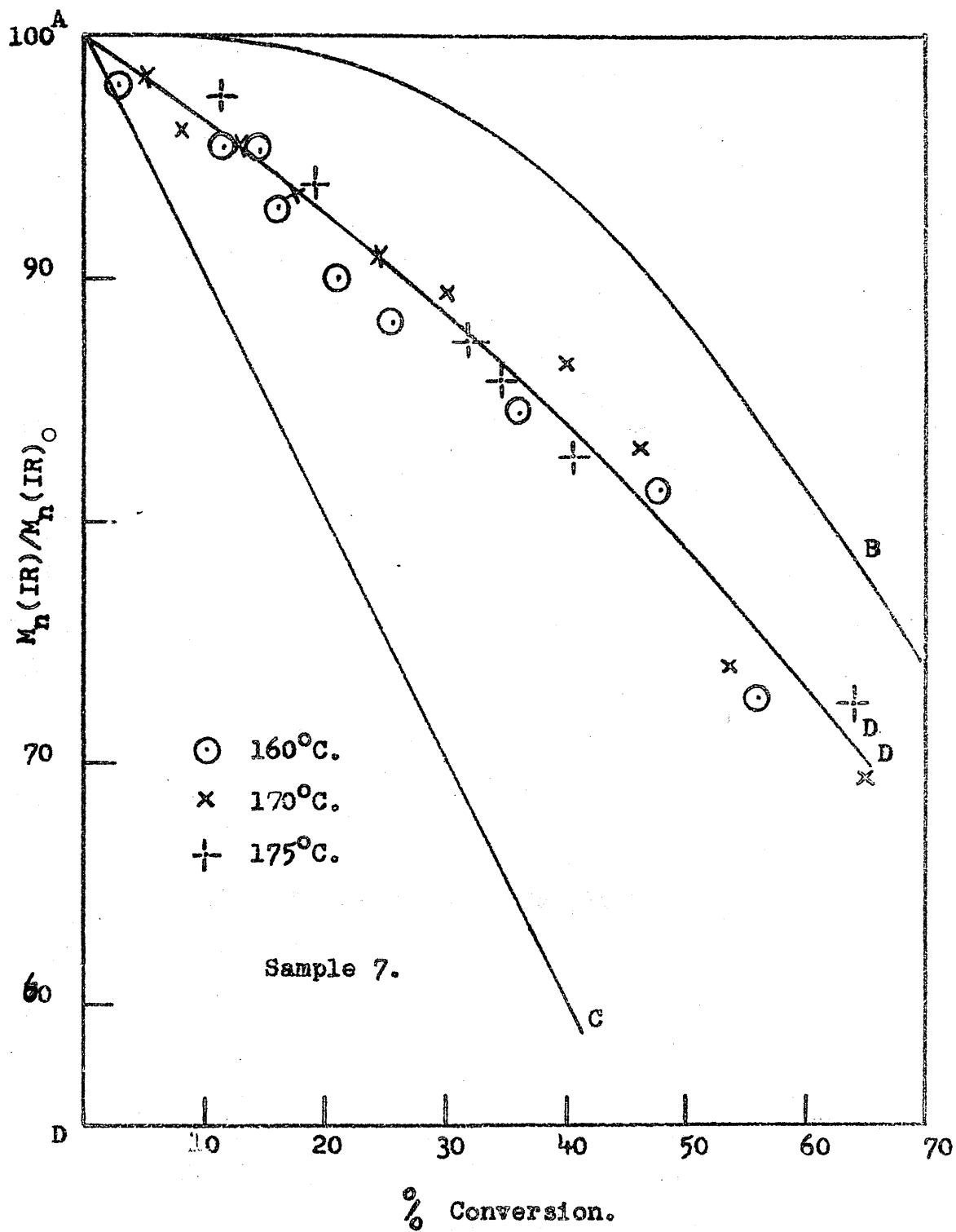


FIGURE 26.

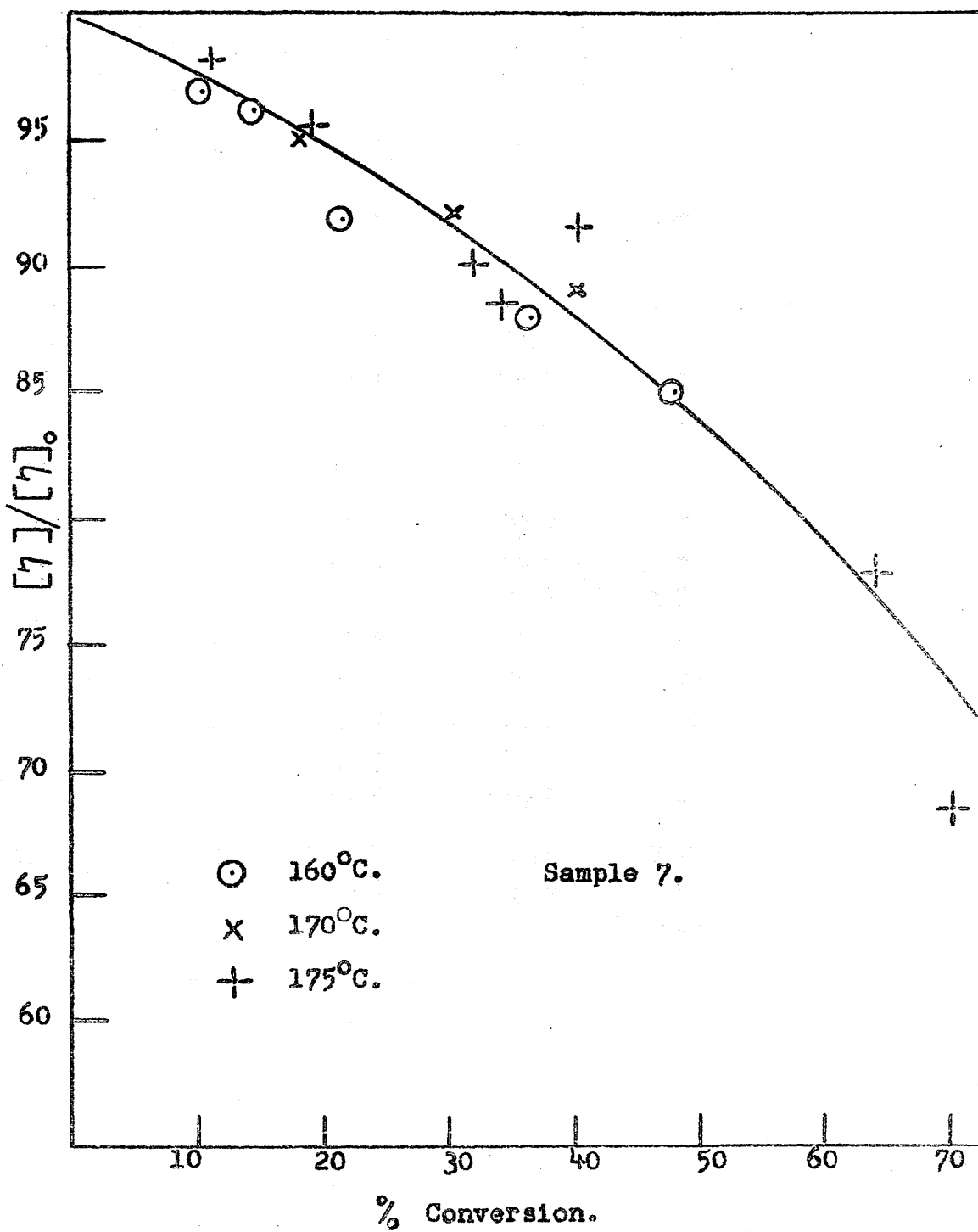




TABLE 9

Temp.	% Conversion	$\bar{M}_n$ (I.R.)	$\bar{M}_n$ (I.R.) <sub>0</sub> = $24 \times 10^3$		$[\eta]_0 = 4.05$		$\alpha$
			$\bar{M}_n$ (I.R.)	$\bar{M}_n$ (I.R.)%	$[\eta]$	$[\eta]/[\eta]_0$	
160	3.2	23.5	97.9	-	-	-	
	10.6	22.9	95.4	3.92	96.8	.60	
	14.5	22.9	95.4	3.89	96.0	.86	
	16.0	22.3	92.9	-	-	-	
	21.4	21.6	90.0	3.72	91.9	.80	
	25.2	21.2	88.3	-	-	-	
	36.4	20.3	84.6	3.56	87.9	.77	
	47.7	19.5	81.2	3.44	84.9	.79	
	56.8	17.5	72.9	-	-	-	
170	5.1	23.6	98.3	-	-	-	
	13.2	22.9	95.4	-	-	-	
	17.2	22.4	93.3	3.85	95.0	.74	
	24.2	21.8	90.8	-	-	-	
	30.2	21.4	89.2	3.73	92.1	.72	
	40.0	20.7	86.2	3.61	89.1	.78	
	46.1	19.9	82.9	-	-	-	
	65.5	16.7	69.6	-	-	-	
175	11.3	23.4	97.5	3.98	98.3	.67	
	18.9	22.5	93.7	3.87	95.6	.69	
	31.8	20.9	87.1	3.65	90.1	.76	
	34.3	20.6	85.8	3.58	98.4	.73	
	40.2	19.8	82.5	3.70	91.4	.47	
	64.0	17.4	72.5	3.15	77.8	.78	
	70.3	15.3	63.7	2.77	68.4	.84	

In order to check the  $\bar{M}_n$  (I.R.) results against the viscosity results, the Mark-Houwink exponent,  $a$ , was calculated where both measurements had been made. Most values lie in the range 0.70 to 0.80 with an average value of 0.74 which compares reasonably well with the value of 0.81 calculated from the data for samples S1, 2, 3, 5 and 7 [Fig. 20, 4.2.2. (b)]. The two methods, therefore, give mutually consistent results for sample 7. It is clear from Fig. 25 that the results are far from precise. As a guide to the interpretation of the results the diagonal AC of Fig. 14 is drawn and the theoretical curve AB, derived by Sinha and Wall<sup>(73)</sup> for chain-end initiated depolymerisation with zip-length greater than the average degree of polymerisation, is also drawn. From Fig. 25 we can deduce that the average zip-length, i.e. the number of monomer units produced by each depolymerising chain, is less than the average degree of polymerisation. The experimental curve AD lies well above the diagonal AC and thus the reaction is not a step reaction and further transfer reactions which would lead to random chain scission and hence an experimental curve below the diagonal AC. The results give no clear indication that the zip-length is a function of temperature. The  $[\eta]$  of sample 8, obtained from S7 by acetylation of the chain-end hydroxyl, was measured as a function of conversion at 175°C up to a maximum conversion of 46%. The results obtained are summarised in Table 410 and fig. 27.

FIGURE 27.

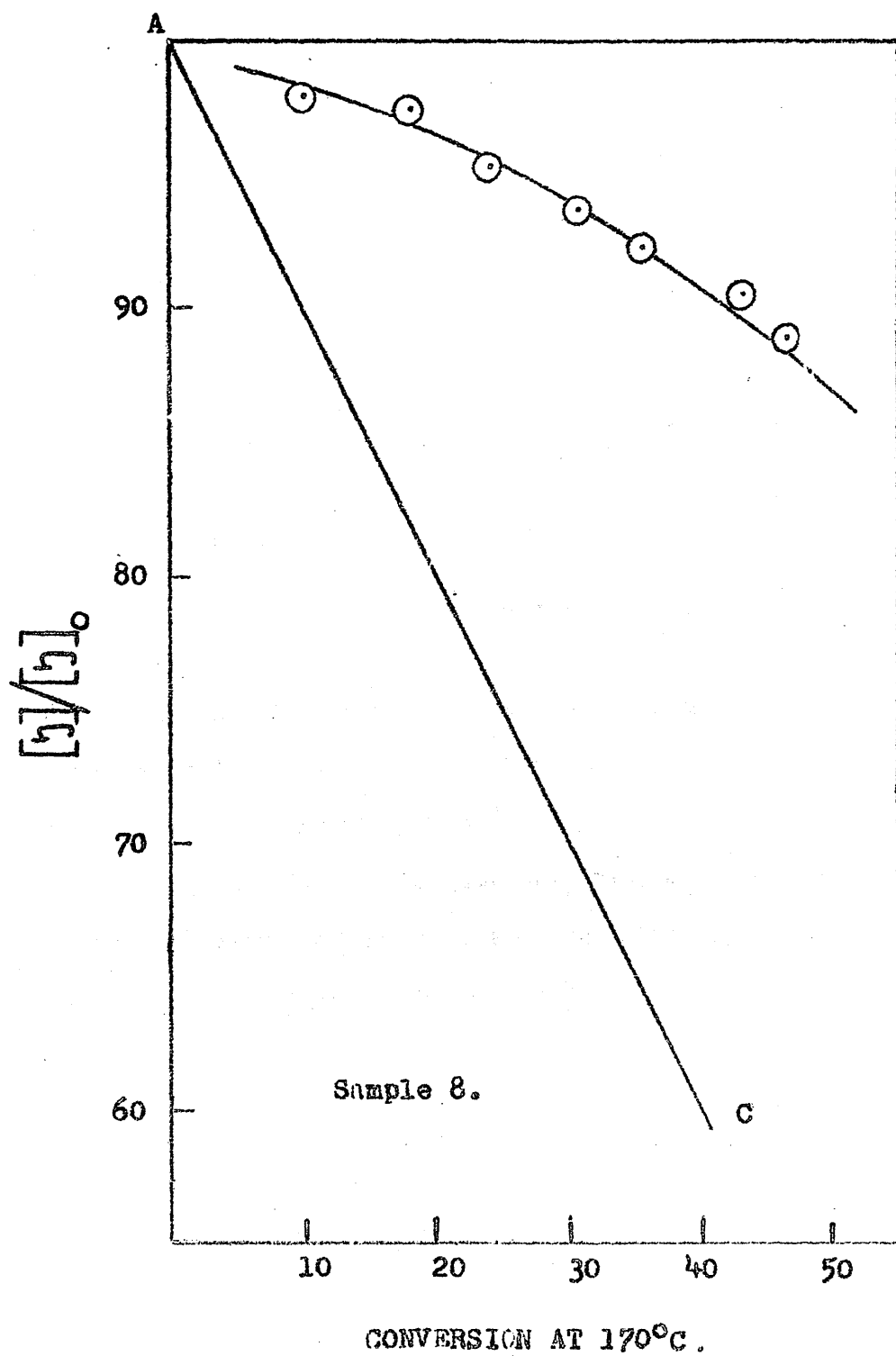


TABLE 4.10

Sample 8, AcO(CH<sub>2</sub>O)<sub>n</sub>Ac,  $[\eta]_0 = 4.01$

<u>% Conversion</u>	<u><math>[\eta]</math></u>	<u><math>[\eta]/[\eta]_0(\%)</math></u>
10.0	3.93	98.1
18.1	3.90	97.4
24.2	3.82	95.3
30.8	3.76	93.7
35.5	3.70	92.2
43.1	3.63	90.6
46.4	3.57	89.0

The results show that the molecular weight changes occurring in the thermal depolymerisation of the acetates are similar to those occurring in the thermal depolymerisation of the parent glycol. This clearly establishes that the depolymerisation of the acetates is chain-end initiated and that the zip-length is large though less than the average degree of polymerisation.

## Chapter 5

### The Thermal Depolymerisation of Polyoxymethylene

#### Part 2 The Mechanism of the Reaction.

##### 5.1 Introduction

The results of product analyses and catalysis and inhibition experiments are reported in this chapter. It will be shown that within the limits of sensitivity of the analytical techniques available evidence for products that could conceivably arise from a free radical reaction, initiated at the polymer chain-end, is lacking and that the action of free radicals inhibitors gives scant support to a free radical mechanism. It will also be shown that depolymerisation is susceptible to catalysis by basic materials, a result confirmed by Czech workers. (74)

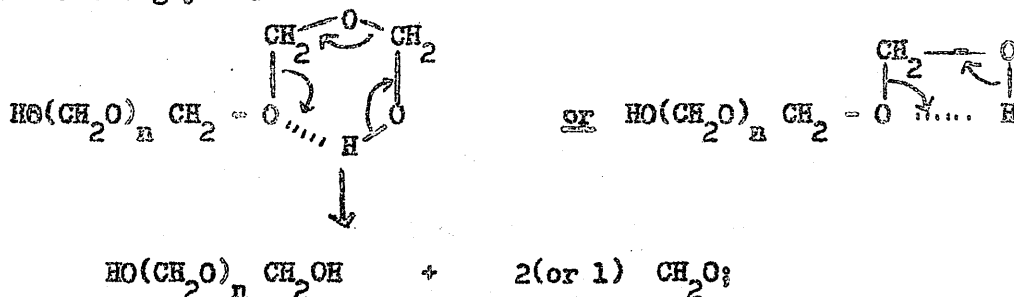
While it is possible to suggest free radical and molecular mechanisms for the depolymerisation of both the glycols and their acetate derivatives in addition to an ionic mechanism for the glycols it is concluded that the molecular mechanism for the thermal depolymerisation of both the glycols and the acetates is the most plausible. The various schemes that can be suggested are discussed in the next section.

## 5.2. Mechanistic schemes - Theoretical

### 5.2.1. The Molecular Mechanism

A mechanism is never completely established for any reaction in the sense that there always remains the possibility that new evidence which it cannot rationalise may be found. In the case of the thermal degradation of polyoxymethylene the situation is superficially clear-cut if we accept the data of earlier workers. Thus Staudinger<sup>(5)</sup> reported that monomer and water or acetic anhydride were produced in quantitative yield in the thermal degradation of polyoxymethylene glycols or their acetate derivatives. We can therefore reasonably suggest an intramolecular mechanism for the depolymerisation of both types of polymer which yields the reported products and no others.

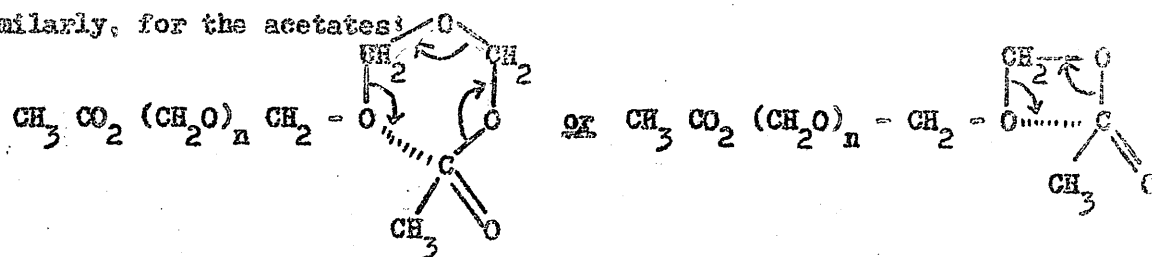
Thus for the glycols:



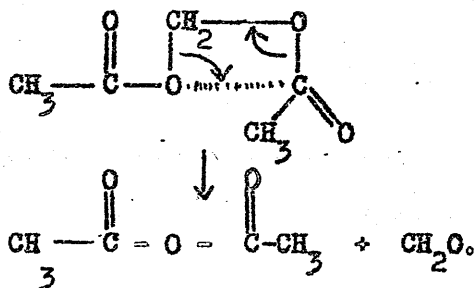
finally:



Similarly, for the acetates:



finally:

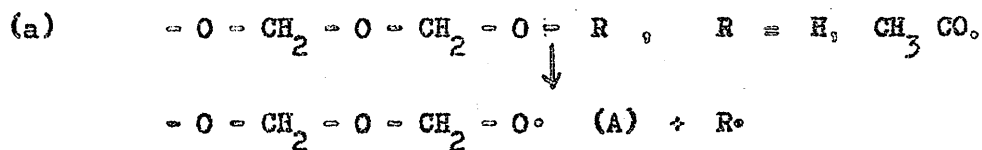


Concerted electron shifts round the postulated 4 or 6 membered transition states would be facilitated: in the glycol by the electrostatic effect of the hydrogen bond and in the acetate by the inductive effect of the carbonyl group.

Two points prompt a consideration of the other two possibilities. Firstly the ubiquity of free radicals in polymer degradation reactions and secondly the fact that the hydroxyl chain-ended polymers are produced by an ionic polymerisation reaction and are known to degrade ionically in aqueous solution<sup>(9)</sup>. Consideration of the nature of the "active centres" through which polymer-monomer equilibrium is established (Chapter 3) led Dainton to the view that they were probably molecular. They could conceivably be ionic and this idea will be explored below (5.2.3.)

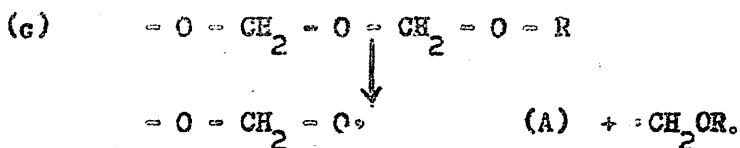
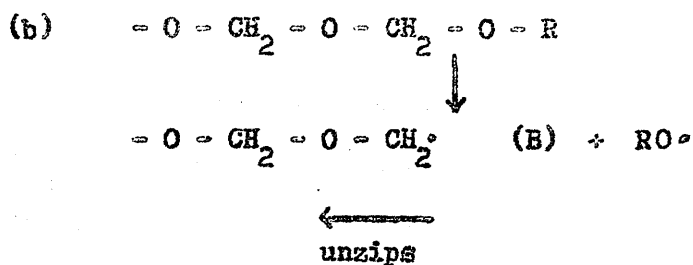
### 5.2.2. The Free Radical Mechanism

The evidence of chapter 4 confirms the conclusion of earlier workers that the thermal degradation of polyoxymethylene is chain-end initiated. Confining our attention to the chain-end we see that there are three possible sites for a chain-initiating homolytic bond-scission, designated (a), (b) and (c) thus



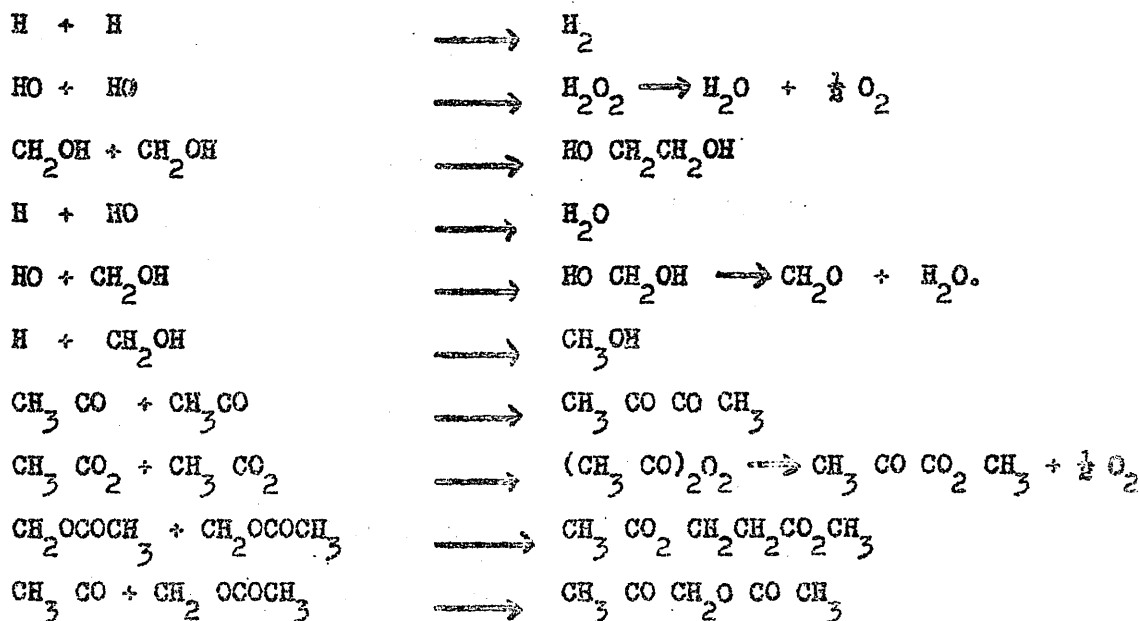
←  
unzips





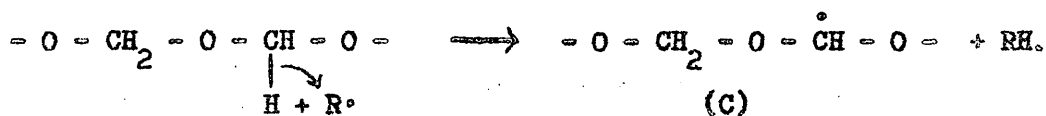
Each of the two polymer radicals, (A) and (B), produced by the bond scissions (a), (b) and (c) would unzip to monomer. The high yields of monomer observed are thus adequately explained by a free radical mechanism. The primary radicals, R , RO , CH<sub>2</sub>OR, could either combine or abstract hydrogen atoms, thus:

Combination



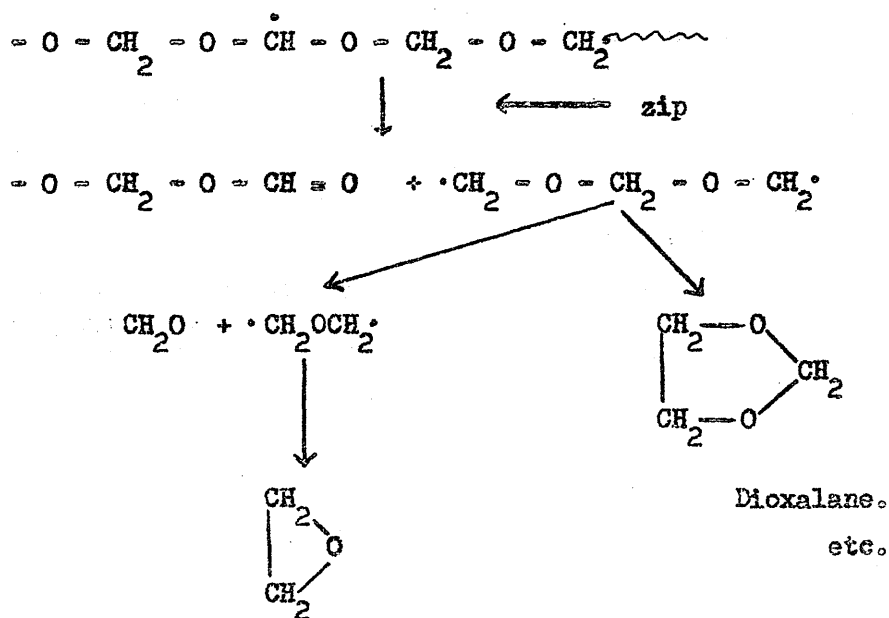
Hydrogen Abstraction

Hydrogen abstraction by the primary radicals,  $\cdot\text{H}$ ,  $\text{HO}\cdot$ ,  $\text{CH}_2\text{OH}\cdot$ ,  $\text{CH}_3\text{CO}\cdot$ ,  $\text{CH}_3\text{CO}_2\cdot$  and  $\text{CH}_2\text{O CO CH}_3\cdot$ , would produce  $\text{H}_2$ ,  $\text{H}_2\text{O}$ ,  $\text{CH}_3\text{OH}$ ,  $\text{CH}_3\text{CHO}$ ,  $\text{CH}_3\text{CO}_2\text{H}$  and  $\text{CH}_3\text{O COCH}_3$ , thus



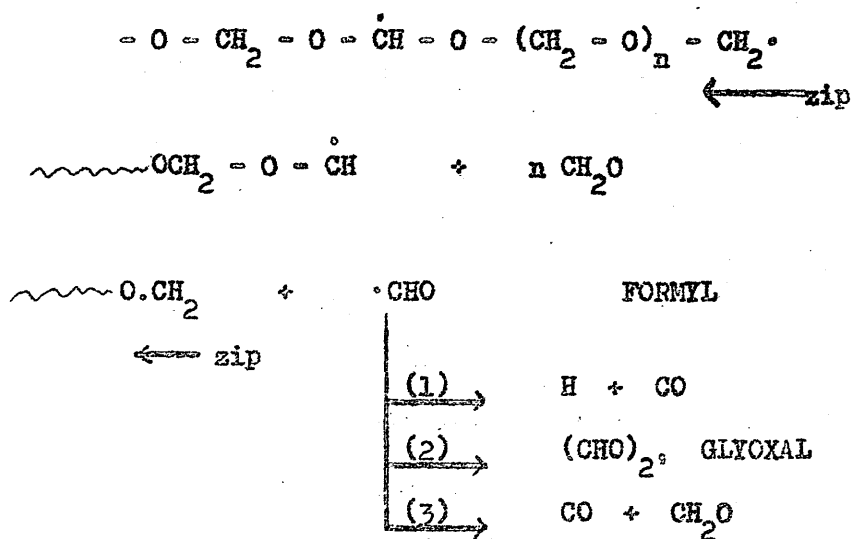
The polymer radical, C, thus produced could either undergo chain scission, yielding a polymer radical capable of depolymerising and an aldehyde chain-end, or survive long-enough to be depolymerised, thus:

Chain scission of (C)

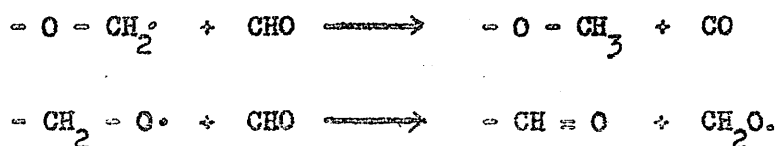


Chain scission is ruled out by the molecular weight evidence presented in Chapter 4.

depolymerisation of (C)



In Kutschke's view <sup>(75)</sup> reaction (3) is the most probable since in the temperature range 80 - 180°C he did not observe hydrogen or glyoxal in the products of the reaction between methyl radicals and formaldehyde. We can also envisage disproportionation with a polymer radical, thus



It is clear therefore that if a free radical mechanism is operating in the thermal degradation of polyoxymethylene at temperatures between room temperature and 200°C the products must include small quantities of the various products which the above theoretical scheme predicts. For convenience these are summarised in Table 5.1.

TABLE 5.1

Predicted Degradation Products of a Free Radical Reaction

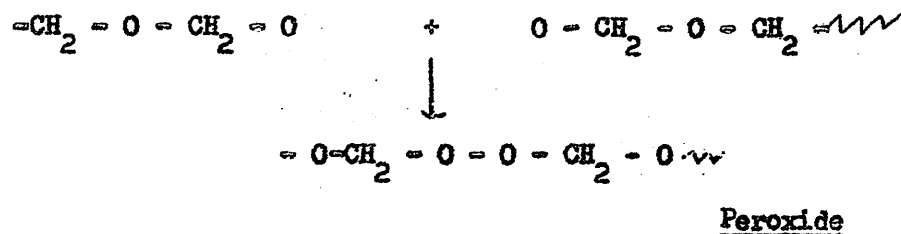
<u>Polymer</u>	$\text{HO}(\text{CH}_2\text{O})_n\text{H}$	$\text{CH}_3\text{COO}(\text{CH}_2\text{O})_n\text{COCH}_3$
<u>Products</u>		
<u>Major</u>	$\text{CH}_2\text{O}$	$\text{CH}_2\text{O}$
<u>Minor</u>	$\text{H}_2\text{O}, \text{H}_2, \text{O}_2, \text{CO}$	$\text{O}_2, \text{CO}_2, (\text{CH}_3\text{CO})_2, (\text{CH}_3\text{CO})_2, \text{CH}_3\text{CHO}$
	$\text{HOCH}_2\text{CH}_2\text{OH}, \text{CH}_3\text{OH}, \text{CH}_2-\underset{\text{O}}{\text{CH}_2}$	$\text{CH}_3\text{CO}_2\text{H}, \text{CH}_3\text{OCOCH}_3, \text{CH}_3\text{COCH}_2\text{CH}_2\text{CO}_2\text{CH}_3$
	$(\text{CHO})_2$ Dioxalane	

If all the initiation reactions, (a), (b) and (c) postulated above were occurring then we envisage bimolecular combination and

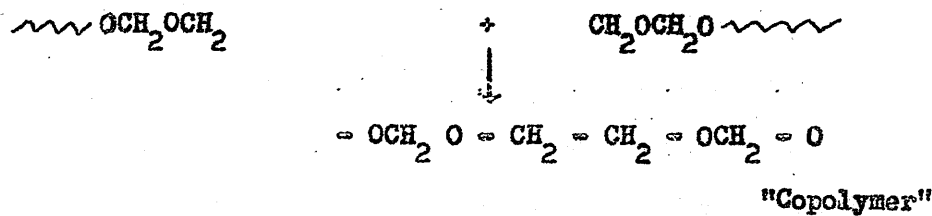
disproportionation reactions as follows:

Combination

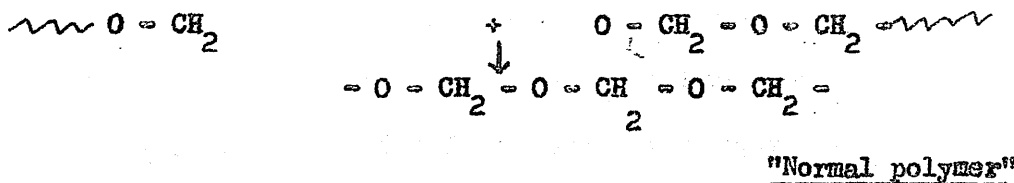
(1) (A) + (A)



(2) (B) + (B)

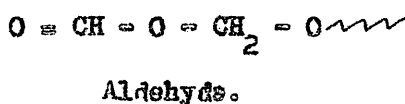
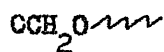
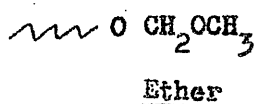


(3) (A) + (B)



Disproportionation

(4)  $\text{O-CH}_2$



Reactions (2) and (4) are stabilising reactions since a copolymer (c.f. "CELCON") and an ether chain-ended polymer are produced, both of which we have already seen to be more stable than the glycol. The aldehyde chain-end is the terminal structure suggested by Carruthers and Norrish<sup>(23)</sup> in their study of the polymerisation of gaseous formaldehyde. Recently it has been suggested<sup>(76)</sup> that the aldehyde chain-end is more stable than the hydroxyl chain-end. Thus reaction (4) produces two fragments with chain-ends more stable than the original chain-end. The peroxide produced by reaction (1) would be unstable at reaction temperatures. Reactions (2) and (4) could explain the negative deviations from first order kinetics reported in Chapter 4.

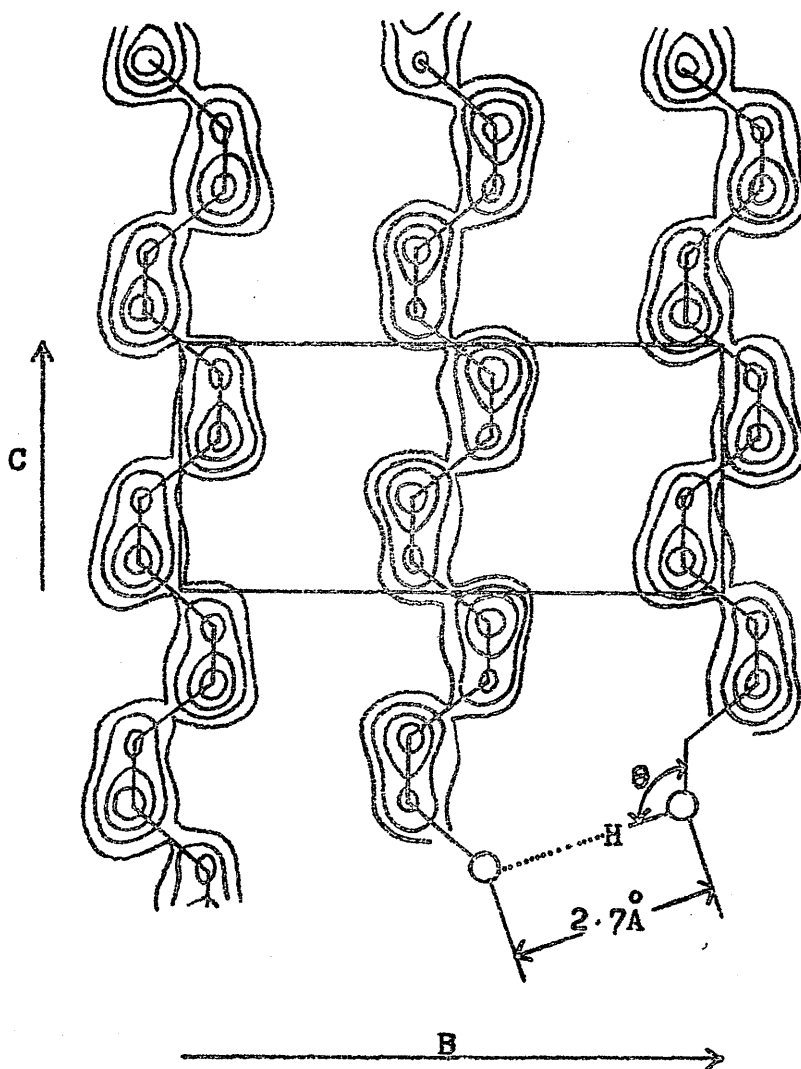
What experimental evidence is there for a free radical mechanism? There is no evidence in the old literature for products other than  $\text{CH}_2\text{O}$  and  $\text{H}_2\text{O}$  from the thermal depolymerisation of the hydroxyl chain-ended polymers. More recently Kern and coworkers<sup>(76)</sup> reported that these were the only products of the thermal depolymerisation found by a gas chromatographic method in complete contrast to the products produced in acidolytic degradation which they were studying.

The most obvious way of checking the free radical mechanism suggested above seemed to be to look for  $H_2$  and CO which are the only compounds, among the products that could conceivably arise from such a mechanism, that are non-condensable at liquid nitrogen temperatures. The results of product analyses will be discussed in section 5.3.

### 5.2.3. The Ionic Mechanism

The ionic nature of the depolymerisation of oligomers in aqueous solutions has been established and the possibility of an ionic mechanism operating in the solid phase decomposition must be considered. The most prohibitive single factor in heterolysis is the large energy required for charge separation. In solution in polar solvents this is invariably compensated by exothermic solvation. In the solid state there is no compensation in the case of molecular compounds. However, as Fig. 28 shows the (O ... O) distance in the bc plane of the POM crystal of 2.7 Å and the  $C - \widehat{O} \dots O$  angle of  $108^\circ$  provide ideal geometry for a hydrogen-bond between a chain-end hydroxyl and an ether oxygen of an adjacent chain. The wave-mechanical representation of the hydrogen-bond<sup>(78)</sup> includes 2% of the canonical form  $(-O^- \text{H} - \overset{+}{O})$  in the resonance hybrid. The next step in a speculative argument of this sort would be to suggest that a

FIGURE 28.



$$b = 7.65 \text{ \AA}; c = 3.56 \text{ \AA}; \theta = 108^\circ.$$

bc plane of POM crystal.

(after Carazzolo and Memmi; ref 28.)



depolymerising Oxanion, identical to the proposed propagating species in the polymerisation of formaldehyde, might be generated by the thermal excitation of the hydrogen bond and that as depolymerisation proceeds the proton keeps within an electrostatically determined "equilibrium" distance by "jumping" from one ether oxygen to the next on the adjacent polymer chain. The proton is thus visualised as a "zipper" unzipping the chain as it tunnels between two adjacent chains. The  $H - O^+$  bond would be formed exothermically and thus the proton "solvation energy" required to bring the overall activation energy within reasonable bounds might be supplied. The oxonium ion,  $-CH_2 - \overset{+}{O} - CH_2 -$ , would lead to chain-scission, thus



and since this would most probably be a random reaction the molecular weight of the polymer would be expected to fall below the diagonal of Fig. 14. The molecular weight results reported in 4.2.4. would suggest that if an ionic mechanism is operating it does not lead to random chain scission.

The principle of microscopic reversibility requires that there should be a depolymerisation route through the oxanionic structure occurring in polymerisation. This suggests that the active centres through which the polymerisation-depolymerisation equilibrium is established might be anionic. The results of "catalysis" experiments (5.4.) with basic catalysts clearly establishes that depolymerising anions can participate in the depolymerisation of polyoxymethylenes though the "half-lives" of the catalysed reactions are very much shorter than that of the purely thermal reaction. This suggests that if an anionic mechanism is operating in <sup>the</sup> latter reaction it is associated with an unfavourable dissociation equilibrium as an initiation step.

### 5.3. Product Analysis

#### 5.3.1. Non-condensables

The gas analysis apparatus described in 2.5 was used for the purpose of detecting and identifying non-condensable products. The sensitivity of the apparatus is determined as follows. Given that the pressure,  $p$ , registered by the McLeod gauge is  $p = (h)^2 \times 2.090 \times 10^{-5}$  m.m. Hg., where  $h$  is the reading on the gauge in m.m., and assuming that a reading of 1 m.m. is the limit of detection the minimum pressure that can be detected by the

Mercurial gauge is  $2.090 \times 10^{-5}$  m.m. Hg.. The volume of the gas analysis unit varied from run to run but was usually between 400 and 410 mls.. The minimum number of moles of non-condensable (NC) detectable at  $0^{\circ}\text{C}$  in 400 mls. is  $2.5 \times 10^{-10}$  moles. In a 300 mg. sample of high molecular weight POM there are  $10^{-2}$  base moles of  $\text{CH}_2\text{O}$  and hence  $10^{-2}$  moles total  $\text{H}_2$ . The number of moles of chain-end hydrogen is  $10^{-2}/\text{D.P.}$ , assuming two hydroxyl groups per molecule. Infra red evidence suggests a DP of about  $10^4$  for sample 7 so in this case there are  $10^{-6}$  moles of chain-end hydrogen in a 300 mg. sample. It is thus possible to detect to 1 part in  $10^4$  if  $\text{H}_2$  is produced in chain-end initiation reactions.

It was found that even at temperatures as low as  $135^{\circ}\text{C}$  non-condensable products were being produced. Table 5.2 gives a summary of the results obtained with Sample 7.

TABLE 5.2.

See page 124.

TABLE 5.2.

Temp °C	P mg	B moles $\times 10^3$	M moles $\times 10^3$	NC moles $\times 10^8$	NC/M% $\times 10^3$	M/B=D%	NC/D $\times 10^6$
135	416.3	13.8	6.5	1.75	2.7	5	35
150	350.6	11.6	1.16	0.21	1.8	10	2.1
172	200.4	6.68	0.93	0.87	9.4	14	6.2
172	204.0	6.80	1.22	1.80	15.0	16	11.2
172	304	10.1	5.65	9.37	16.6	56	16.7
184	208.6	6.95	2.91	5.24	18.0	42	12.5

Key

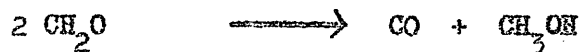
- P = Polymer
- B = Base moles
- M = Monomer
- NC = Noncondensable
- D = % degradation

Blank experiments established that degassing of the glass surfaces in reaction tube, R2, (Fig. 10) at a temperature of 180°C contributed not more than  $5 \times 10^{-10}$  moles to the NC yield.

The results establish beyond reasonable doubt that non-condensables are being produced under the conditions of this experiment.

Combustion analysis with CuO at  $300 \pm 10^\circ\text{C}$  conclusively established that not more than  $5 \times 10^{-10}$  moles of  $\text{H}_2$  per 300 mg. of Polymer is produced after 50% degradation. That is not more than 0.1% of available chain-end hydrogen is reacting according to the initiation reaction (a) above. This conclusion is based on the fact that in all combustion runs using CuO the non-condensable pressure fell to "zero" (at  $-196^\circ\text{C}$ ) after 20-30 minutes combustion to yield a pressure of  $\text{CO}_2$  at  $-80^\circ\text{C}$  that was equivalent to the original NC pressure to within experimental error. If  $\text{H}_2$  had been present the  $\text{CO}_2$  pressure at  $-80^\circ\text{C}$  would have been less by an amount equivalent to the pressure of  $\text{H}_2$  at  $-196^\circ\text{C}$ . The non-condensable fraction of the products could be either CO or  $\text{CH}_4$  on this evidence. To distinguish between the possibilities  $\text{I}_2\text{O}_5$  at  $140^\circ\text{C}$  was used as oxidant since it has been found that at temperatures in the range  $140 - 150^\circ\text{C}$   $\text{I}_2\text{O}_5$  is completely unreactive to  $\text{CH}_4$ .<sup>(54)</sup> The non-condensable was established as CO since it was completely oxidised by  $\text{I}_2\text{O}_5$  in about 45 minutes.

The fact that CO has been established as a minor product does not represent adequate proof for a free radical mechanism because Steacie and Calvert established<sup>(79)</sup> that gaseous formaldehyde undergoes very slow heterogeneous thermal decomposition in the temperature range 150-300°C as follows

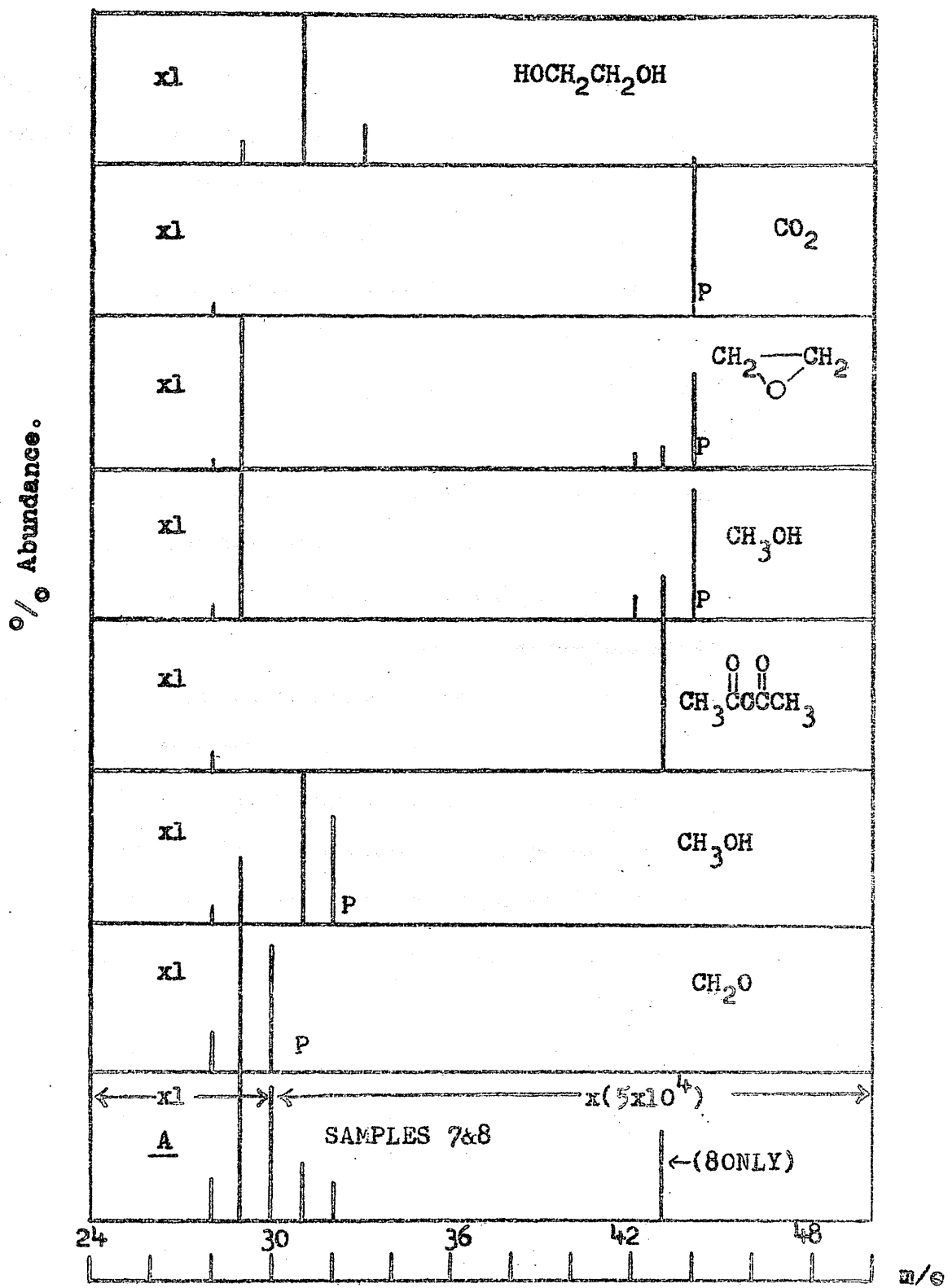


The mechanism of this reaction is still obscure. Its occurrence makes any argument based on CO production ambiguous as far as the thermal decomposition of the polymer is concerned. Analysis for the other possible products is thus essential if the argument is to be taken any further.

### 5.3.2. Mass Spectrometric Analysis

Fig. 29 represents the mass spectra of some of the compounds listed in Table 5.1. These spectra are based on the mass spectral data published by the American Petroleum Institute, Research Project 44. All ions with an abundance less than 5% have been ignored and parent ions, where these occur, have been marked with a P. The mass spectrum has three major peaks at  $m/e = 28, 29, 30$  corresponding to  $\text{CO}^+$ ,  $\text{HCO}^+$  and  $\text{H}_2\text{CO}^+$ . Above  $m/e = 30$  the spectrum

FIGURE 29.  
MASS SPECTRA.



is clear and by turning the ion-current at  $m/e = 30$  up to the point at which a full scale deflection was obtained on the least sensitive galvanometer it was possible to look for ions with the most sensitive galvanometer with a sensitivity of 1 in  $5 \times 10^4$  of the  $\text{CH}_2\text{O}^+$  current. Peaks at  $m/e = 31$  and  $32$  suggested that  $\text{CH}_3\text{OH}$  was present among the products as might be expected if the Steacie - Calvert reaction were operating. A small peak at  $m/e = 28$  in the most sensitive spectrum when a liquid nitrogen trap was placed on compartment B of the apparatus shown in Fig. 12 confirms CO as the non-condensable product discussed <sup>in</sup> 5.3.1.. The only conclusion to be drawn from the fact that all spectra (A) obtained for Sample 7 were "clean" above  $m/e = 32$  and that all spectra for sample 8 had only  $m/e = 43$ , corresponding to  $\text{CH}_3\text{CO}^+$  from acetic anhydride, is that at temperatures up to  $200^\circ\text{C}$  free-radicals play little part in the thermal degradation of polyoxymethylenes.

The mass spectrometric results put a maximum limit of about  $10^{-3}\%$  on the occurrence of most of the minor products listed in Table 5.1. and it is concluded that little support can be given to a free radical mechanism by the available data. The conclusion seems amply justified by the results of the "inhibition" experiments reported in 5.4..



#### 5.4. Catalysis and Inhibition Experiments.

The experiments reported in this section were designed to provide specific information about the mechanism of the thermal depolymerisation of the polyoxymethylene diacetates and their parent glycols. As indicated in 5.2. plausible mechanistic schemes involving all possible intermediates, molecular, ionic and free radical can be postulated. Though the results of product analyses seemed to eliminate the possibility of free radical participation the study of the effect of the free radical inhibitors D.P.P.H. and 1:4 diamino anthraquinone seemed to be worthwhile. Similarly, the possibility that an anionic mechanism might be possible prompted a study of the effect of basic catalysts such as methoxide and acetate ions.

First of all the thermal degradation "half-life" of samples 7 and 8 at 184°C was determined using the apparatus described in 2.4.2. (d). This was considered the most direct way of establishing any effect on the rate of the reaction by additives. The "half-lives" were determined fairly precisely as the average of 5 runs using between 4 to 8 mg. of polymer for each run. Copper powder was used as a heat conductor. The ratio of the "half-lives" of the glycol (57) and its acetate derivative (58) 9.57, is in fairly good agreement with the ratio of specific rates

9.84, as determined in the dynamic molecular still at 184°C. The monomer yields were quantitative suggesting that the accumulation of up to 20 cm. Hg. pressure of monomer has no inhibiting effect on the reaction at this temperature.

Blank experiments, without polymer, established that the volatilisation of all the additives considered was negligible at 184°C. The results obtained in "inhibition" and "catalysis" experiments using 10 mg. Polymer and 10 mg. of each additive are summarised in Table 5.3.

TABLE 5.3.

50% reaction times, mins, at 184°C for Thermal, "catalysed" and "inhibited" depolymerisation of polyoxymethylenes (10 mg.P) + 10 mg. additive.

Sample	Thermal	NaOCH <sub>3</sub>	KCl	NaO <sup>o</sup> CO <sub>o</sub> CH <sub>3</sub>	Ph <sub>3</sub> C <sub>o</sub> Cl	D.P.P.H.	1:4 <sup>o</sup>
S7	28 ± 2	4 ± 1.5	20	12 ± 3	20 ± 2	T	20
S8	268 ± 6	32 ± 5	T	240	T	T	T

Key

D.P.P.H. = ~~phenyl~~<sup>Di</sup> phenyl picryl hydrazyl

1:4 D = 1:4 diamino anthraquinone

T = Thermal time.



The rate of the catalysed reactions suggests that if an anionic mechanism is operating in the uncatalysed thermal reaction the degree of dissociation of the ion pair  $\sim \text{O}^- \text{H}^+$  is not large. Also the ion pair in the catalysed reaction  $\sim \text{O}^- \text{H}^+$ , is "stable" in the sense that an O - H ~~covalent~~ bond is unlikely to be formed. With  $\text{H}^+$  as the counter-ion this is not the case and hence an ionisation step would be required before a depolymerising ion pair could be formed. This initial ionisation could explain the longer half-life of the "thermal anionic" reaction. It is difficult to suggest how direct proof of the participation of ions, or intimate ion pairs, in the purely thermal reaction could be found. Logically there is little difference between the ionic mechanism and the molecular mechanism suggested <sup>in</sup> 5.2.1. since both involve the unzipping of the polymer chain by the chain-end proton. The molecular mechanism is to be preferred on energetic grounds, the necessity for charge separation being overcome by concerted electron shifts round a 4 or 6 membered planar transition state.

The lower rates of depolymerisation of the acetates compared to the parent glycols could be rationalised in terms of the greater difficulty in forming the cyclic transition state in the former case which by virtue of the size of the chain-end acetate group would be formed with some difficulty in the solid below 165°C.

The absence of negative deviations from first order kinetics in the case of the acetates can also be explained on the basis that the rate of the crystalline - amorphous phase transition is greater than the rate of depolymerisation of the acetate and less than the rate of depolymerisation of amorphous glycol. Some support is given to this intuitively plausible explanation of the negative deviation by recent crystallisation studies (80) in which it has been shown that the apparent activation energy of viscous flow in crystallising POM melts is 25.6 k. cal. mole<sup>-1</sup>. The activation energy for melting must be greater than this by 1.59 k. cal. mole<sup>-1</sup>, which is the heat of fusion of POM. Thus it would appear that melting is associated with an activation energy of about 27 k. cal. mole<sup>-1</sup>. This is some 10 k. cal. higher than the activation energy of depolymerisation,  $E_d = \Delta H - E_p = 18$  k. cal. mole<sup>-1</sup> and hence it is reasonable to suggest that melting may become rate determining and thus give rise to the negative deviations observed with the glycols and also the increase in measured activation energies as the reaction proceeds.

## CHAPTER 6

### The Solubility and some solution properties of Polyoxymethylene.

#### 6.1. Introduction

In their study of the effect of solvents on high molecular weight polyoxymethylene<sup>(61)</sup> the Du Pont workers examined 406 compounds of 27 different classes and found no solvent which produced a 1% solution with a gel point lower than 50°C. Phenols were found to be the best solvents. Although many of the phenols considered gave solutions with gel temperatures in the range 50° to 100°C the actual dissolving temperatures were usually 40° to 60° higher. The lowest dissolution temperature, 89°C, is observed with m-chlorophenol.

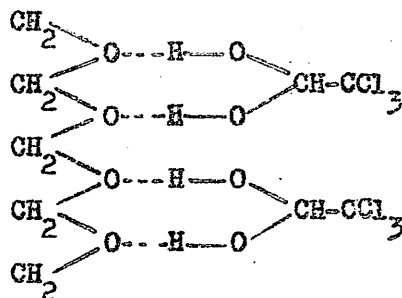
It is clear that specialised experimental techniques would be required in order to characterise the polymer in terms<sup>of</sup> its solution properties in these solvents. The fact that it takes up to one hour to dissolve the polymer at 100°C in phenolic solvents and that the polymer slowly degrades in solution probably accounts for the very poor precision obtained in attempts to measure the intrinsic viscosities of the polymers examined in this study in phenol and

p-chlorophenol. The patent literature has many references to inherent viscosities measured in these solvents but our experience would suggest that they have little more value than as an index of order of magnitude. It soon became clear that the results obtained would be of doubtful value in elucidating the molecular weight changes occurring in the thermal degradation of the polymer. Attempts to develop the technique for measuring viscosities at elevated temperatures were abandoned when a room temperature solvent system was found.

#### 6.2. Perfluoroacetone hydrate as a solvent for polyoxymethylene

Some of the factors affecting the solubility of polymers have been discussed by Small<sup>(81)</sup>. It has been established that the solubility of non-polar polymers in non-polar solvents is determined mainly by the heat of mixing. However, for highly crystalline polar polymers such as POM the heat of mixing alone is not the only factor and specific exothermic interactions between solvent and polymer are necessary for solution to occur. In many systems, e.g. Nylon and Terylene dissolved in phenols, the specific interactions can be identified with hydrogen bond formation. The solubility of POM in phenols can be rationalised in similar terms. In a search for more powerful solvents than the phenols we should

examine molecules containing "bondable" protons which could bond the basic ether oxygens of the polyoxymethylene chain. The notion that a solvent might be more powerful if it had two protons capable of forming H-bonds led us to consider chloral hydrate  $\text{Cl}_3\text{C}\cdot\text{CH}(\text{OH})_2$ , (M.pt.  $51.7^\circ\text{C}$ ), as a solvent since it seemed that it would provide ideal geometry for a specific interaction,



The fact that the polymer dissolves in this solvent at  $60^\circ\text{C}$  without appreciable degradation (95% recovery after 20 minutes at  $60^\circ\text{C}$ ) seems to confirm the above suggestion that the geometry of the gem-diol structure provides for very specific interaction between the molecule and the polymer chain. Chloral hydrate has a number of disadvantages as a solvent for viscosity measurements, however. The two most important are that it degrades to trichloroacetic acid, and that at elevated temperatures it dissociates to the aldehyde and water. The former is perhaps the most serious of these drawbacks



since trichloroacetic acid would lead to random chain scission and make the analysis of results complex. There are few stable gem-diols known and hence the number of potential solvents providing the right geometry for the specific interaction postulated above is limited. These are listed in Table 6.1.

TABLE 6.1.

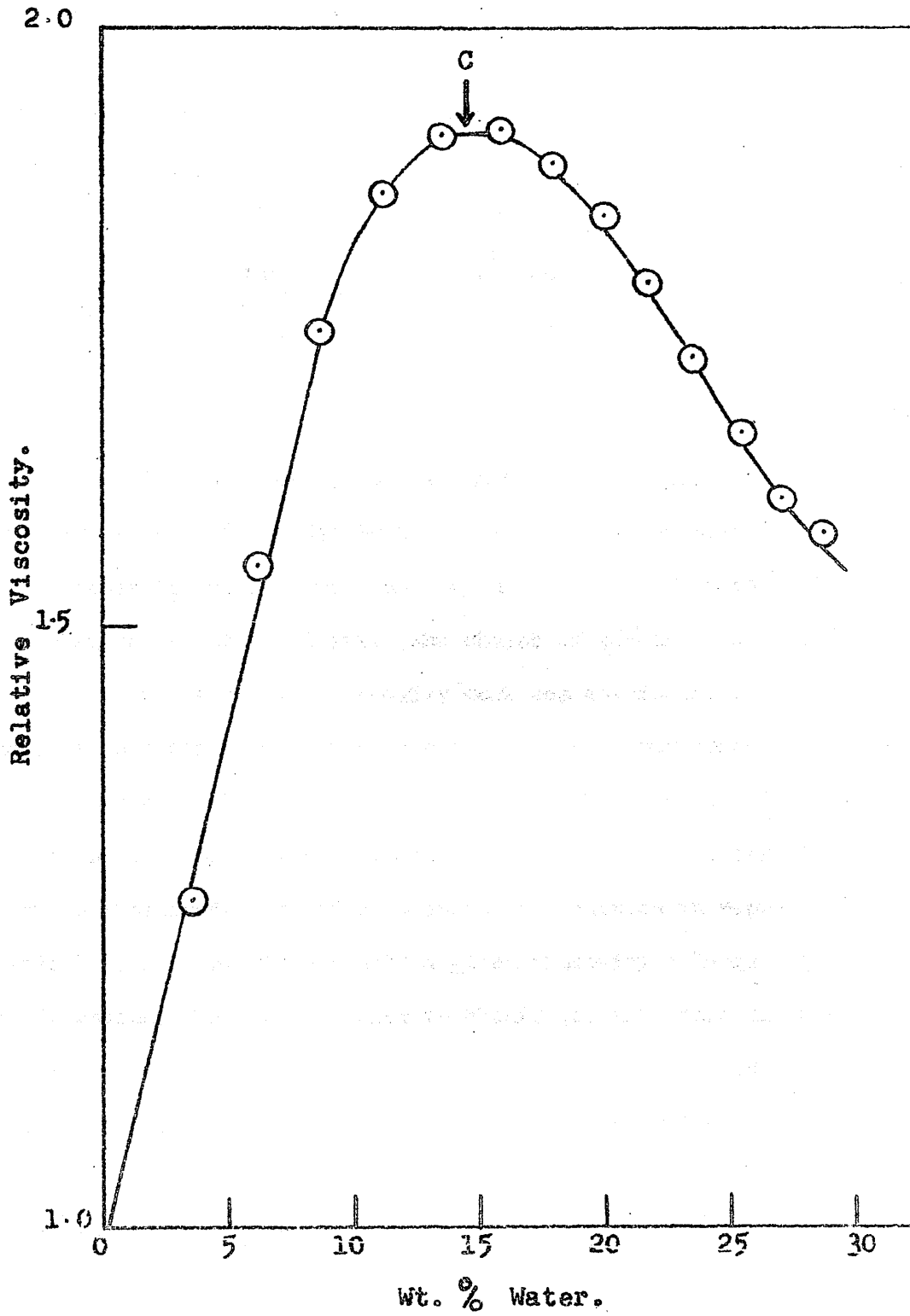
Stable gem-diols

Glyoxylic acid hydrate,	$\begin{array}{c} \text{HO} \\ \diagdown \\ \text{C} \\ \diagup \\ \text{HO} \end{array} \text{CHCO}_2\text{H}$
Mesoxalic acid,	$\begin{array}{c} \text{HO} \quad \text{CO}_2\text{H} \\ \diagdown \quad \diagup \\ \text{C} \\ \diagup \quad \diagdown \\ \text{HO} \quad \text{CO}_2\text{H} \end{array}$
Fluoral hydrate,	$\begin{array}{c} \text{HO} \quad \text{CF}_3 \\ \diagdown \quad \diagup \\ \text{C} \\ \diagup \quad \diagdown \\ \text{HO} \quad \text{H} \end{array}$
Perfluoroacetone hydrate (P.F.A.H.)	$\begin{array}{c} \text{HO} \quad \text{CF}_3 \\ \diagdown \quad \diagup \\ \text{C} \\ \diagup \quad \diagdown \\ \text{HO} \quad \text{CF}_3 \end{array}$

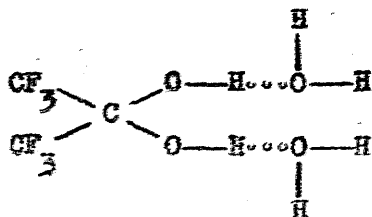
The first two of these are useless as solvents since they would cause hydrolytic degradation of the polymer Fluoral hydrate, like its chlorine analogue, degrades to the corresponding acid and is also eliminated for this reason. P.F.A.H. at its melting point (43-44°C) dissolves POM very rapidly and without degradation. The latter point was established in two ways. The viscosity of the solution obtained at 44°C showed less than 2% decrease over a period of 2 hours. The hot solution was poured into ice cold acetone and the precipitated polymer filtered and weighed (98-99.3% recovery). From these observations it was concluded that pure P.F.A.H. is a non-degrading solvent for POM. It was also found that at 25°C aqueous solutions of P.F.A.H. at concentrations greater than 77% dissolved the polymer in 10 to 20 minutes to give stable 1% polymer solutions. Since the binary solvent mixtures are much less volatile at room-temperature than the pure P.F.A.H. at 44°C it was decided to use 95% aqueous P.F.A.H. in order to minimise concentration errors arising from the volatilisation of solvent.

The viscosity of the binary solvent mixture depends on the concentration of water and as figure 30 shows, the viscosity-concentration function is typical of highly associated mixtures.

FIGURE 30.



The maximum relative viscosity,  $C$ , corresponds to a molar ratio P.F.A.H./ $H_2O = 1:2$ . This, it can be reasonably inferred, is due to the formation of the molecular complex P.F.A.H. $2H_2O$  which probably has the structure:



The mixture is a solvent below the maximum,  $C$ , because the non-solvent water is bonded in this way. Beyond the maximum "free" water is present and hence beyond about 20-25% water content the mixture is not a solvent. The choice of 95% as a suitable concentration for routine viscosity work was considered to provide the best compromise between a lowering of the vapour pressure of the solvent mixture relative to that of the pure hydrate at  $44^{\circ}\text{C}$  and the increasing viscosity of the solvent mixture as the concentration of water is increased. In order to avoid difficulties in reproducing precisely a solvent mixture with a given viscosity a large batch of 95% aqueous P.F.A.H. was used to obtain the intrinsic viscosity data reported in Chapter 4. Using sample 7 exclusively the effect of changing the mole fraction of water in the solvent mixture on

the viscosity of POM was studied. The results are reported in 6.3.

6.3. The Viscosity of POM in P.F.A.H./H<sub>2</sub>O mixtures.

The specific viscosity of a polymer solution,  $\eta_{sp}$ , given by  $\eta_{rel} - 1$ , can be expressed as a power series in polymer concentration,  $C$ , thus

$$\eta_{sp} = A_0 C + A_1 C^2 + A_2 C^3 + A_3 C^4 + \dots \quad (1)$$

The reduced viscosity,  $\eta_{sp}/c$ , is given by

$$\eta_{sp}/c = A_0 + A_1 C + A_2 C^2 + A_3 C^3 + \dots \quad (2)$$

Equation (2) has been found to fit the data well for a very large number of systems. In dilute solutions the  $C^3$  term is negligible, and, except with very high molecular weight polymers, measurements in the usual dilute solution viscosity range ( $C = 0.05$  to  $1.0$  g/dl) give results which indicate a linear relation between reduced viscosity and  $C$ , i.e. the  $C^2$  term is also negligible. The equation (2) then becomes

$$\eta_{sp}/c = A_0 + A_1 C = [\eta] + A_1 C \dots \quad (3),$$

where  $[\eta] = \lim(\text{as } C \rightarrow 0) \eta_{sp}/c = A_0$ .

The coefficient  $A_1$  has been shown to be proportional to  $[\eta]^2$ , i.e.  $A_1 = k_1[\eta]^2$ .

Equation (3) is therefore very often expressed as

$$\eta_{sp}/c = [\eta] + k_1[\eta]^2c \quad (4)$$

This is the familiar Huggins equation<sup>(82)</sup>. Much theoretical work has been done to define the physical significance of the Huggins constant,  $k_1$ . It has been established that  $k_1$  is independent of molecular weight. It is primarily a function of polymer-polymer and polymer-solvent interactions. It has also been established that  $k_1$  is a good criterion of solvent power, whether the solvent power is altered by changing the solvent<sup>(83)</sup> or by varying the composition of a mixed solvent<sup>(84)</sup>. Recent theoretical work<sup>(85)</sup> concludes that  $k_1$  should always be positive and lie in the range 0.2 to 0.5, increasing towards 0.5 as the solvent power decreases. Observed values are not confined to this range, however.<sup>(86)</sup>

Equation (3) was obeyed by all the samples examined in 95% aqueous P.F.A.H. in the concentration range 0.1 to 0.9 g/dl.. The Huggins constant,  $k_1$ , was calculated from the  $[\eta]$  values obtained (see Table 4.5.) using the equation  $A_1 = k_1[\eta]^2$ , where  $A_1$  is the gradient of the reduced viscosity,  $\eta_{sp}/c$ , versus  $c$  plots. The results are summarised in Table 6.2..

TABLE 6.2

The Huggins constant,  $k_1$ , for POM in 95% aqueous P.F.A.H.

Sample	$[\eta]$	$A_1$	$k_1$
1	2.00	2.32	0.58
2	4.59	13.05	0.62
3	4.52	12.46	0.61
4	2.97	5.47	0.62
5	3.04	5.82	0.63
7	4.05	9.84	0.60

$k_1$  lies in the range  $0.60 \pm 0.03$ . This would suggest that the samples were all members of the same homologous series.

The effect of the non-solvent, water, on the solvent power was determined by measuring  $[\eta]$  for sample 7 in a range of solvents containing from 5 to 20% water and calculating  $k_1$ , as above. The results are summarised in Table 6.3.

TABLE 6.3

$k_1$  values as a function of solvent composition

<u>%H<sub>2</sub>O</u>	<u><math>k_1</math></u>
5.0	0.60
8.2	0.61 <sub>6</sub>
11.1	0.62 <sub>5</sub>
16.4	0.64 <sub>7</sub>
18.3	0.66 <sub>4</sub>
20.5	0.67

---

Although the  $k_1$  values lie outside the theoretically predicted range<sup>(85)</sup> the trend of  $k_1$  as the solvent power is increased is in the right direction though the effect is small compared with the magnitude of the effect in other systems<sup>(87)</sup>.

From these results it can be concluded that over the concentration range studied the viscosity of polyoxymethylene solutions in aqueous perfluoroacetone hydrate conforms to the Huggins equation and that changing the solvent has the predicted effect on the Huggins constant,  $k_1$ .



#### 6.4 The Mark-Houwink exponent, $\alpha$ .

According to the theory of Flory and Fox<sup>(88)</sup> the exponent,  $\alpha$ , in the Mark-Houwink equation must lie in the range 0.5 to 0.8 for linear flexible chains without draining effects. The lower limit is for tightly coiled chains in these solvents and the upper limit for highly swollen ~~polymers~~ in very good solvents. The crude value of 0.8 for  $\alpha$ , obtained from intrinsic viscosity and  $M_n$  (IR) data, reported in Chapter 4 would on this basis suggest a highly extended chain if 95% aqueous P.F.A.H. is a good solvent. However, the Huggins constant,  $k_1$ , values obtained suggest a relatively poor solvent. The apparent discrepancy can be due either to the fact that here we are dealing with a polar solvent in a highly polar solvent mixture and hence comparisons with the behaviour of non-polar polymers in non-polymer solvents is not valid or the value of  $\alpha$  is in serious doubt. No further light is thrown on this very interesting topic in this study. Clearly much work remains to be done.

In conclusion we can say, however, that the solvent system P.F.A.H. - H<sub>2</sub>O has proved a valuable tool in elucidating the details of the molecular weight changes occurring in the thermal depolymerisation of polyoxymethylene.

## CHAPTER 7.

### The Photochemical and Photo-oxidative Degradation of Polyoxymethylene

#### 7.1. Introduction

The photochemical and photooxidative degradation reactions of polyoxymethylene are wholly unexplored, which seemed a valid reason for undertaking this preliminary survey of the reactions.

#### 7.2. Photochemical Degradation in high vacuum.

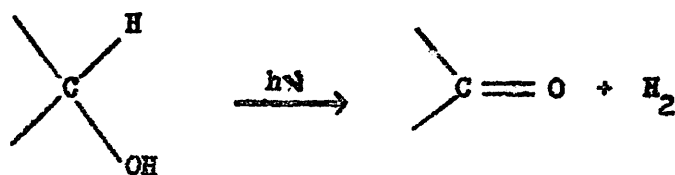
Thin films of samples 7 and 8, weighing 15 to 20 mgs. were irradiated with the light sources described in section 2.8 in the silica vessel, Fh, (Figure 10). With both sources (i.e. with 3650 Å and 2537 Å) a pressure of non-condensable gases was produced from both types of polymer. Combustion analysis of the non-condensable gaseous products (sect 2.5.) established that H<sub>2</sub> and CO were being produced by photolysis. The relative amount of H<sub>2</sub> and CO were determined and it was found that the ratio (H<sub>2</sub>)/CO was between 3.5 and 4.. An ambiguity arises here since it has been found that formaldehyde, which is probably present in small amounts in all polymer samples, is photolysed by 3650 Å and 2537 Å ultraviolet irradiation, the predominant

mode of photolysis at temperatures below 100°C being the first of the two following alternatives (89):

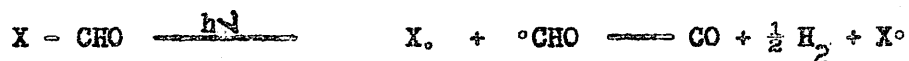


The ratio of  $(\text{H}_2)/(\text{CO})$  found by Calvert and Steacie in their study of the photolysis of  $\text{CH}_2\text{O}$  at high temperatures (79) was always close to unity. If we can assume that a ratio of unity holds for this reaction at room temperature then value of 3.5 to 4 for the  $(\text{H}_2)/(\text{CO})$  obtained in this study is either seriously in error or genuinely arises from polymer photolysis. The main difficulty in explaining the high value of the  $(\text{H}_2)/(\text{CO})$  ratio will be in identifying the primary photochemical process. Since photolysis by active wave lengths greater than about 2000 Å requires the presence of a suitable chromophore to absorb them the difficulty arises in identifying the chromophore in polyoxymethylene. In the case of the polymer with acetate chain-ends (Sample 8) we can plausibly assume that the ester carbonyl would be an efficient chromophore for 2537 Å and 3650 Å. The hydroxyl chain-ended polymers present some difficulty here because they do not contain chromophores which would absorb the active wave lengths. To explain the

production of  $H_2$  and CO in the vacuum photolysis of cellulose by 2537 Å radiation Flynn and co-workers<sup>(90)</sup> postulated the following reactions



and



where X stands for the remaining cellulose chain.

If a similar process occurred in POM glycols the rate of hydrogen production would be molecular weight dependent since the hydroxyl groups occur only at the chain-ends. This possibility was not explored in this study.

### 7.3. The Photo-oxidation of Polyoxymethylene

Kern and Cherdron<sup>(44)</sup> reported that the rate of thermal oxidation of POM is negligible at temperatures below 160°C. We have confirmed this by examining the I.R. spectra of thin polymer films of sample 7 which had been heated in an air oven at 135° to 140°C for periods of up to ten days, after which time the sample had lost 22% of its weight. The infra red spectrum of the sample was obtained at intervals and it was found that except for an increase

in "background" absorption there was no change observed in the spectra except that due to the decrease in molecular weight of the sample due to depolymerisation, i.e. an increase in hydroxyl absorption at  $2.9\mu$ . In complete contrast, ultra-violet irradiation in air at room-temperature produced immediate changes in the polymer structure which were revealed by the infra-red spectra. The most significant changes occurred in the hydroxyl and carbonyl bands.

### 7.3. (a) The hydroxyl band.

By irradiating esterified polyoxymethylene (Sample 8) which has negligible absorption in the hydroxyl band at  $2.9\mu$  it is possible to follow the increasing absorbance in this region due to structures produced in photooxidation without having to allow for absorbing groups present initially. It was found that at a fixed distance of 20 cms. the 30-watt Hanovia "Chromatolite" source [Sect. 2.8. (a)] ( $2537 \text{ \AA}$ ) caused an increase in absorbance in the hydroxyl band at  $2.9\mu$  at about ten times the rate of that produced by the 125-watt Osram MB source ( $3650 - 3663 \text{ \AA}$ ). These observations are summarised in Figures 31 and 32. As shown in Table 2.2. the quantum output of these sources at  $2537 \text{ \AA}$  and  $3663 \text{ \AA}$  are approximately equal and the  $3650 \text{ \AA}$  output is ten times the  $2537 \text{ \AA}$  output. It is clear from these data that the relative

FIGURE 31.

Photo-oxidative Changes in I.R. Spectra.

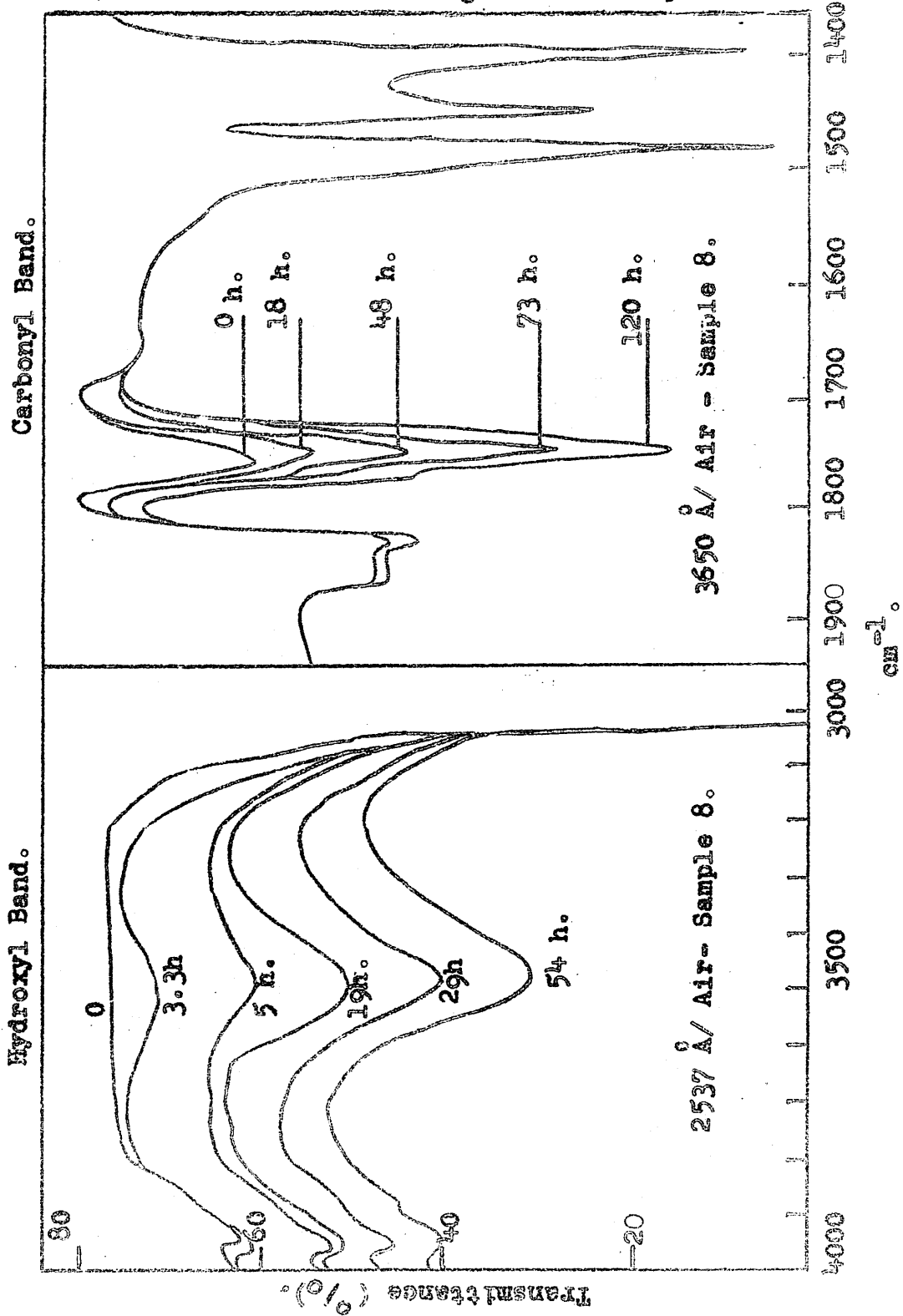
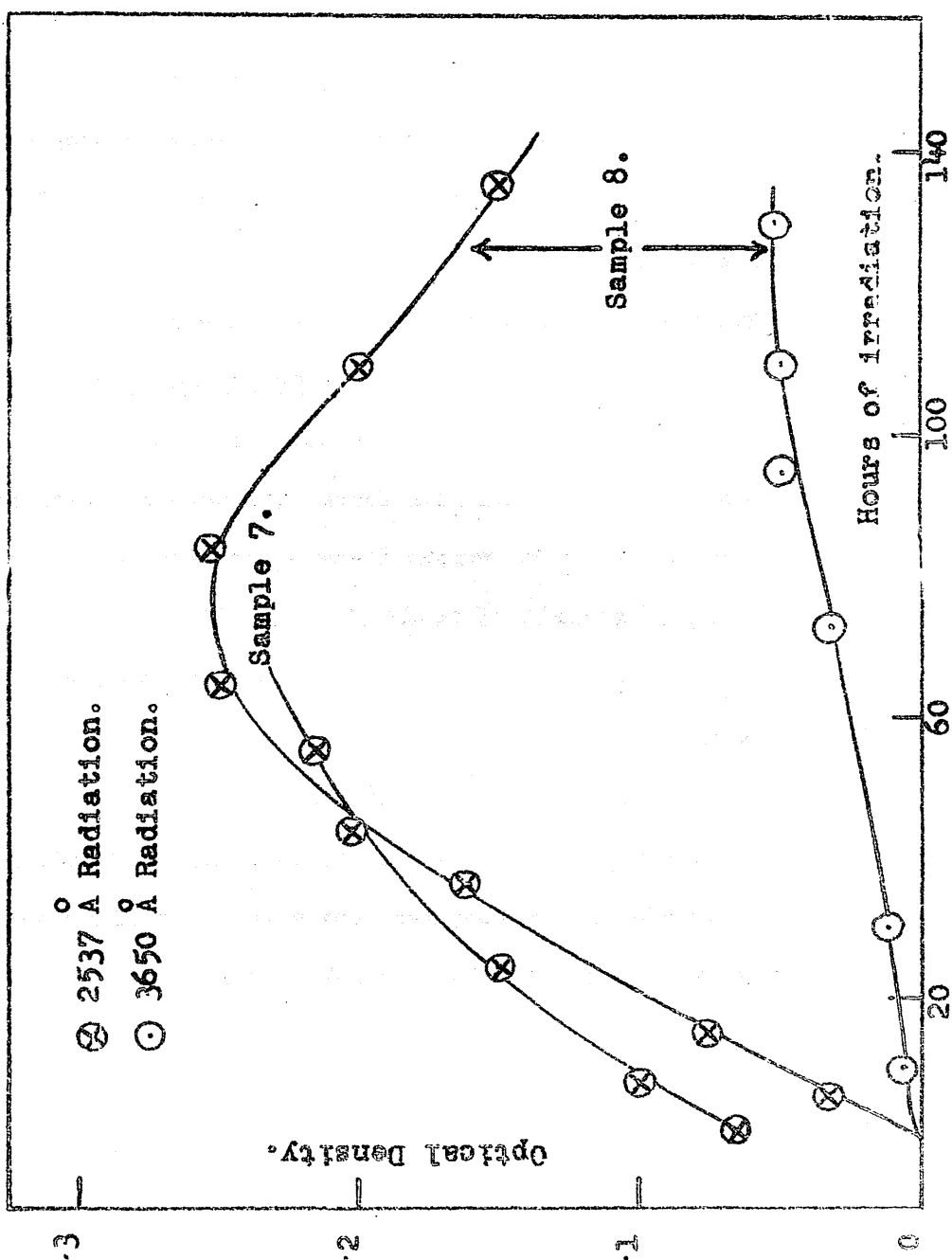


FIGURE 32.

Hydroxyl Band,  $2.9\mu$ .



rates of increase of absorbance caused by the two sources is a true indication of the quantum efficiency of the sources. Thus the quantum efficiency of the 2537 Å radiation is higher for the process producing the absorbance.

The position of the hydroxyl band maximum (2.9 μ), in the irradiated samples is identical to that observed in samples of polymer with hydroxyl chain-ends. As indicated in Figure 32 the unesterified polymer, (Sample 7), showed similar increasing absorbance in the hydroxyl band though at a lower rate.

### 7.3. (b) The carbonyl band.

The increase in absorbance in the carbonyl band (5.4 + 6.0 μ) on irradiation of Sample 7, which initially shows no such absorbance, and of sample 8 which has a small amount of chain-end ester carbonyl present (1750 cm<sup>-1</sup>) is shown in Figures 33 and 34.

The resolution of the infra-red spectrometer was sufficiently high to allow the carbonyl absorbance to be resolved into three components, at 1750, 1785 and 1815 cm<sup>-1</sup>. The 1750 cm<sup>-1</sup> absorbance is attributed to ester carbonyl since it is the wave length of the carbonyl absorbance maximum in the esterified polymer (Sample 8). Small increases were observed at 1785 and 1815 cm<sup>-1</sup> and these are



speculatively assigned to the carbonate,  $-O-\overset{\overset{O}{\parallel}}{C}-O$ , and anhydride,  $(-\overset{\overset{O}{\parallel}}{C}-O-\overset{\overset{O}{\parallel}}{C}-)$ , structures.

The 3650 Å source caused a large increase in the carbonyl absorbance. The data for a typical run are plotted in Figure 33. The ester carbonyl absorbance at  $1750\text{ cm}^{-1}$  increases autocatalytically. In contrast the other carbonyl absorbances ( $1785, 1815\text{ cm}^{-1}$ ) increase linearly and relatively slowly.

Figure 34 illustrates the comparative effect of the two sources on the esterified polymer (sample 8). It is clear from figure 34 that the processes occurring differ markedly. In contrast to the autocatalytic rate of carbonyl production produced by 3650 Å the 2537 Å radiation rapidly produces a "steady-state" concentration of carbonyl groups. By changing the light source from 3650 Å to 2537 Å at points during the irradiation history of the samples (at A and B in Figure 34) it was established that 2537 Å is capable of "destroying" the carbonyl produced by the 3650 Å. This would account for the "steady-state" concentration of carbonyl observed on photo-oxidation with 2537 Å.

A mechanistic rationalisation of these semi-quantitative observations in terms of current theories of oxidation is speculatively attempted in the next section.

FIGURE 33.

Carbonyl Band.

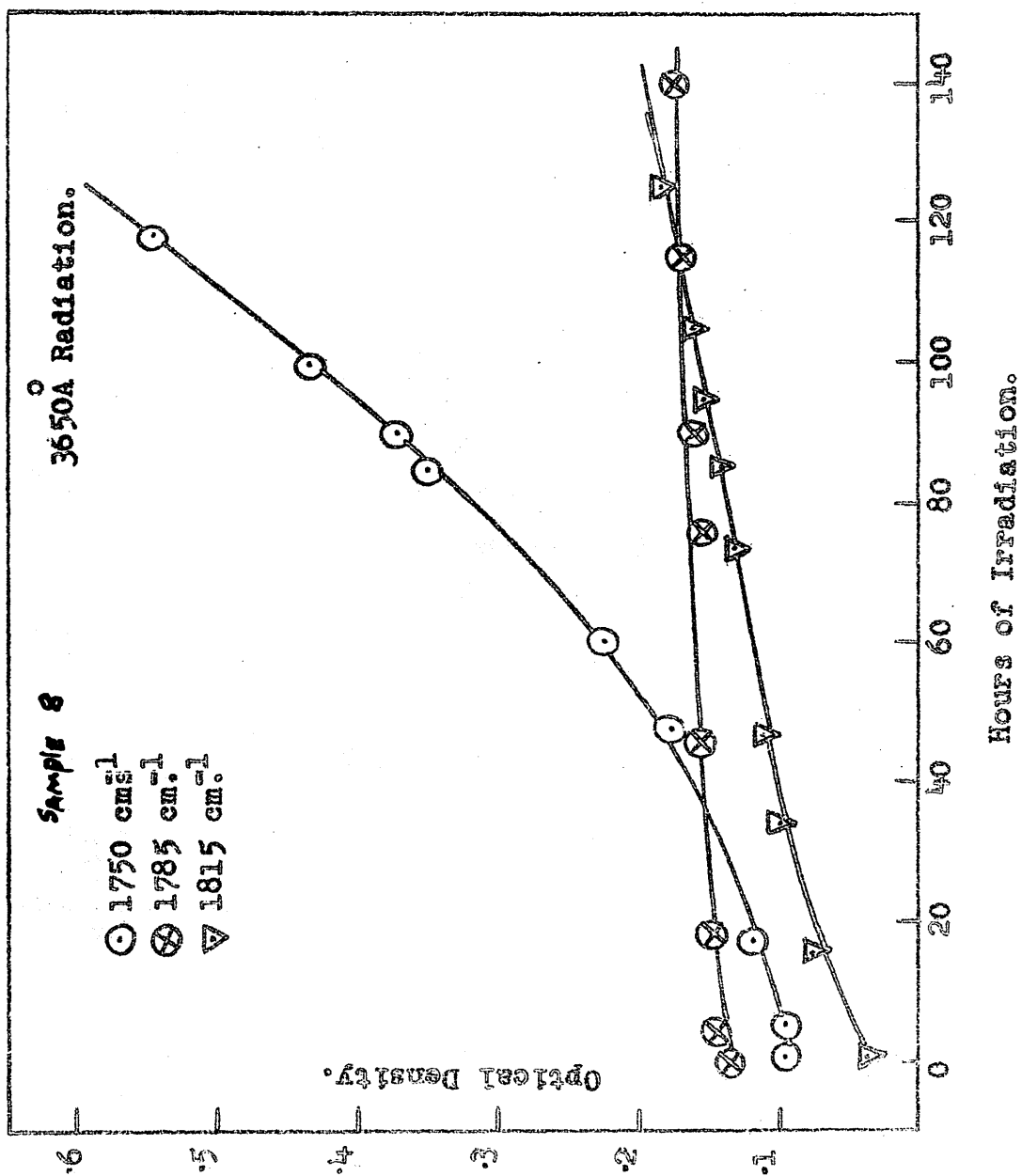
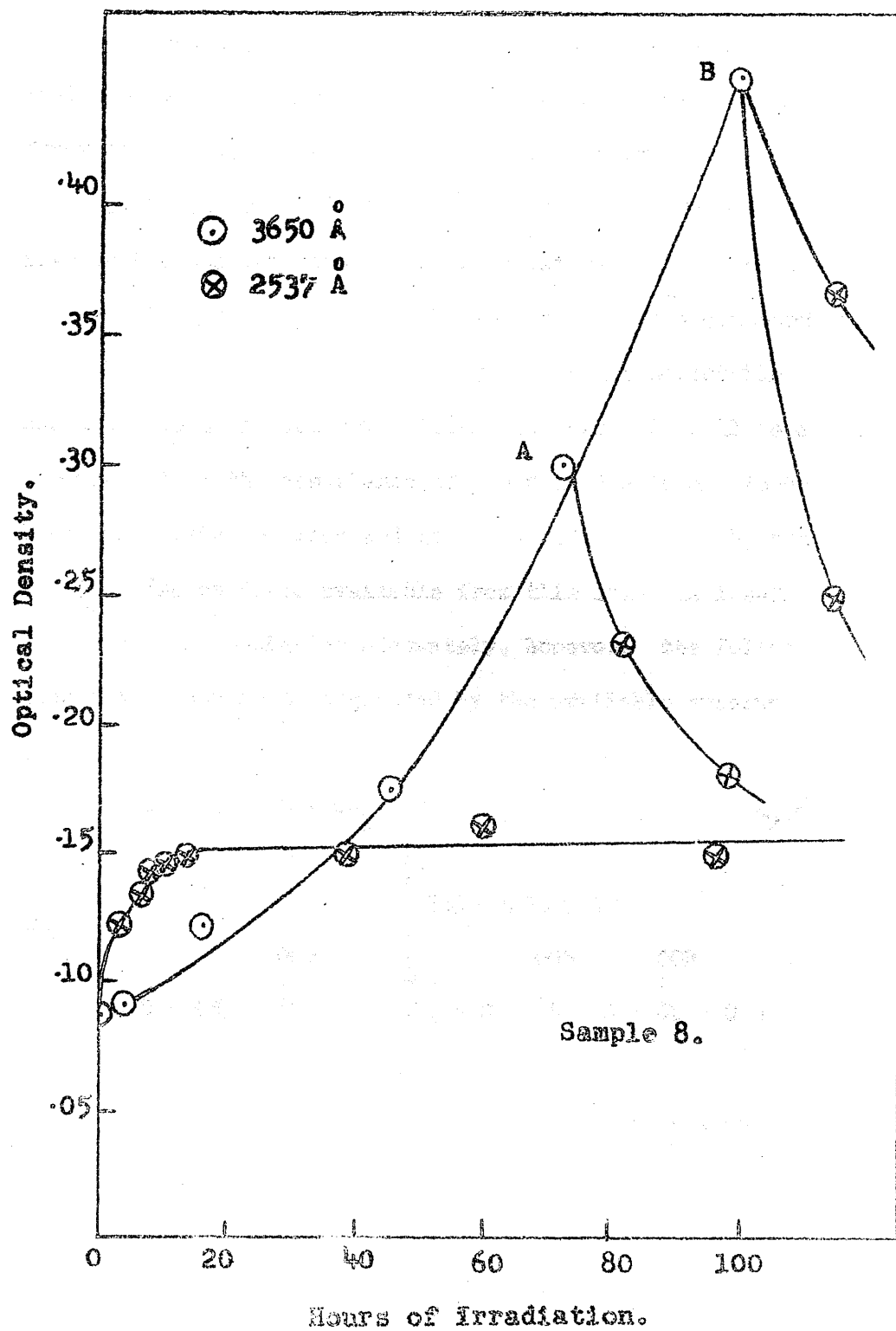


FIGURE 34.

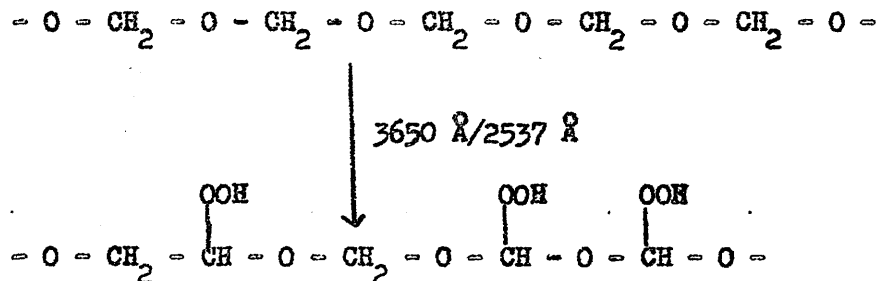


#### 7.4. Discussion

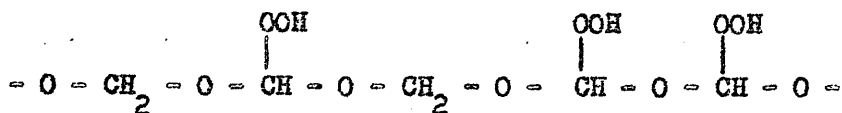
Recently oxidation processes have been extensively reviewed by Lundberg and others<sup>(92)</sup> and this source will be drawn on in this discussion without further reference.

There is now little doubt that organic oxidation processes involve the participation of hydroperoxides as intermediates. However, the photo- and thermal lability of these compounds is such that it is unlikely that they ever reach detectable concentrations in photo-oxidation processes. It will be assumed therefore that the absorbance at 2.9  $\mu$  is due to an alcoholic hydroxyl stretching mode and not to a hydroperoxide hydroxyl.

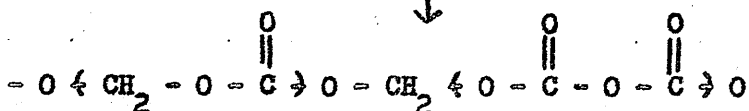
The evidence available from this study is insufficient to support any mechanism adequately, however, the following speculative scheme is suggested by the available evidence:



Hydroperoxide.



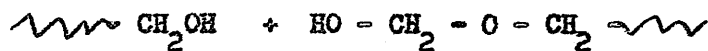
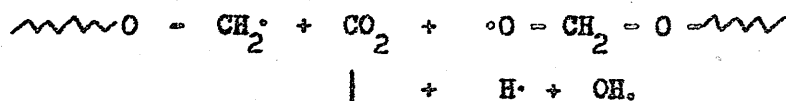
↓ -3H<sub>2</sub>O.



Ester, 1750cm<sup>-1</sup>

poly(carbon dioxide) 1785, 1815 cm<sup>-1</sup>

↓ 2537 Å, chain scission



Clearly, much work remains to be done. Perhaps the best starting point would be a study of the photo-reactions of the oligomeric polyoxymethylene diethers.

APPENDIX I

Perfluoroacetone hydrate

Perfluoroacetone,  $\text{CF}_3\text{COCF}_3$ , was first obtained by Bigelow and Fukuhara,<sup>(93)</sup> among the products of the direct fluorination of acetone. These authors noted that the gaseous ketone (bpt.  $-28^\circ\text{C}$ ) was soluble in water without decomposition and showed some evidence of hydrate formation. Later, Henne et al.<sup>(94)</sup> prepared the ketone by the oxidation of the chlorofluoro-olefin,  $(\text{CF}_3)_2\text{C}=\text{CCl}_2$ . They noted that the isolation of the ketone from the aqueous permanganic oxidation medium was complicated by the formation of a stable hydrate which is soluble in water. Henne et al. did not characterise the hydrate. More recently, Morse et al.,<sup>(95)</sup> in describing an improved synthesis of the ketone describe the hydrate as a liquid  $n_D^{20} 1.3179$  bpt.  $55 - 6^\circ\text{C}$  at 80 m.m.. They also describe the occurrence of an easily sublimed white solid which, they suggest, is the cyclic trimer of the ketone. To obtain the ketone from the aqueous solution of the hydrate it was necessary to use  $\text{P}_2\text{O}_5$  as dehydrating agent<sup>(94), (95)</sup>. From this we can conclude that the hydrate is very stable. There are two possible structures for the hydrate. It is either a hydrogen-bonded molecular complex formed by a molecule of ketone and one or

more molecules of water or it is a gem-diol. The infra-red spectrum of the hydrate (Figure 35), run on a saturated carbon tetrachloride solution treated with molecular sieve to remove "unbound" water, showed no absorption in the carbonyl band. A sharp absorption peak in the hydroxyl band at  $3582\text{ cm}^{-1}$  indicates the presence of "free" hydroxyl groups in the molecule. Thus it can be inferred from the infra red spectrum that the gem-diol structure is the more likely of the above two possibilities.

The negative inductive effect of the trifluoromethyl XXXXXXXXXXXXXXXXXXXX group increases the acidity of the hydroxyl protons and hence the molecule behaves as a weak acid. It is clear from Figure 36, which is the potentiometric titration curve obtained by titrating aqueous P.F.A.H. with N/10 NaOH, that the hydrate is acidic. Thus the titration of an aqueous solution of P.F.A.H. with N/10 NaOH confirms the gem-diol structure.

It soon became clear when the potentiometric titration technique was used as a method of analysing for P.F.A.H. quantitatively that the pure hydrate was in fact the white, easily sublimed solid (Mpt.  $43-44^{\circ}\text{C}$ ) noted by early workers. (95)

I.R. Spectrum of  $(CF_3)_2C(OH)_2$ .

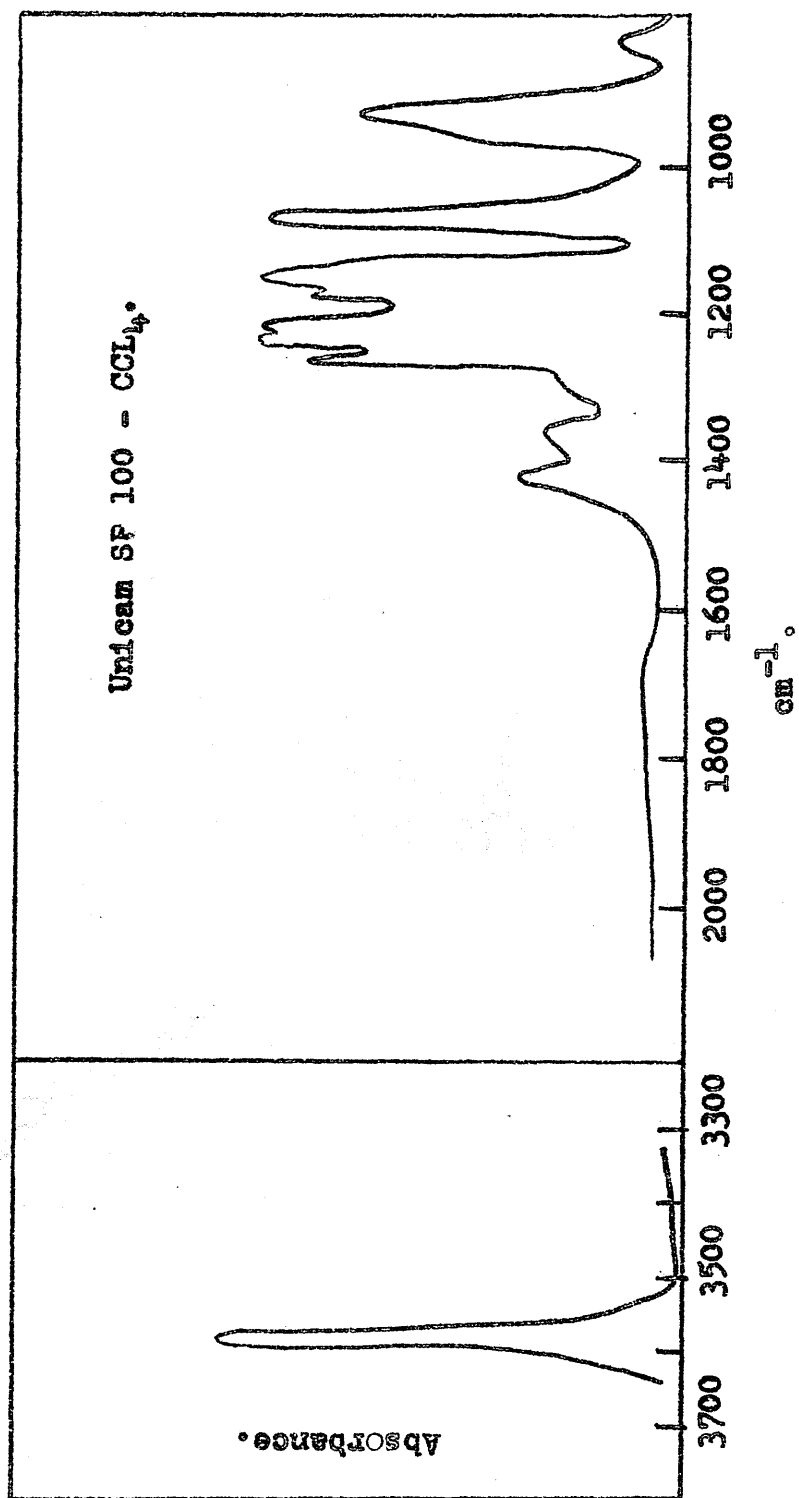
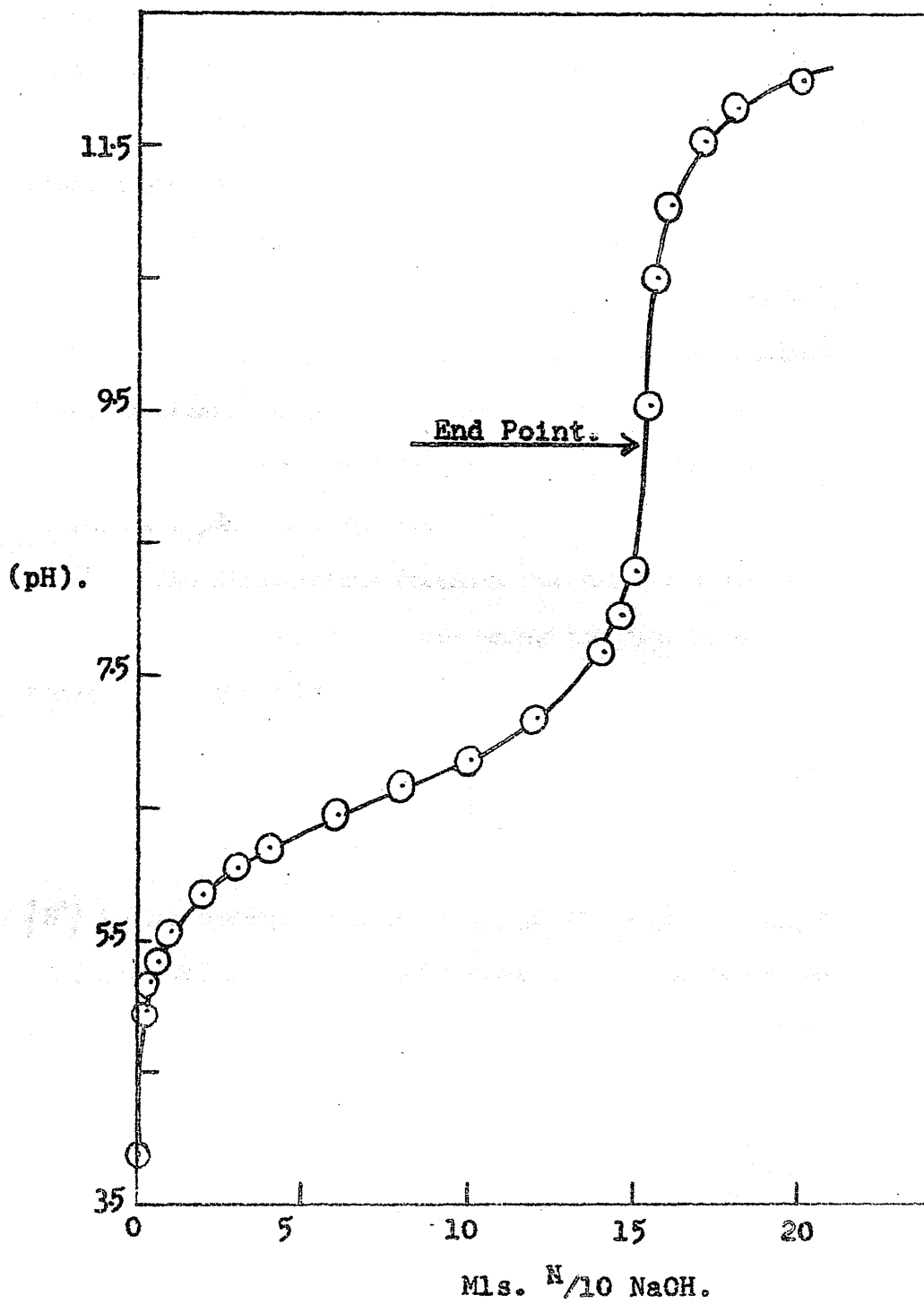


FIGURE 35.



FIGURE 36.

$(CF_3)C(OH)_2$  Versus  $N/10$  NaOH.



When the preparative reaction (section 2.9.) was left for several hours the contents of the reaction flask went solid indicating that the reaction was complete and that all the water present in the flask initially had been used for hydration of the ketone. The ready sublimation of the hydrate suggests that if intermolecular hydrogen bonding occurs in the solid it is not 'polymeric' as in water and other highly associated hydroxylic systems. Kern and Cherdron<sup>(44)</sup> established that at 190°C in nitrogen hydroxy compounds (phenols etc.) with a pKa of less than 6.0 caused appreciable degradation of a P.O.M. dimethyl ether. Thus in 60 minutes at 190°C approximately 1 mole% of p-hydroxy benzoic acid (pKa 4.5) caused 17.8% weight loss. An accurate pKa value for P.F.A.H. is therefore of some interest.

The dissociation constant for the first ionisation stage of P.F.A.H.,  $K_a^0$ , was calculated using the data given in Table A.1., where  $K_a^0$  is given by

$$K_a^0 = \frac{\{H^+\} [A^-] f_A}{[HA] f_{HA}}$$

$\{H^+\}$  is the hydrogen ion activity, given by  $pH = -\log \{H^+\}$  ;

$[A^-]$  and  $[HA]$  are the concentrations of the anions and undissociated acid and  $f_A$  and  $f_{HA}$  are the corresponding activity coefficients.

It is assumed that, at the concentration used in these experiments, the activity coefficient of the P.F.A.H. is unity.  $f_A$  is calculated from the Debye - Hückel limiting law:

$$-\log f_z = 0.5 z^2 (I)^{\frac{1}{2}}; \quad I = \frac{1}{2} \sum (c_i z_i^2)$$

where  $c_i$  is the concentration and  $z_i$  is the charge of the  $i^{\text{th}}$  species.

TABLE A.1.

<u><math>b \times 10^{-5}</math></u>	<u><math>\{H^+\} \times 10^{-5}</math></u>	<u><math>[A^-] \times 10^{-5}</math></u>	<u><math>[HA] \times 10^{-5}</math></u>	<u><math>f_A</math></u>	<u><math>K_a^0 \times 10^{-7}</math></u>
0.91	0.141	1.051	3.31	0.9963	4.47
1.31	0.089	1.399	2.96	0.9959	4.16
1.67	0.063	1.733	2.63	0.9954	4.14
2.31	0.036	2.346	2.01	0.9945	4.15
2.86	0.022	2.882	1.48	0.9938	4.22
3.33	0.013	3.343	1.02	0.9936	4.24

$$\underline{\langle K_a^0 \rangle = 4.23 \times 10^{-7}}$$

$b$  = molar concentration of NaOH at any stage in the titration

$$a = [\text{HA}] + [\text{A}^-] = \text{total P.F.A.H.}$$

$$[\text{NA}^+] + [\text{H}^+] = b + [\text{H}^+] = [\text{A}^-] + [\text{OH}^-].$$

at  $\text{pH} < 7$ ,  $[\text{OH}^-]$  is negligible in comparison to the other concentrations so that

$$[\text{A}^-] = b + [\text{H}^+]$$

$$\therefore [\text{HA}] = a - (b + [\text{H}^+])$$

$a = b$  at the end point.

The  $\text{pK}_a$  value ( $\log K_a^{-1}$ ) calculated from the above data is 6.37. P.F.A.H. is thus fairly acidic and thus heating it to dissolve polymer rapidly was considered inadvisable.

---

### REFERENCES

1. Gaylord, N.G., "Polyethers", Interscience, New York, (1963).
2. I.U.P.A.C. Report, J. Polymer Sci., 8, 257, (1952).
3. Butlerov, A., Annalen, 111, 242, (1959).
4. Auerbach, F., and H. Barschall, Chem. Abstracts, 2, 1125, (1908);  
8, 3087, (1914).
5. Staudinger, H., et al., Annalen, 474, 145-275 (1929);  
Chem. Abstracts, 24, 3754, (1930).
6. Spence, R., and W. Wild, J. Chem. Soc., 506, (1935).
7. Walker, J.F., "Formaldehyde", Reinhold, New York, (1964),  
3rd Edition.
8. Landquist, N., Acta Chem. Scand., 9, 867-92, (1955).
9. Madano, M., et al., Berichte, 67, 174, (1934).
10. Euler, H. von, and T. Lovgren, Z. anorg. Chem., 147, 123, (1925).
11. Illiceto, A., et al., Gazz. Chim. Ital., 81, 915, (1951).
12. Machacek, Z., J. Mejzlik, and J. Pac, J. Polymer Sci. U.S.S.R.,  
4, 238, (1963).
13. Vesely, K., and Mejzlik, J., J. Polymer Sci., U.S.S.R.,  
5, 521, (1964).
14. MacDonald, R.N., et al., J. Appl. Polymer Sci., 1, 158-191 (1959).

15. Kern, W. and Jaacks, V., J. Polymer Sci., 48, 399, (1960).
16. Hammick, D.L., and A.R. Boeree, J. Chem. Soc., 2738, (1922).
17. Wilson, W., and May, H., Chem. and Ind., 412, (1962).
18. Buseti, V., Mammi, M. and G. Carazzolo, Zeit. für Kristall.,  
119, 310, (1963).
19. Kekule, A., Berichte, 25, 2435, (1892).
20. Bevington, J.C., "Polymers from Aldehydes and other Carbonyl  
Compounds", Chap. 2 of "Polyethers", [see ref (1)].
21. Toby, S., and Rutz, E.F., J. Polymer Sci., 60, 841, (1962).
22. Trautz, M., and Ufer, E., J. Prakt. Chem., 113, 105, (1926).  
Bates, J.R. and Spence R., J. Amer. Chem. Soc., 53, 1689, (1931).  
Spence R., J. Chem. Soc., 1193, (1933).
23. Carruthers, J.E., and Norrish, R.G.W., Trans. Faraday Soc.,  
32, 195, (1936).
24. Bevington, J.C. and Norrish, R.G.W., Proc. Roy. Soc. A205,  
516, (1951).
25. Staudinger, H., et al., Ann., 474, 232-7, (1929).
26. Koch, T.A. and P.E. Lindvig, J. Appl. Polymer Chem., 1, 167, (1959).
27. Staudinger, H., et al., Z. physik. Chem., A126, 425, (1927).  
Heingstenberg, J., ibid, A126, 435, (1937).  
Idem, Ann. Physik., 84, 245, (1927).  
Sauter, E., Z. physik. Chem., B13, 417, (1932);  
B21, 186, (1933).

28. Carazzolo, G. and Mammi, M., *J. Polymer Sci.*, 1, 965, (1963).
29. Huggins, M.L., *J. Chem. Phys.*, 13, 37, (1945).
30. Pierce, R.H.H., see ref. (10) page 176.
31. Philpotts, A.R. et al., *Trans. Faraday Soc.*, 51, 1051, (1955).
32. Novak, A., and E. Walley, *Trans. Faraday Soc.*, 55, 1484, (1959).
33. Schneider, W.G., unpublished paper presented at I.U.P.A.C.  
Symposium on Macromolecules, Stockholm, (1953).
34. Walker, J.F., *J. Amer. Chem. Soc.*, 55, 2821, (1933).
35. Staudinger, H., *Oesterr. Chem. Ztg.*, 32, 98, (1929);  
*Chem. Abstr.*, 23, 4340, (1929).
36. Bevington, J.C. *Quart. Reviews Chem. Soc. (London)*, 6, 141, (1952).
37. National Bureau of Standards, Circular No. 525, (1953).
38. Jellinek, H.H.G., "Degradation of Vinyl Polymers", Academic Press,  
New York, (1955).
39. Grassie, N., "The Chemistry High Polymer Degradation Processes",  
Butterworths, London, (1956).
40. Society of Chemical Industry, Monograph No. 13, "Thermal  
Degradation of Polymers", London, (1961).
41. Madorsky, S.L., "Thermal Degradation of Organic Polymers",  
Interscience, New York, (1964).
42. Grassie, N., "Novel Types of Chain Reactions in Polymer  
Degradation", *J. Polymer Sci.*, 18, 79, (1960).

43. Grassie, N., and Kerr, W.W., *Trans. Faraday Soc.*, 53, 234, (1957).
44. Kern, W. and Cherdron, H., *Makromol. Chem.*, 40, 101, (1960).
45. Wadano, M., Trogus, C., and K. Hess, *Berichte*, 67, 174, (1934).
46. Alsup, R.G., et al., *J. Appl. Polymer Sci.*, 1, 185-191 (1959).
47. British Patent, 884, 707, (1961), to the Du Pont Co.,
48. Grassie, N., and Melville, H.W., *Proc. Roy. Soc.*, A199, 1, (1949).
49. Grassie, N., *Trans. Faraday Soc.*, 48, 379 (1952).
50. Jellinek, H.H.G., and J.E. Clark, *Can. J. Chem.*, 41, 355, (1963).
51. Ibsch, H. von, *Anal. Chem.*, 24, 931 (1952).
52. Kline, D.E., *J. Polymer Sci.*, 50, 441, (1961).
53. Eierman, K., *J. Polymer Sci.*, 66, 157, (1964).
54. Adams, E.G., and Simmons, N.T., *J. Appl. Chem.*, 1, 820, (1951).
55. Weir, N.A. Ph.D. Thesis, Glasgow, June 1963.
56. Dainton, F.S., and Ivin, K.J., *Quart. Reviews*, 12, 79, (1958).
57. Walker, J.F., *J. Amer. Chem. Soc.*, 55, 2821, (1933).
58. Dainton, F.S. et al., *Trans. Faraday Soc.*, 55, 61, (1959).
59. Di Giorgio, V.E., and G.W. Robinson, *J. Chem. Phys.*, 31,  
1678, (1959).
60. Cass, R.C., et al., *J. Chem. Soc.*, 1406, (1958).
61. Alsup, R.G., et al., *J. Appl. Polymer Sci.*, 1, 185, (1959).
62. Inoue, M., *J. Polymer Sci.*, 51, S18-20 (1961).
63. Dainton, F.S. et al., *Polymer*, 3, 263 (1962).



64. Ivin, K.J., Pure and Applied Chem., 4, 271, (1962).
65. Ref (7), Page 180.
66. Iwasa, Y., and Imoto, T., Nippon Kagaku Zasshi, 84, 29, (1963).
67. Carruthers, J.E. and Norrish, R.G.W., Trans. Faraday Soc.,  
32, 195, (1936).
68. Roberts, D.E., and R.S. Jessup, J. Res. Nat. Bur. Stand.,  
46, 11, (1951).
69. Hammer, C.F. et al., J. Appl. Polymer Sci, 1, 169, (1959).
70. Linton, W.H., and H.H. Goodman, J. Appl. Polymer Sci., 1,  
179, (1959).
71. Zamboni, V., and Zerbi, G., J. Polymer Sci., C7, 153, (1964).
72. MacCallum, J.R., Trans. Faraday Soc., 59, 2099, (1963).
73. Simha, R., and Wall, L.A., J. Polymer Sci, 5, 615, (1950);  
6, 39, (1951);  
J. Phys. Chem. 56, 707, (1952).
74. Pac, J., Mejzlik, J., and Vesely, K., Chem. Prumsyl, 12,  
575, (1962), Chem. Abstracts, 58, 12698, (1963).
75. Kutschke, K.O. and Toby, S., Can. J. Chem., 37, 672, (1959).
76. Torikai, S., J. Polymer Sci., A2, 239-52 (1964).
77. Cherdron, H., Hohn, L. and Kern, W., Makromol. Chem., 52,  
48, (1962), 52
78. Coulson, C.A., "The Hydrogen Bond", p. 339 in "Hydrogen Bonding",  
ed. Hadzi, D., Pergamon, 1959.
79. Calvert, J.G. and Steacie, E.W.R., J. Chem. Phys. 19, 176, (1951).

80. Inoue, M. and Takayanagi, T., J. Polymer Sci., 47, 498 (1960).
81. Small, P.A. J. Appl. Chem., 3, 71, (1953).
82. Huggins, M.L., J. Amer. Chem. Soc., 64, 2716, (1942).
83. Alfrey T., et al. J. Colloid Sci., 5, 251 (1950).  
Dacoust, H., and Rinfret, M., abid., 7, 11, (1952).
84. Alfrey, T., et al., Trans. Faraday Soc., B42, 50 (1946).  
Iliquori, A.M., and Mele, A., J. Polymer Sci., 13, 589, (1954).  
See also ref. (87).
85. Yamakawa, H., J. Chem. Phys. 34, 1360 (1961).
86. Cragg, L.H., and Bigelow, C.C., J. Polymer Sci., 16, 177, (1955).
87. Bawn, C.E.H., Trans. Faraday Soc., 47, 97 (1951).
88. Flory, P.J., and Fox, T.G., J. Amer. Chem. Soc., 73, 1904, (1951).
89. Klein, R., and Schoen, L.J., J. Chem. Phys. 24, 1094, (1956).
90. Flynn, J.H., Wilson, W.K. and Morrow, J., Res. Nat. Bureau  
Stand., 60, 229, (1958).
91. Burgess, A.R. Ref (37), p. 149.
92. Lundberg, W.O., Ed., "Autoxidation and Antioxidants",  
Vols. I and II Interscience, 1961 and 1962.
93. Bigelow, L.A. and Fukuhara, N., J. Amer. Chem. Soc.,  
63, 788 (1941).
94. Hense, A.L. et al., J. Amer. Chem. Soc., 72, 3577 (1950).
95. Morse, A.T. et al., Can. J. Chem., 33, 453 (1955).